

Advances in 4D Representation: Geometry, Motion, and Interaction

Mingrui Zhao¹, Sauradip Nag¹, Kai Wang¹, Aditya Vora¹, Guangda Ji¹, Peter Chun², Ali Mahdavi-Amiri¹, Hao Zhang¹

¹Simon Fraser University, ²University of Alberta

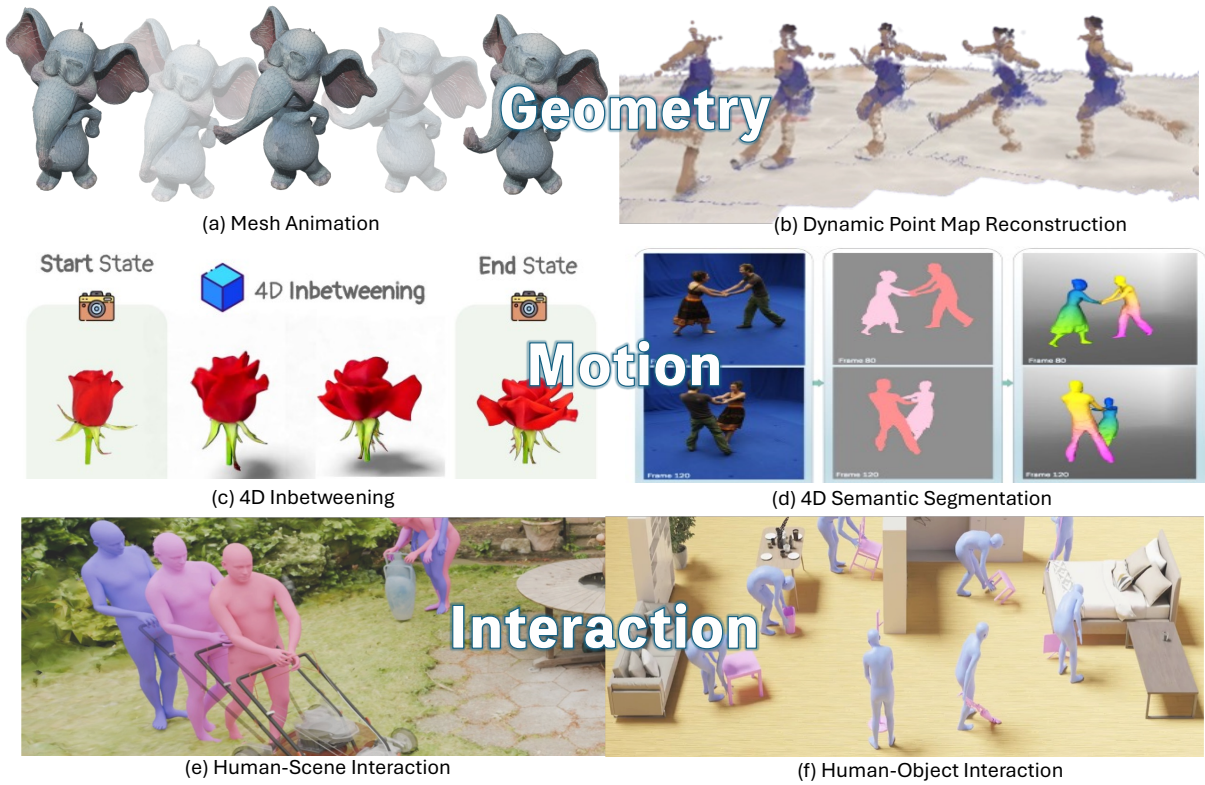


Figure 1: Representative applications for three key pillars of **4D Representation**: (a) (Geometry) mesh animation [CZTW25], (b) (Geometry) dynamic point map reconstruction [WZZ*25], (c) (Motion) 4D inbetweening [NCOZMA25], (d) (Motion) 4D semantic segmentation [MRH22], (e) Human-scene interaction [LYLW24], (f) Human-object interaction [LWL23].

Abstract

We present a survey on 4D generation and reconstruction, a fast-evolving subfield of computer graphics whose developments have been propelled by recent advances in neural fields, geometric and motion deep learning, as well as 3D generative artificial intelligence (GenAI). While our survey is not the first of its kind, we build our coverage of the domain from a unique and distinctive perspective of 4D representations, to model 3D geometry evolving over time while exhibiting motion and interaction. Specifically, instead of offering an exhaustive enumeration of many works, we take a more selective approach by focusing on representative works to highlight both the desirable properties and ensuing challenges of each representation under different computation, application, and data scenarios. The main take-away message we aim to convey to the readers is on how to select and then customize the appropriate 4D representations for their tasks. Organizationally, we separate the 4D representations based on three key pillars: geometry, motion, and interaction. Our discourse will not only encompass the most popular representations of today, such as neural radiance fields (NeRFs) and 3D Gaussian Splatting (3DGS), but also bring attention to relatively under-explored representations in the 4D context, such as structured models and long-range motions. Throughout our survey, we will reprise the role of large language models (LLMs) and video foundational models (VFM) in a variety of 4D applications, while steering our discussion towards their current limitations and how they can be addressed. We also provide a dedicated coverage on what 4D datasets are currently available, as well as what is lacking, in driving the subfield forward.

1. Introduction

Reconstruction and generation of 4D data, i.e., 3D geometry evolving over time while exhibiting motion and interaction, is becoming increasingly critical as computer graphics applications expand into domains requiring dynamic scene understanding, temporal modeling, and motion synthesis. From cinematic visual effects and immersive virtual reality to autonomous robotics, medical imaging, eCommerce and advertising, the ability to capture, represent, and manipulate 4D content has emerged as a fundamental challenge that bridges graphics, vision, and machine learning.

The fourth dimension introduces complexities that extend far beyond simply concatenating spatial coordinates with temporal indices. Temporal coherence, motion continuity, topological changes, interaction dynamics, and the preservation of geometric, appearance, and physical properties across time present unique *representational* challenges that require careful consideration of both spatial and temporal encoding strategies. As the field matures, researchers have developed increasingly sophisticated approaches to handle these challenges, leading to a rich landscape of 4D representation schemes, each with distinct advantages and limitations.

Recent surveys in this domain have primarily categorized methods by applications, approaches, and/or the granularity of the extracted scene signals. Cao et al. [CLH*25] provides a structured review of recent progress in reconstructing 4D spatial intelligence, which is defined as *understanding* 3D scenes and their evolution over time, advancing from extracting low-level geometric cues such as depth, pose, and point maps toward complex reasoning encompassing interactions and physics. This survey does highlight the growing importance of advanced 3D representations while focusing mainly on neural radiance fields (NeRFs) and 3D Gaussian splatting (3DGS). Along the same lines, Fan et al. [FZZ*25] presents a comprehensive survey of recent progress in dynamic scene representation and reconstruction, focusing on the transition from NeRF to 3DGS and their trade-offs. This second survey systematically categorizes the works covered based on motion representation paradigms including rigid, articulated, non-rigid, and hybrid motions, and examines strategies for modeling temporal changes in geometry and appearance. In addition, Miao et al. [MLQ*25] survey the emerging field of 4D *generation* by introducing a taxonomy of low-level geometry representations (meshes, NeRFs, point clouds, and 3DGS), foundational techniques (diffusion models and score distillation sampling), and conditioning methods (text, images, videos, 3D inputs, and multimodal control). This survey further categorizes the algorithmic approaches (end-to-end, via generated data, implicit distillation, vs. explicit supervision) and highlights the growing range of applications for 4D generation.

While the above surveys have advanced our understanding of the field's breadth, they have not sufficiently covered all the relevant representations of geometry (especially higher-level *structured* representations), motion, and interaction, or addressed the fundamental question of why specific representations are chosen for particular 4D tasks and the motion/interaction mechanisms, nor have they provided comprehensive analysis of the inherent trade-offs that different representational choices impose on data preparation, method design, computational requirement, and achievable results.

To close these gaps, our survey adopts a *representation-centric*

perspective. Instead of offering an exhaustive enumeration of many works, we take a more selective approach by focusing on representative works to highlight both the desirable properties and ensuing challenges of each 4D representation under different computation, application, and data scenarios. The main take-away message we aim to convey to the readers is on how to select and then customize the appropriate 4D representations for their tasks.

Organizationally, we separate the 4D representations based on three key pillars: *geometry*, *motion*, and *interaction*. We distinguish between structured representations, i.e., those that maintain explicit primitive or part delineations and relations, and unstructured representations, i.e., those that encode 4D content through implicit functions, point distributions, or learned feature spaces without explicit structural constraints. While the latter category encompasses the most popular representations of today, namely NeRFs and 3DGS, they are both built on *rendering* primitives, mainly for novel view synthesis. They are not best suited to prevalent 4D tasks such as modeling, editing, or interactions, for which more compact and structural representations, built on higher-level primitives, are more appropriate. Hence, we also discuss these representational choices even though they have been relatively under-explored. Throughout our survey, we will reprise the role of large language models (LLMs) and video foundational models (VFM) in a variety of 4D applications, while steering our discussion towards their current limitations and how they can be addressed. We also provide a dedicated coverage on what 4D datasets are currently available, as well as what is lacking, in driving the subfield forward.

Our representation-centric analysis goes beyond traditional surveys in several key ways. First, we examine not only the capabilities of each representation but also their fundamental limitations and the specific 4D challenges they are designed to address. Second, we analyze how representational choices constrain and enable different architectural approaches for learning, predicting, and generating temporal dynamics. Third, we provide comprehensive coverage of motion modeling approaches, temporal consistency mechanisms, and the interplay between representation and motion characteristics aspects that have received limited attention in previous surveys despite their central importance to 4D applications.

Furthermore, this survey addresses the growing importance of motion analysis in 4D representation by dedicating significant attention to temporal dynamics, motion types, and their representational requirements. We examine how different motion characteristics, from rigid articulations to non-linear deformations to topological changes, interact with representational choices and impose constraints on method design. This motion-centric analysis is complemented by comprehensive coverage of datasets, evaluation metrics, and benchmarking protocols that have emerged to support systematic comparison of 4D methods across different representations.

Our survey is organized as follows. Section 2 presents our core representational analysis, examining unstructured representations (mesh, point clouds, NeRFs and 3DGS) and structured representations (template, parts, and graphs). Section 3 focuses on motion and temporal dynamics, analyzing how different motion types interact with representational choices. Section 4 covers representation choices in modeling multiple entities that interact with each other. Section 5 surveys datasets, evaluation metrics, and bench-

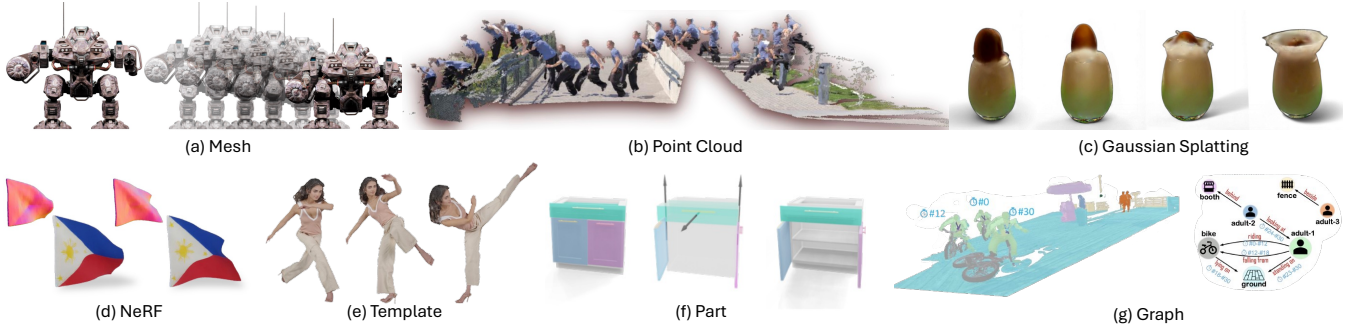


Figure 2: 4D content created with different geometric representations. (a) Mesh [WYWB25]; (b) Point cloud [WZZ*25]; (c) Gaussian Splatting [NCOZMA25]; (d) NeRF [VYB*24]; (e) Template-based representation [ZZY*24]; (f) Part-based representation [LTMAS24]; (g) Spatial-Temporal scene graph [YCP*23]. Figures adopted from the original papers.

marking frameworks that enable systematic comparison across representations. Section 6 provides an overview on training paradigms. Finally, Sections 7 and 8 provide an overall analysis across representations and discuss emerging trends, persistent challenges, and future research directions in 4D representation. The overall taxonomy of our survey is shown in Figure 3.

2. Modeling Geometry

Each 3D representation for 4D carries advantages and disadvantages. We survey geometric representations in state-of-the-art 4D works, examining not only their intrinsic properties but also their integration with the current 4D tasks: which representations are favored for particular applications, what unique capabilities they enable, and what limitations they may have.

We categorize representations into *unstructured* (Section 2.1) and *structured* (Section 2.2) classes based on whether their operational primitives carry explicit functional, hierarchical, or semantic meaning. See Figure 2 for an illustration. Unstructured representations—meshes (Section 2.1.1), point clouds (Section 2.1.2), NeRF (Section 2.1.3), and Gaussian Splatting (Section 2.1.4)—use primitives (vertices, points, ray samples, Gaussians) as independent geometric elements. While local connectivity may exist (e.g., mesh faces), these representations do not impose inter-primitive global structural constraints or functional decompositions.

Structured representations—skeletal templates (Section 2.2.1), part-based models (Section 2.2.2), and graphs (Section 2.2.3)—impose functional decomposition: skeletal joints define kinematic chains, parts carry semantics, graph nodes encode relational structure. Some structured representations build on unstructured primitives (e.g., SMPL uses a mesh but adds skeletal hierarchy and skinning weights); the key distinction lies in whether functional relationships and compositional structure are explicitly encoded as first-class constraints in the representation.

2.1. Unstructured Representation

Unstructured representations form the foundation of most 4D reconstruction and generation pipelines due to their flexibility and

widespread adoption in graphics and vision. We examine four dominant paradigms—meshes, point clouds, NeRF, and Gaussian Splatting—analyzing how each adapts to temporal dynamics and the specific challenges they face in 4D settings.

2.1.1. Mesh-Based Representations

A polygonal mesh represents a 3D object’s surface through vertices (points in 3D space), edges (connecting vertex pairs), and faces (surfaces enclosed by edge loops), explicitly encoding both geometry through vertex coordinates and topology through connectivity relationships. Meshes retain important advantages in graphics applications: compatibility with GPU rasterization enables real-time rendering; explicit structure allows intuitive manipulation and editing; natural decoupling of geometry, topology, and appearance enables motion generation through vertex displacement while maintaining constant topology and texture maps across frames, ensuring temporal coherence and object identity preservation.

Meshes are mainly adopted in object-centric 4D modeling, aimed at producing animated mesh assets from text [DSW*25, CHC*24], video [CZTW25, LCL24], or static 3D assets [WYWB25, SLW*25]. However, mesh representations face several challenges in 4D applications, which we discuss below alongside methods developed to address them.

Spatiotemporal Consistency: Animated mesh sequences require precise vertex-to-vertex correspondence across frames to preserve consistent texture and topology, preventing naive per-frame generation pipelines that can lead to different vertex-connectivity in each generated sample. V2M4 [CZTW25] circumvents this through a reconstruction-and-refine pipeline: it first applies image-to-3D reconstruction models [XLX*25, ZLL*25, LZL*25, LLY*24] to generate per-frame meshes, then sets the first frame as an anchor and deforms it to register with subsequent frames, maintaining consistent mesh correspondence through continuous deformation.

Deformation Learning: Given that most approaches rely on deforming a consistent mesh topology rather than per-frame generation, determining correct vertex displacements becomes the central challenge. Vertices lack inherent semantic meaning, making it difficult to learn meaningful deformation patterns. Two primary approaches have emerged: directly learning per-vertex



Figure 3: Our taxonomy of 4D representations. We separate them into three pillars: (1) Geometry, including both structured and unstructured representations; (2) Motion, including articulation, deformation and tracking based representations; (3) Interaction, including representation of action, affordance, pose, contact and physics.

displacement from data priors [WYWB25] or video diffusion model guidance [DSW*25], or introducing an intermediate rigging structure—either explicit [SZL*25, SLY*25] or approximated [LCL24]—followed by skinning-based articulation to propagate skeletal motion to vertex displacements.

Open Challenges: Despite recent progress, fundamental limitations remain. Topological inflexibility prevents meshes from representing splitting or merging. Their inflexible topology and connectivity struggle with volumetric phenomena such as clouds, smoke, and fire, motivating the adoption of topologically flexible alternatives such as NeRF (Section 2.1.3) and point clouds (Section 2.1.2) for such scenarios. Additionally, current mesh-centric generation and reconstruction methods predominantly focus on object-level rather than scene-level modeling. The latter has recently been studied on static 3D scene reconstruction [YZY*25] through generative methods, while most existing works rely on mesh database retrieval [WIR*24]. Key difficulties include: (1) generating and tracking separate mesh topologies for multiple objects at varying scales, (2) handling inter-mesh physical constraints, and (3) maintaining temporal coherence when objects move independently with different deformation patterns. Addressing these challenges remains an open problem for the research community.

2.1.2. Point-cloud-based Representation

A point cloud represents 3D geometry as an unordered set of points $P = \{p_i\}_{i=1}^N$, where each point p_i is defined by spatial coordinates (x, y, z) and optional attributes including color (RGB), intensity, surface normals, and timestamps. Their unstructured, unordered nature enables representation of arbitrary and changing topologies without connectivity constraints. Point clouds also serve as the primary output format for real-world acquisition mechanisms. This direct sensor correspondence has established point clouds as the standard representation for large-scale scene capture, particularly in autonomous driving (KITTI [GLSU13], nuScenes [CBL*20]), where their geometric scalability outperforms alternatives. On native 4D point cloud sequences, numerous works focus on improving point cloud quality through denoising [HH25], upsampling [LLF21, BBBB23], and mesh reconstruction [TADTBS*22, RBZ*20, NMOG19]. Another research direction addresses dynamic point cloud understanding, including motion recognition [LHL*25, DZLY23], object detection and tracking [HGH*22, WNGO24, CLZ*24], scene flow estimation [LQG19, WWL*20, TD20], forecasting [KHHR23, WYW*24], and motion interpolation [ZQZ*22, ZWL*23, LCQ*21]. With the emergence of large feed-forward geometric models like DUST3R [WLC*24] and VGGT [WCK*25], a new promising branch of work is to create dynamic point map sequences from videos [ZHH*24, WZH*25, WZZ*25, TZW*25] and incorporate tracking within the inferred point maps [XWX*25].

Below we discuss the main challenges in applying point clouds to 4D contexts and representative works addressing them.

Temporal Correspondence: Different frames in dynamic point cloud sequences exhibit varying noise patterns, point counts, and no guaranteed point-to-point correspondence. FlowNet3D [LQG19] pioneered end-to-end scene flow learning,

estimating vector displacements between consecutive frames without assuming point-to-point correspondence. St4RTrack [FZW*25] generates dynamic point cloud sequences from videos and tracks point motion using an attention-enabled tracking branch that leverages video inputs. Alternatively, correspondence can be enforced by interpolating between adjacent frames. FastPCI [ZQXY24] applies pyramidal transformer blocks to extract motion and structure features, facilitating in-betweening generation.

Appearance Modeling: The discrete, isolated nature of point clouds prevents complete appearance modeling, leaving void spaces between points unlike surface or volumetric representations. PAPR-in-Motion [PZL24] addresses this by associating each point with view-dependent features and rendering through attention-weighted feature interpolation, achieving void-free rendering while enabling dynamic visualization through point displacement.

Open Challenges: Point clouds remain the primary interface with real-world sensor captures (LiDAR, RGB-D cameras), and this abundance of point-based training data has recently enabled pointmap-based methods to achieve impressive 4D reconstruction from monocular videos. However, a reconstruction-generation asymmetry persists: while point clouds excel at capturing dynamic geometry from observations, their inherent limitations—discrete sampling without explicit surface connectivity—make them less suitable for generation tasks. Incorporating physical motion remains challenging: the lack of topological structure complicates enforcement of physical constraints such as collision response, conservation laws, and contact dynamics. Future work should focus on efficient bidirectional conversion between point clouds and other representations, enabling knowledge transfer of mesh topology, NeRF appearance modeling, and physical constraints to point-based frameworks while preserving their computational efficiency and sensor correspondence advantages.

2.1.3. Neural Radiance Fields (NeRF) based Representation

Neural Radiance Fields (NeRF) [MST*20] represent 3D scenes by mapping 3D query points and view directions to density and color using an MLP. Final pixel colors are obtained by integrating these color predictions along camera rays via volume rendering [KVH84]. This continuous representation achieves high visual fidelity from only 2D images and can capture topologically complex phenomena like smoke and fluids, and compactly store dynamic scenes within an MLP [PSH*21, AHR*23]. Despite its promise, NeRF faces several key challenges in 4D modeling.

Flickering and Unrealistic Deformations: A direct extension of NeRF to the 4D domain models temporal variations by introducing time-varying fields. This is typically done by conditioning the representation on a time signal or by learning a unique embedding for each timestamp [GSKH21, LSZ*22, WZT*22, OMT*21]. Another approach models dynamics by predicting deformation or flow fields using a separate deformation network, which warps the scene over time [LNSW21, SCL*23]. Each frame’s color and density are then composited and rendered using the standard NeRF volume rendering framework. However, this approach often suffers from temporal flickering and unrealistic deformations. These issues are typically alleviated through temporal consistency losses and rigidity constraints [GSKH21, LNSW21].

Slow Convergence: NeRF-based representations often suffer from slow convergence due to the heavy computational cost of training large MLPs for dynamic scenes. To accelerate training, several methods introduce learnable spatial-temporal data structures such as Hex-planes and K-planes [CJ23, SSP*23, FKMW*23, JZG*24], which trade memory for speed. These approaches sample positional features from planar decompositions via bilinear interpolation before passing them through a smaller MLP for color and density prediction. By offloading computation from the MLP to explicit plane-based storage, convergence accelerates significantly compared to standard NeRFs. However, planar decompositions may sacrifice fine-grained spatial details. Alternative data structures have also been explored, including voxel grids [LCM*22, FYW*22, SZT*23, YYPZ24] that provide denser spatial sampling, and hash grids [BSR*24, ZYX*23, ZCW*24] that offer adaptive resolution through learned hash encodings.

Handling Sparse Input Scenarios: NeRF representations, in general, require dense multi-view video captures as input. To improve robustness under sparse input conditions, recent works incorporate flow supervision [WMJL23, YHR*24] to train models with only monocular video supervision. Other methods approach this problem through motion-adjusted feature aggregation [LWC*23] or enriching input data from generative models [YXV*25, XYV*24].

Open Challenges: Despite these improvements, temporal flickering and unrealistic motion artifacts remain persistent issues, particularly when training from sparse or limited input views. Motion synthesis and editing in NeRF-based methods are also less intuitive, as manipulations occur in latent deformation spaces rather than through direct geometric controls. Additionally, NeRF’s ray marching mechanism incurs significant computational overhead during inference, leading the community to increasingly favor Gaussian Splatting (Section 2.1.4) as a more efficient alternative for real-time dynamic scene rendering.

2.1.4. Gaussian Splatting based Representations

3D Gaussian Splatting [KKLD23] represents 3D scenes using a set of Gaussian primitives and renders images through rasterization. Each Gaussian is defined by its 3D covariance matrix and spatial position, and is optimized using photometric loss after rasterization. This explicit, discrete representation offers several advantages: it avoids redundant computation in empty regions by only evaluating non-zero Gaussians, enables real-time differentiable rendering through efficient tile-based rasterization [KKLD23], and supports motion modeling more explicitly through deforming each Gaussian. Gaussian Splatting’s explicit formulation and efficient rendering pipeline have made it increasingly favored for dynamic scene applications. Despite these benefits, several challenges remain for this representation in 4D settings.

Temporal Coherency: A straightforward way to model dynamic scenes is to generate per-frame 3D Gaussians [RXM*24, VNZ25] from an input video. However, maintaining temporal coherence across frames remains difficult due to flickering and blurriness caused by dynamically learned Gaussian colors. To mitigate this, many methods opt for continuous deformation field [JZJ*24, YXW*23, WGP*25, YXL*25, XFYX24, SSP*24]

or tracking-based deformation [SHU*24, LWH*25] or attention-based deformation [SGW*24] to enforce temporal coherency through local regularization. Another emerging trend is to use native 4DGS that encodes space-time variations within the geometry representation [DWD*24, WYF*24].

Sparse Input Conditions: Similar to NeRF, the most comprehensive input for Gaussian Splatting is also multi-view synchronized videos. However, such data scales drastically in volume with video length and number of view angles, along with the induced computational burden, such data is also harder to acquire. Thus it is a natural choice for the community to shift toward a sparse input paradigm. Existing methods include simultaneously learning canonical static Gaussian and deformation field from monocular videos [YPZ*24], leveraging additional physical priors such as optical flow [GXC*24, LDZY24], depth [LLW*25] and video diffusion guidance [NCOZMA25, RXM*24, WGP*25].

Open Challenges: Improving spatial-temporal coherence, training efficiency, and adaptation to sparse inputs remain active research areas. Beyond these, modeling large-scale motion in Gaussian Splatting poses significant challenges, as it requires carefully calibrated covariance matrices to properly reorient and deform Gaussian primitives across frames. Additionally, while volumetric rendering methods inherently couple appearance and geometry, extracting high-quality explicit meshes from dynamic Gaussian representations remains an important open problem.

2.2. Structured Representation

Structured representations impose compositional priors that enable more controllable and interpretable 4D modeling. We survey three primary approaches—template-based, part-based, and graph-based methods—examining how explicit structural constraints facilitate motion modeling and the challenges they present.

2.2.1. Template-based Representation

Template-based representations combine a parametric mesh with an underlying skeletal structure (kinematic tree). Mesh vertices are bound to the skeleton through a *skinning* function that determines vertex deformation during skeletal articulation. Animation occurs by manipulating skeletal pose parameters, which drive mesh deformation through skinning weights (detailed in Section 3.1.1). This representation models object categories sharing common topology and articulated structure—humans, hands, or animals—while allowing individual variation in shape and pose. Examples include SMPL [LMR*15] for human bodies, MANO [RTB17] for hands, SMAL [ZKJB17] for animals, FLAME [LBB*17] for heads, and compositional variants like SMPL+X [PCG*19] for body, hand, and face. Templates offer distinct advantages for 4D modeling. They inherently couple motion within parametric structure, provide compactness while maintaining anatomical plausibility, and encode category-specific priors enabling realistic motion and facilitating motion transfer. By decomposing 4D modeling into per-frame pose [GPR*23], templates effectively handle long-term sequences, establishing foundations for digital avatars, human-object interactions, and hand manipulation applications. Despite these advantages, templates face challenges.

Sub-realism: Models like SMPL represent bare bodies with rigid motion, leaving gaps in realistic digital human modeling. Enhanced personalization requires deforming meshes to mimic cloth [MYR*20], texturing for appearance [LYX*24b], or generating garments and hair with simulators [XYDM*24, ZZY*24]. Soft-SMPL [SGOC20] introduces soft tissue dynamics as a preliminary step toward realism.

Temporal Consistency: Per-frame pose estimation can produce temporal jitter from frame-level errors, resulting in unrealistic motion despite correct per-frame geometry. This can be addressed by temporal smoothness constraints through sequential models [KZFM19, KAB20, CMCL21] that leverage temporal context from adjacent frames, or physics-based priors [SGXT20] that enforce motion continuity and physical plausibility.

Open Challenges: While template-based representations exhibit excellent motion transferability within categories, cross-category transfer remains limited. Developing generalizable template learning frameworks that automatically infer skeletal structures, skinning weights, and shape spaces from sparse examples would greatly boost the representation’s applicability [LXY*25, SZL*25]. Furthermore, integrating physics simulation with learned skinning functions to enable realistic contact dynamics, collision response, and soft tissue deformation represents a promising direction.

2.2.2. Part-based Representation

Part-based representations decompose 3D entities into individual parts and model overall motion through their collective dynamics. Unlike unstructured representations with holistic motion models, part-based approaches assign semantic meaning to decomposed parts and functional meaning to their motion. Parts can be represented using various formats such as NeRF [LMS23], point clouds [YHY*20], or meshes [JMCS22]. This representation is commonly used for modeling articulated objects [LTMAS24, LIC*25, IJZ*24, LDS*23]—such as cabinets with opening doors, pulling drawers, and rotating hinges—with applications in embodied AI and robotic manipulation.

Part-based representation faces two primary challenges: decomposing 3D entities into functional parts and correctly articulating each primitive. The decomposition process requires functional understanding of component relationships and involves both segmentation and completion during part reconstruction. Early approaches rely on segmented datasets [XQM*20] but show limited generalizability due to dataset scale constraints. Recent work leverages large language models for semantic reasoning in part segmentation and completion [QYW*25, LIC*25, XSM*25, LLT*25]. These methods use LLMs to identify functional parts and plausible articulated motions, then apply amodal completion on segmented 3D parts or retrieval-based reconstruction. An alternative approach learns kinematic part decomposition directly from visual data. SP4D [ZYD*25] jointly generates multi-view RGB videos and corresponding kinematic part segmentation from monocular inputs. The method lifts the generated 2D part maps to 3D to derive skeletal structures and harmonic skinning weights, enabling articulated 3D asset creation for extended categories.

Open Challenges: Part-based representation remains

a growing field. Active research continues in both 2D [LZRV24a, LZRV24b, VNZ25, SJSC24, WGPYZ24] and 3D [ZWY*24, YQZ*24, YGH*25, YHZ*25], with many techniques yet to be transferred to 4D content creation. Precisely segmenting and articulating parts of 3D models remains an open problem, with current applications concentrated on specific object categories such as furniture and relatively simple motions—prismatic translation, rotation, and revolution. The underlying challenge still lies in functional understanding. Extending to more complex behaviors such as per-part non-rigid deformation and generic objects requires a deeper functional understanding of 3D assets and their constituent parts. These directions warrant further investigation by the research community.

2.2.3. Spatio-Temporal Scene Graphs

Scene graphs are a popular representation for describing multiple geometries in an environment and the relations between them. 3D scene graphs could be generalized to include a temporal dimension through multiple means. A straightforward approach is to represent a 4D spatio-temporal scene graph as a collection of 3D scene graphs at different time stamps [JKFFN20, RCJ*21]. While each slice is a standard 3D scene graph, temporal edges can be used to connect the same entity across slices. It is also possible to generalize a linear sequence into an arbitrary graph, where edges link temporally proximal concepts [KGP02]. A collection of slices could also be grouped to represent entire events.

While such representations are effective, they are computationally expensive—when the size and length of the 4D scene grow, because all nodes are still in 3D. A natural generalization is to adopt 4D nodes, where each node describes a tube/trajectory of 4D geometries over time [BT11], rather than a single 3D geometry. In addition to concrete geometries, 4D nodes can also represent abstract concepts such as events. Doing so drastically reduces the size of the graph, removing the need for a node at every time slice. Edges can also be generalized to work with 4D nodes. Instead of distinguishing between spatial (at 3D slices) and temporal (connecting adjacent 3D nodes) edges, a single edge connecting 4D nodes can represent spatio-temporal concepts over time, including time-restricted properties (e.g. co-visibility) [RGA*20], evolving actions (e.g. falling from) [YCP*23], or causal relationships.

Open Challenges: While 4D Spatio-Temporal scene graphs naturally describe structural relations and semantics better, they are more complex than the unstructured counterparts. Curating compatible 4D data and developing specific learning algorithms for such representation also require significant efforts [BT11, YXL18, BPL*16]. Consequently, achieving comparable geometric fidelity and temporal granularity to unstructured 4D representations remains challenging. Connecting such 4D graphs as an additional layer of abstraction over aforementioned unstructured 4D representations is an important future research direction.

3. Modeling Motion

The core of motion representation is establishing how geometry evolves across temporal frames. This can be formulated as determining the geometric state \mathcal{G}_t as time t evolves. We distinguish four

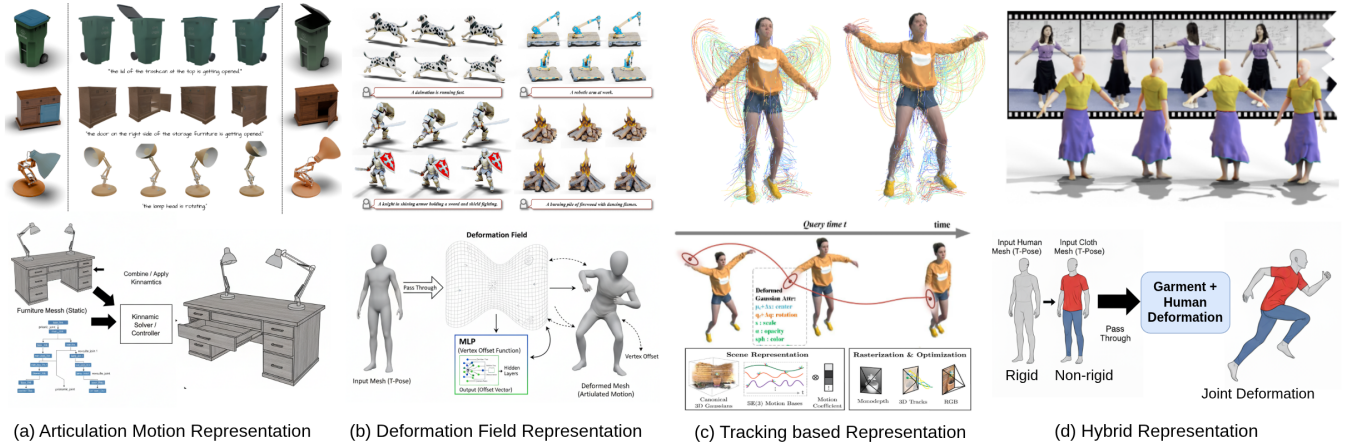


Figure 4: Various examples showing how motion is added to the geometry. From left to right: [VNZ25, DSW*25, LKLR24, QCZ*23]

principal motion classes in 4D representations: articulated motion, deformation-based motion, tracking-based motion, and hybrid motion (Fig. 4), discussed below.

3.1. Articulated Motion

Articulated motion consists of rigid segments connected by joints that move relative to each other, producing globally non-rigid behavior while each segment undergoes only rigid transformations (translation and rotation). This motion is commonly seen in biological systems (e.g., skeletons) and engineered mechanisms.

Articulated objects are modeled as kinematic trees [ATK19]-hierarchical structures where joints define degrees of freedom (revolute, prismatic, or fixed) and govern transformation propagation through the hierarchy. Methods for articulated motion fall into two categories. **Template-based methods** utilize predefined parametric models that encode a known shape and/or skeletal structure for specific object categories. **Template-free methods** infer geometry and kinematics directly from observations without category-specific priors, enabling generalization to arbitrary articulated objects at the cost of increased computational complexity and ambiguity in joint inference.

3.1.1. Template-based Articulation

Among available template choices (see Section 2.2.1), we take SMPL [LMR*15] as an exemplar for the following discussion, as most template-based methods share similar motion modeling mechanisms. To articulate a standard template mesh from a rest pose to a target pose, SMPL deforms its template mesh using *linear blend skinning (LBS)*, which assigns blend weights to vertices to quantify each joint’s influence. The deformed position \mathbf{p}_i^m of a canonical point \mathbf{p}_i^c is computed as:

$$\mathbf{p}_i^m = \mathcal{D}_\theta(\mathbf{p}_i^c, \mathbf{w}(\mathbf{p}_i^c); \tau(J)) = \sum_{j=1}^J w_j(\mathbf{p}_i^c) \mathbf{T}_j \mathbf{p}_i^c, \quad (1)$$

where $w_j(\mathbf{p}_i^c)$ is the blend weight for the j -th joint and $\mathbf{T}_j \in \mathbb{R}^{4 \times 4}$ is its transformation matrix. This provides natural support for in-domain applications such as human motion synthesis [YSI*23] and

reconstruction [GPR*23], where tasks are accomplished through template parameter prediction. Further combination with visually rich representations such as Gaussian Splatting [LZWL24] allows realistic motion and appearance to be generated simultaneously.

Neural skinning fields address off-surface deformation challenges by learning skinning functions directly from data. A neural network maps 3D points to blend weights:

$$\mathbf{w}(\mathbf{x}) = \mathcal{S}_\theta(\mathbf{p}; \tau(t)), \quad (2)$$

where $\tau(t)$ provides time-varying conditions such as pose parameters. Instead of using the fully equipped SMPL template, this branch of work, at minimum, takes only the skeleton as input and derives the skinning weight. HumanNeRF [WCS*22], TAVA [LTV*22], and A-NeRF [PDW*21] employ off-the-shelf modules to predict posed skeletons as the prior and model motion sequence from input videos. LS-Avatar [SWS*25] applies part-based neural skinning fields, enabling realistic avatar animation from monocular video. NeuroSkinning [LZT*19] and SNARF [CZB*21] take the skeletons as input and infer skinning weights to synthesize motion, with the former demonstrating applicability on cloth animations once the skeleton is provided.

3.1.2. Template-Free articulation

Template-free methods reconstruct articulated objects without predefined models, discovering geometry and kinematics from observations. This presents three challenges: (1) inferring movable parts, (2) identifying joint locations and axes, and (3) estimating motions from limited data—compounded by diverse articulation patterns, occlusions, and sparse observations. Solutions typically employ two approaches: explicit joint parameter estimation or kinematic tree discovery.

Joint Parameters: Joint parameters provide a structured representation specifying motion properties including joint type, axis, state, and limits [LXF*22]. Common 1-DoF joints (revolute, prismatic) dominate everyday objects, while multi-DoF joints (e.g., ball joints) appear in complex mechanisms. The joint axis encodes orientation and pivot location; joint state represents current configuration (rotation angle or translation distance) [CSWK24].

Kinematic Tree: The kinematic tree provides a hierarchical abstraction capturing part dependencies through explicit structural relationships [LDS*23, EZH22]. This graph-based representation—with parts as nodes and joints as edges—proves essential for multi-component objects [CWM*24]. However, topology extraction is challenging due to object-specific variations in part count and structural configuration [LXL*24, KHK*25]. Recent advances address this through graph neural networks that learn connectivity patterns and enhanced representations supporting complex structures like kinematic loops [CSWK24].

3.1.3. Integrating physical priors

Physical priors ensure plausible reconstructions across both paradigms. Template-based models embed constraints in learned spaces [LMR*15], model continuous velocity [SFT*25], or learn efficient dynamics [ATFS24]. Collision detection employs spatial partitioning and CCD [RKLM04]. Template-free methods infer consistency from observations, through enforcing SDF and kinematic constraints [WLL*25] or incorporating probabilistic limits [SSB11]. Alternatively, integration via neural priors [ATFS24] or physics constraint injection [YSI*23] enables physically consistent reconstructions for robotics, animation, and simulation.

3.2. Deformation-guided Representation

This paradigm factorizes dynamic scenes into a static *canonical space* and time-varying *deformation fields* [HSY*24, PSB*21, GCD*22, LCM*22, ZYX*23, RPT*23]. The canonical space serves as a reference from which all frames derive via learned deformations. For rigid or articulated cases, it corresponds to a neutral pose; for general scenes, it preserves sufficient structure for reliable temporal correspondence.

Deformation fields, implemented as neural networks, formalize the canonical-to-observation relationship. Forward deformation Φ_θ maps canonical to observation space at time t :

$$\Delta_{b \rightarrow f}(\mathbf{p}_b) = \Phi_\theta(\mathbf{p}_b; \tau(t)), \quad (3)$$

while backward deformation Φ_θ^{-1} provides the inverse and $\tau(t)$ is a function of time. Invertibility ensures bidirectional consistency through regularization or invertible architectures [LLW*25, WCC*23, CFF*22]. NeRF frameworks typically use backward deformation to query canonical attributes [PSB*21, PCPMN21, PSH*21], while explicit representations like 3D Gaussians employ forward warping [YGZ*24, LLW*25]. For long sequences with substantial motion, multiple local canonical spaces over temporal subwindows maintain coherence while handling large transformations [AHR*23, NCOZMA25].

Deformation-based motion representations in 4D tasks encounter key limitations. *Topological variations* such as object emergence, disappearance, or merging break the bijective mapping assumption, leading to correspondence failures [LNSW21, TTG*21]. *Large inter-frame motions* challenge the smoothness and invertibility of learned deformations, often entangling geometry and appearance [PSH*21, PCPMN21]. *Ambiguous correspondences* arise under occlusion or low-texture regions

where multiple deformations fit equally well [YLSL21, WWXL23] while *computational overheads* grow rapidly with sequence length and bidirectional consistency [YGZ*24, LKLR24]. Lastly, *non-rigid or fast motions* remain difficult to capture due to temporal discretization limits [PZX*21, LSZ*22]. Deformation fields model two main types of motion: (a) rigid and (b) non-rigid motion.

3.2.1. Rigid Motion

Rigid motion preserves geometry through rotation and translation, maintaining shape, size, and internal distances. A rigid transformation is expressed by a rotation matrix $\mathbf{R} \in SO(3)$ (or quaternion $\mathbf{q} \in \mathbb{R}^4$) and translation vector $\mathbf{t} \in \mathbb{R}^3$:

$$\mathbf{p}_t = \mathcal{D}_\theta(\mathbf{p}_{t-1}) = \mathbf{R}\mathbf{p}_{t-1} + \mathbf{t}. \quad (4)$$

Rigid bodies include manufactured items (boxes, chairs, kitchenware) and vehicles, which are often approximated as rigid despite minor internal deformations [PYL*22, YAK*20, XH22].

3.2.2. Non-Rigid Motion

Non-rigid motion involves local point deformations essential for modeling cloth [QCZ*23], facial expressions [WWY*25], and fluids [GYZW25]. Unlike rigid or articulated motion with structured parametric models [LMR*15], generic non-rigid deformation lacks compact formulations due to topological changes and infinite degrees of freedom.

Recent approaches model non-rigid motion as learnable neural fields estimating continuous displacement:

$$\mathbf{p}_t = \mathcal{D}_\theta(\mathbf{p}_{t-1}; \tau(t)) = \mathbf{p}_{t-1} + \Delta_\theta(\mathbf{p}_{t-1}; \tau(t)), \quad (5)$$

where Δ_θ predicts displacements conditioned on temporal code $\tau(t)$. These fields are trained from 2D observations via differentiable rendering, eliminating 3D supervision. However, sparse views complicate learning, requiring regularization for robustness.

3.2.3. Integrating physical priors

Physics-based 3D deformation integrates simulation with neural representations. Material Point Method (MPM) [SSC*13] handles large deformations and topology changes. PhysGaussian [XZQ*24] treats 3D Gaussians as simulation particles, which has been extended to language-driven property assignment [QYZW24] and text-to-3D synthesis. NeRF methods embed continuum mechanics: PIE-NeRF [FSL*24] and PAC-NeRF [LQC*23] enable interactive elastodynamics, while Nerfies [PSB*21] regularizes deformation with elastic priors. Alternative frameworks explore finite elements, spring-mass systems [ZYWL24], and position-based dynamics [ACRDS23]. [CZH*25] uses elasticity as a constraint in point cloud modelling, while differentiable physics [HZL*24, LSY23] leverages neural networks to distill physical laws.

3.3. Tracking-based Representation

Rather than relating observations to a shared reference, tracking-based methods capture motion between consecutive frames. This frame-to-frame approach leverages incremental deformations, naturally accommodating topology changes and extreme deformations that challenge canonical-space methods.

3.3.1. 2D Tracking

Reliable 2D tracking establishes temporal correspondences foundational for 3D motion recovery. Classical methods include sparse feature matching (e.g., ORB [RRKB11]) and optical flow [SYLK18, TD20]. Sparse matching supports localization but fails for dense non-rigid motion; optical flow provides dense correspondences but struggles with occlusion and large viewpoint changes. Recent neural rendering methods [WELG21, WCC*23, LKLR24] enable dense, long-range 3D tracking by jointly optimizing scene representation and a continuous trajectory field:

$$\mathbf{p}_t = \mathcal{J}_\theta(\mathbf{p}_{t-1}; \tau(t)), \quad (6)$$

Here, \mathcal{J}_θ models per-point 3D motion guided by 2D tracking priors $\tau(t)$, achieving global temporal coherence [CGJ*23, SHU*24, WYG*24].

Despite its accessibility, 2D tracking faces several critical challenges for 4D tasks: (a) *Depth ambiguity*: 2D projections lose 3D geometric information, making it difficult to distinguish between different 3D motions that produce similar 2D displacement. (b) *Occlusion handling*: Points disappear and reappear in 2D views, breaking temporal correspondence. (c) *Perspective distortions*: 2D tracking doesn't capture actual 3D motion—camera viewpoint changes confound object motion. (d) *Requires lifting*: An additional step is needed to reconstruct 3D/4D information from 2D observations, introducing errors and ambiguity.

3D tracking and scene flow overcome these limitations by directly estimating motion in 3D space, preserving geometric information throughout the temporal sequence.

3.3.2. 3D Tracking

The 3D *scene flow* provides a compact representation of frame-to-frame motion in 4D reconstruction. In the continuous setting, a velocity field $\mathbf{v}(\mathbf{x}, t)$ assigns each point a motion vector describing its instantaneous change [NMOG19, WMJL23], where a point's new position can be approximated as

$$\mathbf{p}_t = \mathbf{o}_{t-1} + \int_{t-1}^t \mathbf{v}(\mathbf{p}(\hat{t}), \hat{t}) d\hat{t}, \quad (7)$$

where $\mathbf{v}(\mathbf{x}(\hat{t}), \hat{t})$ denotes the velocity at intermediate time \hat{t} . Although theoretically elegant, acquiring continuous ground-truth velocities is typically infeasible in practice. In discrete form, the scene flow $\mathbf{O}(\mathbf{p}, t) = \mathbf{p}_t - \mathbf{p}_{t-1}$ directly encodes per-point displacements between frames, serving as the practical counterpart of continuous velocity fields for learning temporally coherent 4D motion.

Scene flow offers key *advantages*: it resolves depth ambiguity in 2D tracking, ensures geometrically consistent 3D motion, and naturally handles topology changes [NMOG19]. Neural methods such as NeRFlow [DZY*21] couple flow and radiance fields for continuous spatiotemporal modeling, while Neural Scene Flow Fields [LNSW21] predict forward and backward flows to capture sharp motion boundaries and enable smooth interpolation.

However, scene flow methods have notable *limitations*: they are sensitive to occlusions and visibility constraints, leading to tracking failures [LYXZ22]. Highly deformable or low-texture scenes

exacerbate self-occlusion and reduce accuracy [DMY*24], while frame-wise processing struggles with topology changes and temporal inconsistency. Moreover, limited sensor visibility restricts motion estimation to observed surfaces, leaving discontinuities in the reconstructed motion field [LTT*21].

3.3.3. Integrating physical priors

Integrating physics into 2D tracking regularizes the ill-posed monocular reconstruction problem through *motion constraints and physical priors*. *Optical-flow-based methods* [WYG*24, GXC*24] combine flow and depth cues with physical motion models to enforce coherent spatio-temporal dynamics. *Deformation-based approaches* apply physics-inspired constraints including as-rigid-as-possible (ARAP) regularization [LWH*25] to preserve local rigidity. Meanwhile, *learning-based frameworks* [FZW*25, NMOG19] exploit 2D correspondences and monocular depth through reprojection or implicit dynamic modeling, achieving 4D reconstruction without explicit supervision.

Physics integration in 3D tracking depends on the *choice of 3D representation*. For *rigid-body/mesh models*, physics-based filters like [KSS24] embed differentiable simulators into Extended Kalman Filters (EKF) to track pose, velocity, and friction, while [PPN21] applies differentiable EKFs to simpler 1D sliding motion. *Gaussian/particle representations* couple dynamics with rendering: [LKL24] models scenes as moving 3D Gaussians with local rigidity constraints, [ZZL24] learns dynamics via Graph Neural Networks on sparse particles, and [XZQ*24] enriches Gaussians with Newtonian mechanics (strain, stress, inertia). For *extended object tracking*, [KO21] uses Gaussian processes to jointly infer shape and kinematics, while [BRD*24] employs object-centric Gaussian splatting to reconstruct and track dynamic objects from RGBD.

3.4. Hybrid Representation

While we have examined explicit motion representations that integrate motion into geometric structures, several approaches extend beyond this paradigm—either by leveraging multiple concurrent motion models or by adopting alternative formulations for motion representation. We discuss them below.

Joint representation Most real-world environments involve a blend of motion types—rigid, articulated, and non-rigid—whose coexistence gives rise to hybrid dynamics. The human body is a canonical example: an articulated skeleton undergoes global rigid motion, while soft tissue, loose garments, and hair introduce highly non-rigid variations [QCZ*23, JHBZ22]. Modeling such interplay requires a representation that enforces global structure yet retains flexibility for localized deviations.

A common strategy is to decompose motion into complementary components:

$$\mathbf{p}_t = \underbrace{\mathcal{T}_{\theta_1}(\mathbf{p}_{t-1}; \tau(t))}_{\text{coarse, e.g. rigid/articulated}} + \underbrace{\Delta_{\theta_2}(\mathbf{p}_{t-1}; \tau(t))}_{\text{fine, e.g. non-rigid residual}}. \quad (8)$$

Here, \mathcal{T}_{θ_1} denotes a structured, interpretable global motion model (e.g., rigid or articulated transformations), while Δ_{θ_2} is typically realized as a neural field that predicts residual displacements for local deformations. Beyond human and animal motion, this

paradigm has been extended to deformable objects with near-rigid parts and to multi-object scenes exhibiting heterogeneous dynamics [CYH*24, FKB*24]. Such hierarchical factorization offers several benefits: it preserves interpretability by isolating coarse transformations; simplifies learning by restricting the neural component to residuals; and enables explicit control over global motion while retaining the capacity to model fine-scale variations.

4D space-time 4D space-time methods represent dynamic scenes as unified spacetime volumes using explicit 4D primitives [DWD*24, YPZ*24], where motion is inherently encoded within the 3D representation itself, eliminating the need for deformation fields [KVN24]. Geometry, appearance, and motion are jointly modeled in a single neural field, allowing density, color, and opacity to evolve over time without explicit motion vectors. Formally,

$$I_o = \mathcal{R}_\theta(\mathbf{p}, \tau(g, t)) \quad (9)$$

where \mathcal{R}_θ is the rendering function, $\tau(g, t)$ captures geometric variations such as 4D Σ, σ in Gaussian Splatting or color density in NeRFs, and t denotes direct time input (e.g., frame index or learnable per-frame latents). The key design choice lies in modeling $\tau(g, t)$: feed-forward models [XLD*25, MCY*25] decode per-pixel 4D Gaussian vectors via DiT heads, while [DWD*24, YPZ*24] instead use 1D temporal Gaussians. NeRF-based approaches progress from MLPs to 4D neural voxels for faster rendering [PSJ*23, GXH*23]. In all cases, motion is implicitly embedded in the scene’s geometry and supervised purely from 2D images, making this paradigm computationally efficient and well-suited to recent feed-forward 4D generation models [MCY*25, XLD*25].

Per-frame modeling Per-frame 4D reconstruction methods treat each timestep as an independent or weakly coupled 3D reconstruction task [WZH*25], producing discrete per-frame 3D representations that are subsequently assembled into a 4D sequence. L4GM [RXM*24] generates frame-wise Gaussian representations from LGM [TCC*24] conditioned on predictions from previous timesteps, while point-based approaches [WZH*25, CCX*25a, ZHH*24] adopt Dust3R [WLC*24] independently for each frame to obtain 4D outputs. However, this frame-by-frame generation strategy typically necessitates interpolation or post-processing to enforce temporal smoothness. For example, [RXM*24] employs a video interpolation model [BRL*23] to refine renderings, and [CCX*25a] incorporates temporal attention modulation to enhance overall reconstruction fidelity.

4. Modeling Interaction

Thus far, we have focused on modeling the geometry and motion of 4D entities, in isolation. It is often necessary, however, to model the interactions between multiple 4D entities: between human and human, human and object, or object and object. Such interactions can be learned either from data priors [LHB*25] where knowledge of dynamics and causality is implicitly captured from large-scale observations, or from physical simulations [LKJ20] where interactions are explicitly governed by forces, materials, and physics-based rules. We refer readers to surveys dedicated to these two perspectives [ZMR*23, SGH*26, FHCD25]. In this section, we take

a complementary angle, surveying explicit interaction representations that describe the structure of interactions, independent of specific objects or scenes (Figure 5). We begin by surveying the overall representation strategies for entities involved in interactions. We then delve deeper into three aspects crucial in interaction: pose, contact, action and affordance. Finally, we examine strategies for integrating physical priors into interaction representations.

4.1. Representing Interaction Entities

Interaction occurs between multiple entities, each having its individual motion. Naturally, one could model an interaction I involving N entities as a collection of motion sequences

$$I = \{M_1, M_2, \dots, M_N\},$$

where each $M_i = \{\mathbf{x}_i^1, \mathbf{x}_i^2, \dots, \mathbf{x}_i^T\}$ is a sequence of states \mathbf{x}_i^t describing the motion of entity E_i over time steps $1 \dots T$. The representation choice of each entity depends on both its individual properties, as well as the property of the entire interaction. Humans are most commonly represented with skeletal poses or template meshes (Section 2.2.1), as these excel at modeling long motion sequences which are central to most interaction events. Given the complexity of interaction data, simpler representations are sometimes favored to make the problem tractable. To address the weaknesses of template meshes, a growing trend is to couple them with neural field based representations to obtain increased geometric fidelity [PSX*24, QLC*25] and more flexible, differentiable optimization of poses and contact objectives [OGK*25, WHZ*25, LYLW24, CPH*24]. For other objects, meshes (Section 2.1.1) are the popular choice due to having explicit surface representations, which enables more efficient modeling of contact and physics. Despite these advances, the assumption of object rigidity remains a major simplification. Extending to articulated objects brings more flexibility, but also introduces the need for a unified representation that captures part connectivity, motion patterns, and pose variations beyond fixed templates.

4.2. Pose

To accurately model interactions, it is crucial to precisely describe the poses of the interacting entities. The fundamental design choice is between storing poses in global coordinates, or storing relative poses. While single-entity methods often canonicalize poses by removing global position and orientation, recent interaction-focused works preserve global coordinates to maintain spatial relationships [XLY*24, BXP*22, LZL*24]. This preservation is essential because relative positions and orientations between entities *are* the interaction signal—canonicalizing to a single reference frame discards this critical information. Independent of coordinate choice, the rotation parametrization itself requires careful consideration. Most modern works adopt 6D continuous rotation [ZBL*19] instead of traditional representations (quaternions, axis-angle, Euler angles) to avoid discontinuities during neural network optimization. While global coordinates preserve spatial context, they create challenges: similar interactions at different world locations have completely different coordinate values. The solution is to store global poses but compute relative features for learning. Common relative features include inter-entity distances, relative orientations,

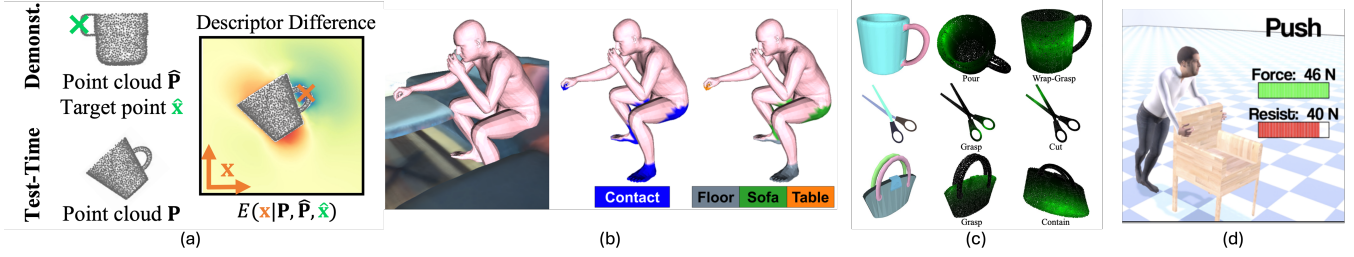


Figure 5: Interaction specific representations. (a) Parametrizing poses between interaction entities [SDT*22]; (b) Representing contacts [HGT*21]; (c) Representing affordances [DXW*21]; (d) Representing physical properties [ZBS*24].

and facing directions. Beyond these handcrafted features, learned representations like Neural Descriptor Fields [SDT*22] provide SE(3)-equivariant encodings that generalize across different global configurations, while maintaining relative spatial relationships. Hybrid representations [TCBT22] that combine global poses and relative features is an interesting direction in addressing the challenges for pose representation.

4.3. Contact

Interacting entities make contact with each other. Accurately representing contact can either be an end goal, or a means for more accurate interaction modeling. Explicit representations of contact, such as *contact maps* [BHKH19, BTT*20, TGBT20] and *neural distance fields*, have been shown to improve motion generation. [MHS*22] shows that predicting future contact maps enhances both local and global motion consistency. GanHand [CPA*20] refines contact modeling at finger and force levels to improve pose estimation. Neural distance fields (NDF) emerges as an auxiliary contact representation. NDF [KYZ*20, TAL*22, WHMM22, UFPC22, KRG*24] expands the single-frame local contact information into a spatially-dense field to guide motion generation. Grasping Fields [KYZ*20] encodes the distances to valid grasps, and PoseNDF [TAL*22] learns to encode full-body pose into the field. NIFTY [KRG*24] encodes the body pose gradient towards interacting frame into the fields. All these works demonstrate that explicit contact modeling improves generation. Most existing research, however, relies on SMPL or MANO, which are rigid representations and naturally induce penetration. Another future step might be to extend contact modeling beyond the visual domain to incorporate mechanical realism and force reasoning.

4.4. Action and Affordance

While geometry, poses and contact implicitly describe the type of actions, it is also common to explicitly model the affordances [Gib77] and actions, describing both possibility of interaction and the actual interaction events. Such actions and affordances are commonly represented with explicit [SCH*16] or neural implicit [SZKS19] graph structures. It is also common to directly add additional labels (e.g. "hook pull", "key press") either at object/part level [DTT*24] or as dense per point labels [DXW*21, XCW*22]. Motion/articulation annotations can be added for affordances that

involve movable parts. Instead of explicit labels, one could also adopt a field-based representation [WCJ*24, KRG*24] to support continuous queries. Other types of queries, such as motion parameters, force, etc. can also be integrated into such representations. With the emergence of foundation models, more works have opted to adopt open-vocabulary representations [LZX*24, QCB*24].

4.5. Ensuring Physical Plausibility

Physical plausibility is also fundamental for interaction related tasks. It is important to ensure plausible contact without floating and penetration, accurate object dynamics with respect to various forces, and valid interaction with the environment overall. A wide range of techniques have been adopted to ensure such physical plausibility. First, one could directly apply physics and interaction aware losses during training and optimization [CPA*20, JLWW21, GTT*21, YZL*21, TWH*22, XZY*24]. Metrics include foot sliding, average and maximum penetration depth or volume, hand-to-object distance, contact IoU and normal alignment, etc. It is also possible to perform physics simulation and contact-based optimization, and incorporate them through post-processing [ZWZ*22], correction steps [YSI*23, XLWG23], learnable surrogates [WML23], or combination with reinforcement learning [CKA*22, HGW*23]. Another line of work directly injects physics-aware encoding into the network structure, encoding physical properties like force, resistance and contact [ZBS*24].

5. Datasets and Benchmarks

Unlike other computer vision tasks with abundant labeled data, 4D representation learning faces a data scarcity problem. Ideal datasets would contain real-world dynamic scenes with complete ground-truth geometry, appearance, motion and interaction annotations. However, such datasets remain limited due to technical and economic challenges in capturing high-quality spatio-temporal data. To address this, the current 4D field leverages a mixture of datasets ranging from 2D to 4D dimensions to guide 4D representation learning (Figure 6). This section surveys the current dataset in use from the perspective of learning geometry, motion and interactions.

5.1. Geometry Datasets

Geometric learning in 4D works primarily leverages two data paradigms: static 3D object datasets for feed-forward reconstruc-

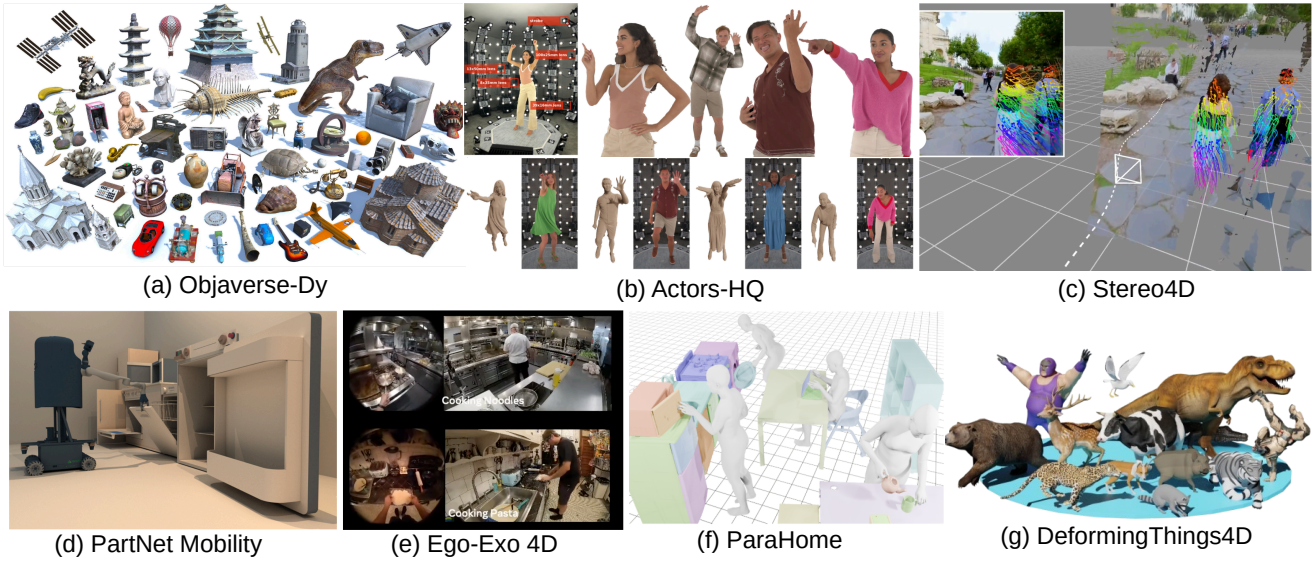


Figure 6: Overview of key datasets in 4D representation research: (a) *Objaverse-Dy* [YXV*25] provides a large-scale collection of synthetic animated 3D assets, serving as the primary source for current 4D generation works after filtering; (b) *Actors-HQ* [IRG*23] is a high-fidelity, multi-view human performance capture dataset with per-frame 3D mesh reconstructions for dynamic human motion; (c) *Stereo4D* [JTL*24] represents emerging large-scale datasets capturing native 4D data from real-world scenarios; (d) *PartNet-Mobility* [XQM*20] offers an articulated object database that facilitates part-based representation and articulated motion learning; (e) *Ego-Exo4D* [GWT*24] is a multi-camera synchronized video corpus capturing first-person (egocentric) and third-person (exocentric) views of skilled human activities; (f) *Parahome* [KKNJ25] is a dataset capturing 3D human–object interaction in a natural home environment, and (g) *DeformingThings4D* [LTT*21] is a large-scale synthetic dataset of non-rigidly deforming 3D objects (humanoids and animals) with dense 4D annotations.

tion and large-scale 2D image collections for score-distillation-based generation.

Static 3D Object Datasets. Modern 4D generation systems [CZTW25, SLY*25] employ feed-forward 3D generation models [XLX*25, LZL*25, ZLL*25] to first synthesize static geometry, then animate it through video guidance or rigging techniques. These feed-forward models are enabled by large-scale 3D object collections. Primary datasets in early time include ShapeNet [CFG*15] (51K objects) and ModelNet [WSK*15] (12K objects), while the more recent Objaverse-XL [DLW*23] dramatically scales to 10+ million models, becoming one of the most widely adopted datasets in current research. However, Objaverse exhibits significant quality variance, leading researchers to create high-quality filtered subsets [XLX*25, ZWZ*24]. Other smaller high-quality 3D collections, including ABO [CGD*22], 3D-Future [FJG*21], OmniObject3D [WZF*23], Toy4K [STR21], HSSD [KMJ*24], and GSO [DFK*22] are commonly used as training set additives or benchmark datasets. These datasets provide native supervision for high-quality 3D reconstruction.

Large-Scale 2D Image Collections. Score distillation sampling (SDS) based 4D generation [BSR*24, LKT*24, SSP*23] leverages foundational image diffusion models to generate 2D supervision for 3D scene reconstruction through volumetric rendering. The generalizability of this paradigm—enabling arbitrary 4D scene generation from text prompts—is inherited from web-scale training on LAION-5B [SBV*22] (5.85 billion image-text pairs). However, standard image diffusion models lack 3D awareness, causing multi-

face artifacts (the Janus problem [ASS*23]). To address this, multi-view diffusion models [SWY*24, LWVH*23, SCZ*23, LLZ*23] are fine-tuned using rendered multi-view images from filtered Objaverse objects, significantly improving geometric reconstruction quality in 4D pipelines through enhanced multi-view consistency.

5.2. Motion Datasets

Temporal dynamics learning in 4D generation relies on four primary data sources: large-scale video collections for learning general motion patterns, specialized multi-view captures for high-fidelity scene dynamics, parametric motion libraries that provide explicit temporal supervision and deformable object collections for native non-rigid motion learning.

Large-Scale Video Collections. Video diffusion models serve as key components for guiding motion synthesis in 4D works [LZZ*24, LZRV24b, VNZ25, JYC*24]. Unlike images that capture only static geometry, videos encode both geometric structure and temporal dynamics. WebVid-10M [BNV21] and HD-VILA-100M [XHZ*22] represent two prominent large-scale video datasets that enable training models like Align Your Latents [BRL*23] and Make-a-Video [SPH*23]. These foundational video diffusion models have been successfully adapted for 4D generation [SSP*23, LKT*24]. Following strategies used to enhance image diffusion models, recent work finetunes video diffusion models [XYV*24, YXV*25, WYWB25, LYX*24a] on filtered dynamic objects from Objaverse, significantly improving

multiview motion consistency. The primary advantage of video diffusion models lies in their generalizability from large-scale training data, enabling motion synthesis across diverse applications. However, 2D video supervision prioritizes frame-level visual realism over 3D geometric constraints, often producing sequences that appear locally plausible but violate physical continuity when reconstructed as coherent 3D trajectories.

Specialized Multi-View Captures. Domain-specific datasets provide high-fidelity temporal ground truth through controlled multi-view recording systems. For human motion, representative datasets include ZJU-MoCap [PZX*21], DynaCap [HLX*21], ActorHQ [IRG*23], and Human3.6M [IPOS13]. For general dynamic scenes, D-NeRF [PCPMMN21], Nerfies [PSB*21], HyperNerf [PSH*21], and Plenoptic Video [LSZ*22] capture real-world deformations with varying complexity. These datasets preserve authentic physical dynamics and provide strong multi-view supervision for consistent 3D motion reconstruction. However, limited scale—typically dozens to hundreds of sequences compared to millions in large-scale video collections—and substantial capture infrastructure requirements constrain their broader applicability.

Animated Motion Libraries. Synthetic motion captures offer perfect ground truth with structural priors for controllable animation. AMASS [MGT*19] consolidates over 40 hours of motion capture from 15 datasets into unified SMPL [LMR*15] parametric representations for human motion synthesis. Mixamo [Ado15] provides thousands of professionally rigged character animations, while Truebones Zoo [Tru] extends coverage to 75+ non-humanoid creatures. For animated objects, curated Objaverse subsets [LYX*24a, XYV*24, LZRV24b, LZZ*24] provide hundreds of thousands of animated assets filtered by motion quality and temporal coherence. Articulation-XL [XLX*25] provides 48K+ models featuring automated skeleton quality assessment via Vision-Language Models. These synthetic collections enable large-scale training with explicit motion annotations, though they exhibit domain gaps and simplified physics compared to real-world capture, particularly for complex interactions and environmental effects.

Deformable Object Collections provide ground truth for non-rigid motion learning. DeformingThings4D [LTT*21] contains 1,972 synthetic animation sequences spanning 31 categories (humanoids and animals) with dense 4D annotations including signed distance fields, volumetric motion fields, and scene flow at multiple hierarchical resolutions. The most recent effort, Stereo4D [JTL*24] offers 100K+ real-world clips mined from Internet VR180 videos, providing pseudo-metric 3D point clouds with long-range world-space trajectories derived through careful fusion of stereo depth estimation, 2D tracking, and structure-from-motion. These datasets address the scarcity of real-world 4D supervision—DeformingThings4D through high-quality synthetic rendering and Stereo4D through scalable data collection.

5.3. Interaction Dataset

Interaction-focused datasets capture relationships between objects, humans, and environments through three approaches: articulated object collections that encode structural priors, human-object interaction datasets capturing co-evolving dynamics, and multi-entity scenarios modeling complex relational behaviors.

Articulated Object Collections. Structured representations of articulated objects provide functional-aware supervision for controllable 4D generation. Available datasets span multiple sources: synthetic object-centric collections include PartNet-Mobility [XQM*20] and its successors ACD [IJZ*24] and Phys-X 3D [CCPL25]; real-world scans include object-centric AKB-48 [LXF*22] and scene-level Multi-Scan [MZJ*22] with articulatable components; and GPartNet [GXZ*23] combines both synthetic and real sources. These datasets provide kinematic constraints and structural annotations essential for physically plausible 4D animation, though coverage remains limited to specific object categories with explicit articulation mechanisms.

Human-Object Interaction. HOI datasets capture the coupled dynamics between humans and manipulated objects during interaction sequences, spanning multiple levels of granularity. At the finest level, hand-object interaction datasets including DexYCB [CYX*21], ARCTIC [FTT*23], OAKINK2 [ZY*24], and TACO [LYS*24] capture single-hand or bi-manual grasping and manipulation with rigid objects, while Obman [HVT*19] provides synthetic data pairing MANO [RTB17] hand models with ShapeNet [CFG*15] objects. Whole-body interaction datasets extend this scope, with CIRCLE [ALV*23] capturing reaching motions in virtual home environments, COUCH [ZBS*22] and CHAIRS [JLC*23] focusing on sitting-based furniture interactions, and GRAB [TGBT20], BEHAVE [BXP*22], and OMOMO [LWL23] providing diverse activities such as grasping, carrying, and moving household objects. At the broadest level, Human-Scene Interaction (HSI) datasets such as ParaHome [KKNJ25], SAMP [HCV*21], TRUMANS [JZL*24], and HUMANISE [WCL*22] incorporate environmental navigation by capturing humans moving through spaces while interacting with multiple scene objects. These datasets enable learning of contact-rich interactions and object affordances, though capture complexity and annotation requirements limit dataset scale and diversity. Given the breadth of this field, the datasets presented here are not exhaustive; we refer readers to [ZMR*23] for a comprehensive discussion of HOI datasets.

Multi-Entity Scenarios. Large-scale datasets capturing multiple interacting entities provide supervision for complex relational dynamics. Egocentric datasets like Ego4D [GWB*22] and Ego-Exo4D [GWT*24] capture first-person interaction perspectives during daily activities with synchronized multi-view data. Autonomous driving datasets including Waymo [SKD*20, ECC*21] and nuScenes [CBL*20] provide dense spatio-temporal supervision for multi-agent urban scenarios with point clouds and 3D trajectories. Social interaction datasets such as CMU Panoptic [JSL*17] and CHI3D [FZO*20] focus on multi-person scenarios. These datasets enable learning of relational behaviors and spatial reasoning, though their domain-specific focus limits direct transfer to general 4D generation tasks.

5.4. Benchmarks and Evaluation Metrics

4D evaluation requires assessment across geometric fidelity, temporal consistency, and semantic alignment, progressing from reconstruction-centric evaluation with clear ground truth to generation-centric assessment emphasizing perceptual quality.

Specialized Benchmarks. Recent benchmarks target specific 4D challenges: WideRange4D [YZT*25] focuses on wide-range spatial object movements in synthetic scenes, Inter3D [CHY*25] benchmarks human-interactable 3D object reconstruction, SEED4D [KGB*25] provides annotated driving videos with synchronized ego-exo captures for autonomous driving tasks; InterAct [XLZ*25] provides 22 hours of HOI data for 6 HOI task benchmarks; 4D-Bench [ZLZ*25] benchmarks MLLM understanding on 4D by assessing captioning abilities. Despite progress, unified benchmarks for core generation tasks (text-to-4D, image-to-4D, dynamic NeRF reconstruction) remain absent. Current practice relies on small-scale datasets like Consistent4D [JZG*24] and D-NeRF [PCPMMN21] without standardized protocols.

Quantitative Metrics. Evaluation metrics span multiple objectives. *Appearance fidelity* uses PSNR and SSIM for pixel-level correspondence, complemented by perceptually-aligned LPIPS [ZIE*18] that better correlates with human judgments. *Temporal consistency* employs Fréchet Video Distance (FVD) on 4D video renders [JZG*24, ZJZ*24], STREAM [KKY24] for disentangled evaluation of temporal coherence, visual fidelity, and diversity without length constraints, and VBench [HHY*24] providing comprehensive assessment across 16 dimensions, including subject consistency and motion smoothness. *Semantic alignment* measures input-output consistency through CLIP-score [RKH*21] for text-to-image tasks and R-Precision for text-to-motion alignment via retrieval accuracy. *Geometric integrity* employs Chamfer Distance for bidirectional point cloud similarity, Earth Mover’s Distance (EMD) [RTG98] for optimal transport cost between point distributions, 3D IoU for volumetric overlap, Hausdorff Distance for maximum deviation, and physics-based constraints for interaction validity [LHB*25]. *Human evaluation* complements automated metrics, assessing faithfulness, aesthetic quality, and physical plausibility through structured user studies [NCOZMA25, ZYW*24].

Current Limitations. Contemporary 4D evaluation faces fundamental challenges. *Geometric functionality assessment* remains inadequate, with metrics emphasizing shape alignment while overlooking functional correctness, structural balance, and design complexity. *Long-duration motion evaluation* lacks appropriate protocols, as temporal metrics assess only short sequences (<32 frames) without extended temporal consistency evaluation. *Unified benchmark scarcity* limits systematic progress assessment—the field lacks comprehensive benchmarks encompassing diverse object categories, motion types, and conditioning modalities comparable to ImageNet [DDS*09] on 2D tasks. *Perceptual alignment gaps* between quantitative scores and human perception necessitate heavy reliance on manual evaluation, motivating efforts toward automated perception-aligned metrics [WZM*24]. Addressing these requires functionally-aware metrics, extended temporal assessment, comprehensive benchmarks, and improved perceptual alignment.

6. Training Strategy

The training strategies employed in 4D tasks reflect fundamental trade-offs between generalization, fidelity, and efficiency. For single-entity geometry and motion modeling, these strategies fall into three categories: per-scene optimization (Section 6.1), feed-forward models (Section 6.2), and hybrid approaches that combine

both (Section 6.3). Training interaction models, however, introduces distinct challenges, namely coordinating multi-entity dynamics under physical constraints, that warrant separate treatment (Section 6.4). Building upon the geometric representations (Section 2) and motion modeling approaches (Section 3) discussed above, we provide a comprehensive taxonomy of selected papers organized by these dimensions in Table 1.

6.1. Per-Scene Optimization

Per-scene optimization treats each dynamic scene as an independent problem, directly optimizing model parameters (geometry, appearance, motion fields) from input observations without large-scale pre-training. This approach delivers high fidelity by dedicating computational resources to scene-specific refinement, operates without 4D training data by leveraging pre-trained 2D/video diffusion models [SSP*23, ZJZ*24], and supports flexible scene-specific constraints with interpretable representations [ZLN*24, WYG*24].

Below, we discuss some of the popular strategies used in per-scene optimization for both 4D generation and reconstruction tasks.

6.1.1. Data-driven Priors

Foundation model priors provide implicit knowledge from large-scale datasets as substitutes for scarce 4D supervision. Multimodal diffusion priors address complementary quality aspects: image diffusion [RBL*22] for appearance detail, 3D-aware image diffusion [SCZ*23, LGL*23] for spatial consistency, video diffusion [BDK*23, SPH*23, GYR*23] for temporal dynamics, and multi-view diffusion [SWY*24, LLZ*23] for 360° consistency. 4D-fy [BSR*24] alternates supervision across all three types, achieving 67% user preference over MAV3D [SSP*23]. Recent work utilizes MLLMs/VLMs for 4D generation [ZL25] and LLM reasoning for object composition [XLB*24].

Auxiliary priors such as depth offer geometric cues, optical flow offers motion cues, and semantic priors enforce region- or part-level consistency across time, thus stabilizing optimization, improving spatial-temporal coherence, and enhancing both geometric fidelity and perceptual realism in 4D tasks. Depth supervision improves joint learning of radiance and motion fields [CFF*22, WKS*22], particularly in outdoor scenes [WLL*23, TLH*24, YCW*23]. Monocular depth estimation [RLH*20, YKH*24] provides geometric cues despite scale ambiguity [WYG*24, LLW*25]. Optical flow models [XZC*23] supply dense inter-frame correspondences [YVN*22, LCM*22], while visual foundation models like DINO [ODM*24] deliver semantic features consistent across views and time [YJB*23, WLJ*23]. SA4D [JWF*24] lifts SAM [KMR*23]-style 2D masks into 4D Gaussian representations by learning a temporal identity feature field. In dynamic scenes, object-level semantic segmentation provides valuable silhouettes or foreground masks that help localize dynamic objects and decompose scenes into static backgrounds and dynamic foregrounds [YLL23, LGXC24]. For object articulation [GXL*25], instead of using foundational model priors, it uses physics-based optimization [IMH05] to learn motion parameters.

Table 1: A summary of representative methods in 4D representations organized by underlying geometry type. Each method is characterized by its geometry, motion type, input condition, and training strategy. Motion types: Articulation (ART), Deformation Field (DF), Tracking (TRK), Space-Time (ST) and Per-frame (PF).

Methods	Geometry	Motion	Input Condition	Training Strategy
TextMesh4D [DSW*25]	Mesh	DF	Text	Per-scene
V2M4 [CZTW25]	Mesh	DF	Video	Per-scene
Puppeteer [SLY*25]	Mesh	ART	Text/Mesh	Per-scene
AnimateAnyMesh [WYWB25]	Mesh	DF	Mesh	Feed-forward
MagicArticulate [SZL*25]	Mesh	ART	Mesh	Feed-forward
DreamMesh4D [LCL24]	Mesh+Gaussian primitive	DF	Video	Per-scene
RigAnything [LXY*25]	Mesh	ART	Text+Mesh	Feed-forward
NeuralPCI [ZWL*23]	Point Cloud	DF	Point Cloud	Per-scene
Cut3R [WZH*25]	Point Cloud	PF	Image	Feed-forward
Monst3R [ZHH*24]	Point Cloud	TRK	Image	Feed-forward
St4RTrack [FZW*25]	Point cloud	TRK	Video	Feed-forward
PAPR-In-Motion [PZL24]	Point cloud	DF	Image	Per-scene
RPMNet [YHY*20]	Point cloud	DF	Point Cloud	Feed-forward
MAV3D [SSP*23]	NeRF	DF	Text	Per-scene
4D-fy [BSR*24]	NeRF	DF	Text	Per-scene
Consistent4D [JZG*24]	NeRF	DF	Video	Per-scene
SV4D [XYV*24]	NeRF	DF	Video	Hybrid
Dream-in-4D [ZLN*24]	NeRF	DF	Text/Image	Per-scene
Animate124 [ZYX*23]	NeRF	DF	Text+Image	Per-scene
4Diffusion [ZCW*24]	NeRF	DF	Video	Hybrid
V4D [GXH*23]	NeRF	ST/DF	Video	Per-Scene
TempInt [PSJ*23]	NeRF	ST/DF	Video	Per-Scene
4DGen [YXW*23]	Gaussian primitive	DF	Video	Per-scene
4D-Rotor [DWD*24]	Gaussian primitive	ST	Video	Per-scene
4D-GS [WYF*24]	Gaussian Primitive	ST/DF	Video	Per-scene
Dynamic 3DGS [LKL24]	Gaussian Primitive	ST/TRK	Video	Per-scene
CAT4D [WGP*25]	Gaussian primitive	DF	Video	Hybrid
DG4D [RPT*23]	Gaussian primitive	DF	Image	Per-scene
4D-LRM [MCY*25]	Gaussian primitive	ST	Few-Image	Feed-forward
L4GM [RXM*24]	Gaussian primitive	PF	Video	Feed-forward
STAG4D [ZJZ*24]	Gaussian primitive	DF	Text/Video	Per-scene
GenXD [ZLL*24]	Gaussian primitive	DF	Image	Hybrid
Mosca [LWH*25]	Gaussian primitive	TRK	Video	Per-scene
Gaussian Marbles [SHU*24]	Gaussian primitive	TRK	Video	Per-scene
In-2-4D [NCOZMA25]	Gaussian primitive	DF	Few Image	Per-scene
Free4D [LHC*25]	Gaussian primitive	DF	Text+Image	Per-scene
EG4D [SGW*24]	Gaussian primitive	DF	Image	Per-scene
MVTokenFlow [HLZ*25]	Gaussian primitive	TRK	Video	Per-scene
4Real [YWZ*24]	Gaussian primitive	DF	Text+Video	Per-scene
SC4D [WYJ*24]	Gaussian primitive	DF	Video	Per-scene
PhysAvatar [ZZY*24]	Template/Mesh	ART/DF	Video+Mesh	Per-scene
AvatarGO [CPH*24]	Template/Gaussian primitive	ART/DF	Text	Per-scene
TADA [LYX*24b]	Template	ART/DF	Text	Per-scene
ANYTOP [GRT*25]	Template	ART	Skeleton	Feed-forward
Human3R [CCX*25b]	Template/Point Cloud	ART	Video	Feed-forward
MVP4D [TZT*25]	Template/Gaussian Primitive	ART	Image	Hybrid
Avatar Artist [LWW*25]	Template/Mesh	DF	Image	Feed-forward
Disco4D [PLC*25]	Template/Gaussian Primitive	ART/DF	Image	Per-scene
CAP4D [TZTL25]	Template/Gaussian Primitives	ART	Image	Feed-forward
Vid2Avatar [GJC*23]	Template/NeRF	ART/DF	Video	Per-scene
Paris [LMS23]	Part/NeRF	ART	Image	Per-scene
ArticulatedGS [GXL*25]	Part/Gaussian primitive	ART	Image	Per-scene
ArtGS [LJL*25]	Part/Gaussian primitive	ART	Image	Per-scene
SP4D [ZYD*25]	Part/Mesh	ART	Video	Hybrid
ArticulateAnyMesh [QYW*25]	Part/Mesh	ART	Mesh	Per-scene
SINGAPO [LIC*25]	Part/Graph/Mesh	ART	Image	Feed-forward
GeoPard [GPA*25]	Part/Point Cloud	ART/DF	Point Cloud	Feed-forward
MeshArt [GSLD25]	Part/Mesh	ART	Mesh	Feed-forward
3DSG [RGA*20]	Graph	Scene Graph	Video	Per-scene
4D-PSG [YCP*23]	Graph	Scene Graph	Point Cloud	Per-scene
PSG-4D-LLM [WFY*25]	Graph	Scene Graph	Video	Feed-forward

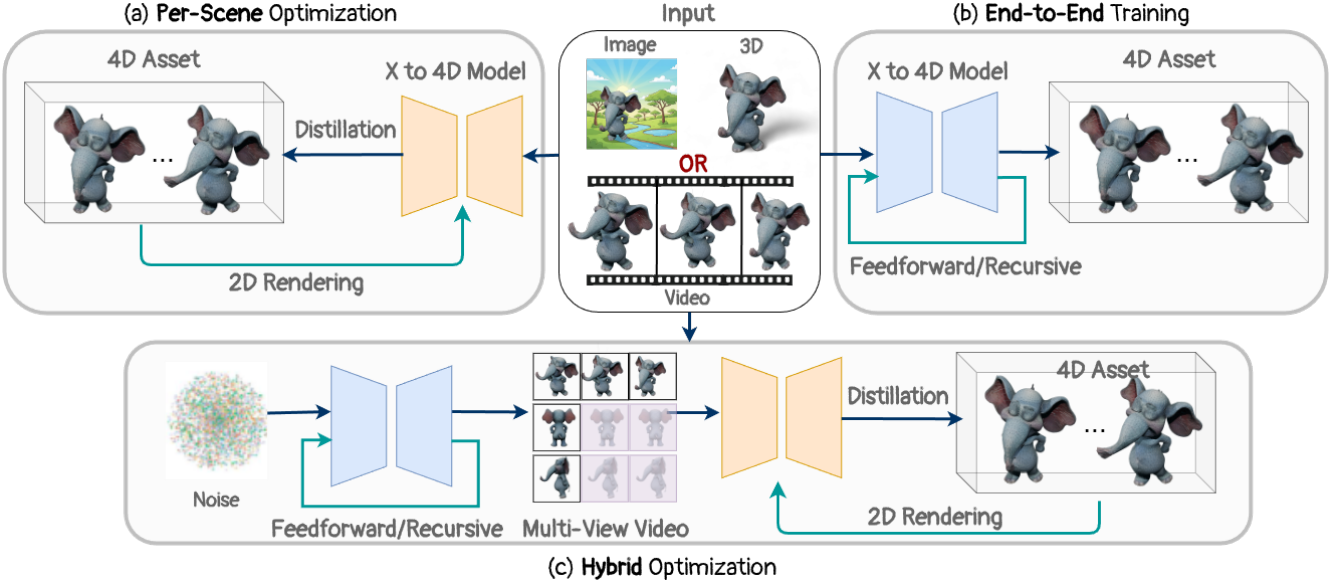


Figure 7: Overview of three main training paradigms for 4D generation: (a) Per-scene optimization treats each scene as an individual optimization problem, leveraging information distilled from large foundation models (e.g., image and video diffusion models via score distillation sampling) to optimize a 4D representation; (b) End-to-end training employs feed-forward models trained on large-scale native 4D assets to learn strong data priors; (c) Hybrid optimization combines both approaches by training a customized feed-forward multi-view video generator, then using the generated videos to optimize individual scenes.

6.1.2. Design Choices

Converting 2D or textual inputs into 3D (and subsequently 4D) structure depends heavily on how the input modality is encoded and lifted. Here we discuss some of the design choices that have influenced 4D literature in the realm of per-scene optimization.

3D lifting models differ in how they convert 2D/textual inputs into 3D structure. Multi-view generation approaches like Zero-1-to-3 [LWVH*23] and MVDream [SWY*24] for objects, as well as ViewCrafter [YXY*24] and SEVA [ZGV*25] for scenes, synthesize novel views and reconstruct structure through NeRF or Gaussian Splatting. This has recently been improved by multi-view video generators [VYB*24] for better geometry quality. Direct feed-forward methods [XLX*25, TCC*24, JN23] infer 3D structure from single images via learned mappings. Multi-view synthesis ensures stronger geometric consistency; feed-forward prediction offers faster, generalizable inference at reduced fidelity cost.

Disentanglement methods decouple static and dynamic components for easier optimization. Two-stage approaches dominate: Consistent4D [JZG*24], STAG4D [ZJZ*24], and 4D-fy [BSR*24] optimize static 3D assets before adding motion through deformation learning. MAV3D [SSP*23] uses three stages: static, dynamic, and super-resolution.

Deformation fields model motion patterns using MLPs [BKY*24, HSY*24, LKLR24], spatial-temporal planes [DMY*24, LDZ*24, WYF*24], polynomial functions [LCLX24], Fourier series [KVN24], or combinations [LDZY24]. These methods directly learn motion patterns from independent time inputs, neglecting cross-time relationships. Recent work [JKZ*24] adaptively learns temporal relationships

via transformer attention. Most methods optimize deformation frame-by-frame from multi-view videos [YXV*25, ZJZ*24], while articulation-based methods [LJL*25, GXL*25] estimate motion from heuristics or input geometry.

6.1.3. Optimization Objectives

Score Distillation Sampling (SDS) distills prior knowledge for 4D generation. Originating with DreamFusion [PBJM22], SDS iteratively optimizes representations by rendering views, adding noise, denoising with diffusion models, and computing gradients:

$$\nabla_{\theta} L_{\text{SDS}} = \mathbb{E}_{t, \epsilon} [w(t) (\epsilon_{\phi}(x_t, t, c) - \epsilon) \nabla_{\theta} x_t] \quad (10)$$

This distills 2D priors into 3D/4D space without 3D training data [AKS24, PBJM22], typically driving deformation fields from generated multi-view videos [BSR*25, ZJZ*24].

Reconstruction loss provides direct supervision when reference views exist. Shape of Motion [WYG*24] optimizes photometric consistency between rendered and captured views, depth supervision from monocular depth priors, and 2D tracking consistency with long-range point tracks. The photometric reconstruction loss is implemented as L2 distance between the generated/reconstructed source view with the target view as follows:

$$\mathcal{L}_{\text{rec}} = \frac{1}{\mathcal{T}} \sum_{\tau=1}^{\mathcal{T}} \|f(\tau, o_{\text{Ref}}) - I_{\text{Ref}}^{\tau}\|_2^2, \quad (11)$$

where \mathcal{T} is the frame count, $f(\cdot)$ is the rendering function and o_{Ref} is the reference camera. For object centric scenes [JZG*24], a separate foreground mask loss [WYG*24, ZJZ*24] is also estimated. These reconstruction losses complement or replace SDS

when ground truth video supervision is available. These losses primarily enhance per-frame appearance and reduce floating artifacts.

Regularization losses ensure physical plausibility. Temporal and spatial smoothness use Total Variation loss [LSS*19, FKMW*23, HWZ*24] and Laplacian regularization [HLX*21]. Structural integrity is preserved via As-Rigid-As-Possible constraints [IMH05], isometric loss, and divergence loss. ArtGS [LJL*25] uses Chamfer distance for geometry preservation during articulation.

6.1.4. Open Challenges

Optimization-based 4D methods achieve high visual fidelity, but remain impractical for large-scale use due to computational expense, instability, and slow convergence, limiting scalability and motion complexity in real-world applications. Key limitations include:

Compute cost. These methods are extremely time-consuming, with [ZJZ*24] and [JZG*24] requiring around 2 hours per scene and [SSP*23] or [BSR*24] taking several to 10+ hours. This makes them 10–1000x slower than feed-forward models, preventing real-time or interactive use. They also demand high-end GPUs like V100/A100 and large memory budgets (at least 24 GB GPU RAM), posing significant hardware barriers.

Scalability. Each scene must be optimized independently, eliminating the possibility of batch or parallel generation. Such slow, scene-specific pipelines are impractical for large-scale or commercial deployment, where generating hundreds of 4D assets for gaming, film, or AR/VR would be prohibitively costly. Moreover, learned representations do not generalize across scenes.

Limited motion complexity. Current pipelines perform well for simple, object-scale motions but fail to capture large, scene-level dynamics, non-rigid deformations, or topological changes. Realistic physics is rarely enforced, and long-range motion across extended sequences remains unsolved. Modeling the appearance or disappearance of objects over time remains particularly challenging for continuous representations.

6.2. End-to-End Training

Feed-forward models learn global mappings from 2D observations to 4D representations using large pre-trained networks. Once trained, these models infer novel scenes in single forward passes, enabling real-time generation (e.g., L4GM [RXM*24] at 0.3s, 4DGT [XLD*25] at 25 ms/frame) and cross-dataset scalability with learned spatiotemporal priors that handle ambiguity and sparse views, and provide deterministic inference with stable quality and fixed runtime regardless of scene complexity.

6.2.1. Data-driven Priors

Motion priors. Some methods leverage video diffusion models for joint motion-appearance learning. 4DNeX [CLZ*25] integrates RGB and 3D sequences using DiT architectures. Geo4D [JZL*25] extends image-to-video diffusion to output explicit geometry with point maps. Other works, such as AnimateAnyMesh [WYWB25] and Motion 3-to-4 [CCZ*26] directly learn motion prior from large animated 3D assets.

Geometry priors. Large 3D backbones are widely adopted to anchor geometry priors: L4GM builds on LGM [TCC*24], 4D-LRM [MCY*25] extends LRM [HZG*23], and Forge4D [HHC*25] adopts VGGT. MonST3R [ZHH*24] and Geo4D [JZL*25] employ DUS3R encoders. Human-object interaction methods [WHZ*25, LSCK23, LSN*24] anchor on pre-defined template geometries [PCG*19, RTB17]. Together, these priors transfer pre-trained 3D spatial understanding to dynamic 4D tasks, achieving high-quality results with minimal 4D supervision.

6.2.2. Design Choices

The fundamental design of a 4D model is defined by how it represents 3D space and captures the evolution of that space over time.

3D lifting models. Most recent works adopt 3D Gaussian Splatting (3DGS) [KKLD23] for its balance of realism, efficiency, and differentiability. Two main extensions adapt it to 4D:

Unified 4D Representations: Methods like 4DGT [XLD*25] embed temporal attributes (e.g., velocity, lifespan) directly into each Gaussian, while 4D-LRM [MCY*25] models space-time jointly via anisotropic 4D Gaussians for fast reconstruction.

Sequential or Deformable Fields: Other approaches construct sequential 3DGS scenes linked by interpolation [RXM*24], continuous flow [LXZ*24] or conditioned on timestamps [LRM*24]. Beyond GS, [WYWB25, CCZ*26] handle mesh animations through vertex displacement maps. Overall, current trends favor explicit, geometry-aware, and temporally coherent 3D lifting frameworks that unify appearance and motion in a feed-forward manner.

Motion models have evolved beyond simple interpolation. Explicit motion prediction methods [LLP*25, HHC*25] use transformer heads to predict dense 3D motion fields or per-pixel displacements. Temporal transformers [RXM*24] incorporate attention for cross-frame dependencies, enabling implicit learning of complex interactions—a popular choice in human-object interaction [LSN*24, XSW*23], recently replaced by diffusion methods [RTSB25, SZL*24]. Together, these paradigms transition from per-frame fitting, in-between bridging to learned feed-forward representations, improving temporal continuity and scalability.

6.2.3. Optimization Objectives

Reconstruction losses optimize photometric consistency using MSE/L1, SSIM, and LPIPS for perceptual sharpness [RXM*24, MCY*25]. Extensions include segmentation-aware L1 [LXZ*24] for static-dynamic decoupling. These losses ensure visual accuracy and serve as universal reconstruction anchors across Gaussian, mesh, and diffusion systems.

Diffusion-based losses minimize noise prediction errors in latent video space [CLZ*25, JZL*25], predicting ϵ conditioned on frames or camera embeddings. AnimateAnyMesh [WYWB25] adopts flow-matching objectives for continuous-time supervision. These losses align generated sequences with learned diffusion manifolds, ensuring smooth motion and appearance trajectories.

Geometry losses ensure metric realism. 4DGT [XLD*25] uses depth [YKH*24] and normal [YQG*24] supervision. DrivinRecon [LXZ*24] employs a DepthNet for depth integration.

MonST3R [ZHH*24] imposes pointmap alignment and flow-projection consistency, while Geo4D [JZL*25] merges multiple geometric terms. Interaction methods [LSN*24, RTSB25, XLWG23] employ physics-based losses to penalize interpenetration, enforce contact constraints, and regularize trajectories.

6.2.4. Open Challenges

End-to-end training enables joint learning of geometry, appearance, and motion within a unified framework but introduces limitations in data requirements, generalizability, and architectural flexibility. We discuss some of the drawbacks below:

Training data. Feed-forward models require massive-scale 4D data that is costly to acquire. Existing methods [XLD*25, RXM*24, MCY*25, CLZ*25] train on mixed 3D datasets [ZTF*18, DLW*23] or limited explicit 4D datasets [GWT*24, JTL*24]. L4GM [RXM*24] requires 12M synthetic videos (300M frames), while 4DGT [XLD*25] uses 5K real-world videos. Training demands days on 64–128 GPUs with complex multi-stage optimization, making academic-scale training infeasible due to computational and storage costs.

Limited generalizability. Models trained on narrow distributions struggle beyond training conditions. L4GM [RXM*24] assumes fixed camera elevation and fails on egocentric or occluded motion; 4DGT [XLD*25] performs poorly on new camera types; 4DNeX [CLZ*25] degrades under occlusion or lighting changes. Domain shift from synthetic to real scenes remains critical—models trained on Objaverse-Dy [YXV*25] fail to generalize to real-world scenarios, limiting practical applicability.

Lack of flexibility. Fixed architectural designs limit adaptability. L4GM [RXM*24] directly predicts Gaussian splats, tightly coupling the network to this representation—switching to meshes or implicit fields requires full retraining. Similarly, 4DGT [XLD*25] and St4RTrack [FZW*25] hard-code 4D Gaussians or pointmap assumptions. This contrasts with per-scene optimization frameworks that can swap representations or regularizations without retraining, offering greater experimental flexibility.

6.3. Hybrid Optimization

Hybrid methods combine the strengths of the two extremes. Typically, a feed-forward backbone provides a strong initialization or prior, which is then refined through scene-specific optimization. This two-stage paradigm balances reconstruction quality and inference speed—leveraging global priors for generalization and local optimization for fidelity.

Two-stage paradigm. A distinct family of 4D methods adopts a *two-stage design*: Stage 1 performs feed-forward multi-view or video generation, while Stage 2 refines or reconstructs explicit 4D geometry. This combines the scalability of diffusion-based appearance synthesis with the precision of geometric optimization. CAT4D [WGP*25] first generates view-consistent videos using a multi-view diffusion model (CAT3D + Lumiere), then reconstructs 4D motion via deformable Gaussian splatting. SV4D [XYV*24] and SV4D 2.0 [YXV*25] similarly use Stable Video Diffusion for multi-view synthesis followed by dynamic NeRF optimization. Splat4D [YCPH25] predicts coarse 3D Gaussians before

refining temporal coherence with DynamiCrafter, while DreamArt [LLT*25] synthesizes articulated motion via video diffusion and reconstructs textured meshes through dual-quaternion optimization. Overall, this two-stage *feed-forward + optimization* framework balances generative realism and geometric consistency, yielding high-fidelity and temporally stable 4D reconstructions.

SDS-Free optimization. A notable trend in hybrid 4D methods is the shift away from score distillation sampling (SDS) to direct photometric, geometric, and temporal supervision—enabling Stage 2 optimization to remain lightweight and fast. This trend is also broadly observed across per-scene and feed-forward paradigms. Hybrid methods like AR4D [ZHY*25], Splat4D [YCPH25], SV4D [XYV*24], and SV4D 2.0 [YXV*25] rely on flow alignment, uncertainty minimization, and SDS-free NeRF optimization, respectively. Per-scene methods like EG4D [SGW*24] and In-2-4D [NCOZMA25] optimize deformation fields using photometric and geometric losses. Feed-forward methods such as BTimer [LRM*24], 4DGT [XLD*25], DrivingRecon [LXZ*24], MoVies [LLP*25], and Forge4D [HHC*25] leverage depth, flow, photometric, and perceptual losses, making SDS unnecessary.

6.4. Interaction Training

Interaction training aims to generate physically coherent motion sequences for multiple entities from conditioning signals such as text [DD24], audio [SGY*24], objects [LWL23], scenes [HCV*21], or action classes [XSW*23]. Human entities are predominantly modelled with template-based representations—either fully-parametric meshes or skeletons—sometimes augmented or replaced by neural representations such as NeRF and Gaussian Splatting for photorealism, whereas object entities span both structured and unstructured representations. The central challenge lies in capturing not only individual motions but also inter-entity relationships. Existing approaches broadly divide into data-driven and reward-driven paradigms; we briefly overview both below and refer readers to [SGH*26] for in-depth discussion.

6.4.1. Data-Driven

Data-driven methods learn to map input conditions to interaction motion sequences from captured data priors (see Section 5.3). Architectures have evolved from RNNs [KBM*20] and GANs [XSW*23] through VAEs [TCBT22, WWZ*22] to the now-dominant diffusion models [LZL*24, LWL23] and transformers [GZD*25]. Training can be further regularized by contact [WZM*25], affordance [ZSY*25], collision [ZHN*20], and physical priors [ZBS*24]. While this paradigm produces natural motions grounded in real human data, physical plausibility remains only implicitly enforced, GOAL [TCBT22] and SAGA [WWZ*22] resort to post-hoc optimization to reduce penetration, and HOI-Dyn [LW25] introduces explicit driver–responder synchronization via a transformer to improve inter-entity coherence.

6.4.2. Reward-Driven

Reward-driven methods instead train agents via reinforcement learning coupled with a physics simulator, making physical plausibility an intrinsic guarantee rather than a learned prior. The central design problem is the reward function. [HGW*23] combines

Table 2: Comparison of 4D geometric representation properties across seven key dimensions relevant to dynamic scene modelling.

Representation	Motion Representation	Visual Fidelity	Scalability	Temporal Consistency	Topology Handling	Editability	Generalization	Efficiency
Mesh	Vertex displacement Skinning weights	Medium	Medium	High (explicit tracking)	✗ Fixed connectivity	Medium	High	Low
Point Cloud	Scene flow vectors	High	Excellent	Low (no structure)	✓ Natural (add/remove points)	Medium	High	High
NeRF	Deformation field Time-conditioned MLP	Very High	High	Medium	✓ Implicit (no topology)	High	Medium	Low
Gaussian Splatting	Space-Time Gaussian Deformation field	Very High	High	Medium (Gaussian tracking)	✓ Adaptive (splat birth/death)	High	High	High
Graph	Edge relationships Node attributes	Medium	High	Very High (node tracking)	✓ Dynamic (edge operations)	Very High	Medium (structure transfer)	Medium
Part	Articulation	Medium	Medium	Very High (parametric)	✓ Limited (fixed primitive set)	Very High	Excellent (within category)	Medium
Template	Deformation basis Articulation	Medium	High	Very High (correspondence)	✗ Fixed (topology-preserving)	Very High	Excellent (within category)	Medium

a task-completion reward with a learned realism reward derived from motion data; [WZY*25] extends this design to real humanoid robots. SMP [MZS*25] repurposes a pretrained motion diffusion model as a frozen, task-agnostic reward, enabling a single prior to guide diverse policies. A key limitation is that most methods train separate per-task policies. [XLWG25] addresses this via teacher-student distillation across diverse HOI datasets, correcting MoCap artifacts through physics simulation. Nevertheless, reward-driven approaches remain constrained by per-task reward engineering and reliance on reference motions, limiting generalization.

6.4.3. Open Challenges

Realism. Template-based body representations cannot capture soft deformation upon contact, limiting realistic grasping and collision-free close interaction. MoCap artifacts such as floating contacts further degrade supervision quality across both paradigms.

Generalization. Neither paradigm generalizes well beyond its training distribution. LLM-guided methods partially address this by decomposing open-vocabulary instructions into structured subgoals for low-level controllers [XWW*23, WPD*25, CPH*24], yet LLM-generated plans remain physically inconsistent. Tighter integration of LLM semantic reasoning with physics-based execution is a key open direction.

7. Representation Comparison and Trade-off

We compare representations covered so far across seven key metrics; see below. Table 2 outlines the fundamental trade-offs.

Visual Fidelity (Quality of reconstructed appearance, including photorealism and geometric detail preservation). Volumetric rendering (NeRF [PSH*21], 3DGS [LWH*25]) achieves the highest fidelity through view-dependent effects and continuous radiance modeling. Point clouds [WZH*25] and meshes [ZLL*25] follow: point clouds directly use input pixel colors despite discrete surfaces, while meshes provide continuous geometry but require PBR modeling for photorealism. Structured representations (graph, part, template [LIC*25, LYX*24b]) exhibit medium fidelity as appearance depends on node or part attributes rather than direct modeling.

Scalability (Quality and efficiency when extending from simple objects to large, complex scenes with multiple entities). Point clouds excel at large-scale scenarios (autonomous driving [CBL*20], urban reconstruction [LLH*22]), while NeRF [AHR*23], Gaussian Splatting [ZLS*24], and graphs handle unbounded multi-entity scenes through volumetric fusion and explicit modeling. In contrast, mesh, part, and template methods face constraints from connectivity complexity and category-specific design.

Temporal Consistency (Motion smoothness and coherence, i.e., absence of flickering, jittering, and discontinuity). Structured methods (graph, part, template [ZYD*25, PZX*21]) achieve the highest consistency through explicit functional motion modeling, while meshes [WYWB25] maintain high consistency via vertex tracking. NeRF [PCPMN21] and 3DGS [BSR*24] exhibit moderate consistency as learned deformation fields require temporal regularization. Point clouds demonstrate variable performance: per-frame reconstruction with tracking [FZW*25] achieves consistency, but native 4D sequences suffer from lack of explicit correspondence. Tracking-based motion representations can provide better and efficient temporal consistency in a zero-shot manner [WYG*24], but may introduce errors when projecting 2D priors into 3D.

Topology Handling (Topological changes during motion: splitting, merging, and appearance/disappearance of structures). Implicit and adaptive methods (NeRF, Gaussian Splatting, point clouds, graphs) naturally accommodate topological changes through volumetric representation or dynamic structure modification. In contrast, fixed-connectivity approaches (mesh, template, part) require consistent topology throughout sequences.

Editability (Ease of manipulation and control, including both semantic-level and fine-grained modifications). Parametric representations (graph, part, template) achieve the highest editability through intuitive semantic controls, while explicit geometry (mesh, point clouds) provides straightforward but limited manipulation. Learned methods (NeRF, 3DGS) offer powerful editing capabilities but require less intuitive latent space manipulation.

Generalization (Transferability to unseen scenes/objects without per-instance optimization or retraining). Category-level methods (part, template) achieve excellent generalization, while the rest re-

sults in moderate cross-instance capability when trained on large-scale data [XLX*25, WCK*25, HZG*23, TCC*24]. Deformation-field motion representations [LME*23, YRH*24] offer flexible optimization over diverse inputs and enable stronger motion control. Being learning-based, they generalize better than zero-shot tracking, which is often prone to 2D-to-3D projection errors.

Efficiency (*Motion-coupled inference speed*). Point clouds [WZH*25] and Gaussian Splatting with space-time motion [DWD*24] achieve the highest efficiency: point clouds through per-frame reconstruction without temporal dependencies, and space-time Gaussians by baking motion directly into the representation. Graph [FPB*24], template [PLC*25] and part-based [GPA*25] methods follow, benefiting from their compact parametric structure and inherent motion coupling (e.g., node motion or articulation). Methods requiring per-frame deformation evaluation—including mesh with vertex displacement [DSW*25], NeRF [BSR*24] and 3D Gaussians [LKT*24] with learned deformations—are less efficient due to the computational overhead of temporal motion decoding.

8. Conclusion, Emerging Trends, and Future Directions

We provide a representation-centric synthesis of recent advances in 4D modeling, highlighting how the choice of representation (e.g., structured vs. unstructured) fundamentally shapes the design, capability, and limitation of methods to reconstruct and generate 4D content. By examining the interplay between representation, motion type, and temporal dynamics, as well as the associated datasets, metrics, and benchmarks, we reveal the underlying trade-offs that govern efficiency, fidelity, and generalization. This unified perspective not only bridges prior efforts focused on specific techniques, but also establishes a conceptual framework to guide future research toward more principled and scalable approaches to capturing, understanding, and synthesizing motions and interactions.

We conclude the survey by discussing emerging trends or paradigm shifts, and open challenges to stimulate future work.

Trend #1: Feed-Forward Reconstruction. The transition from per-scene optimization to feed-forward inference represents a fundamental shift in computational efficiency. Traditional approaches requiring hours of optimization per scene are being replaced by Large Reconstruction Models (LRMs) for 4D through a single forward pass [RXM*24, CLZ*25], achieving 100-1000× speedups. This trend mirrors similar transitions witnessed in 2D [RBL*22] and 3D [ZWZ*24] generation, establishing feed-forward architectures as a dominant paradigm across dimensional barriers.

Trend #2: Hybrid Generation-Reconstruction Pipelines. The boundary between the two has become increasingly blurred, with state-of-the-art methods employing generative models such as “data amplifiers” to overcome sparse-view limitations. Multi-stage pipelines first employ diffusion models to synthesize missing multi-view observations from monocular inputs, then apply optimization-based reconstruction to the generated data [WGP*25, ZYD*25]. This paradigm addresses fundamental data scarcity through generative priors rather than improved capture hardware, but generation errors may be unavoidable and propagate into the reconstruction.

Trend #3: Integrating World Knowledge. Capturing 4D con-

tents with real-world fidelity requires incorporating high-level semantic understanding and physical plausibility. The use of LLMs has become prevalent for multi-modal reasoning and common-sense guidance in 4D tasks [WYWB25, LIC*25], encoding abstract knowledge that would be impractical to specify as mathematical inductive biases or require prohibitive amounts of training data to learn. Complementarily, physics-based constraints are being integrated through differentiable physics losses [LHB*25] or reconstruct-then-simulate pipelines [XZQ*24, ZYW*24], to enforce the generated dynamics to obey fundamental physical laws.

A key direction for future research lies in developing unified, adaptive, and structure-aware representations that can seamlessly handle transitions across motion types, spatial scales, and topological changes while preserving temporal coherence and physical plausibility. Current methods often balance efficiency, fidelity, and generalization. However, since each representation offers its own benefit and shortcoming, *hybrid representations* that combine the explicit geometric hierarchy and interpretability of structured models with the flexibility and expressiveness of implicit neural representations would be an interesting direction to explore.

The role of structure remains particularly underexplored, especially how hierarchical, part-based, or physically grounded representations can enhance motion reasoning, interaction modeling, and compositionality in 4D learning. In addition, prominent adoptions of structured representations are often found in CAD domains, with Constructive Solid Geometry (CSG), Sketch-and-Extrude, and Boundary Representations (B-Reps) offering precise geometry and compact parameterization. While many 4D applications in CAD can be envisioned, e.g., assembly or mechanical reconstruction, animation, and visualization, robot training and simulation, as well as any sub-task in the realm of 4D digital twins, a key open challenge is the *lack of industrial precision* by current methods, as CAD imposes stringent geometric and topological constraints across time. Making matters worse is the fact that high-quality dynamic CAD datasets are virtually nonexistent.

Indeed, we are still faced with a general 4D dataset bottleneck. Current 4D datasets are generally small in scale with limited motion and interaction diversity, and they often lack complete, measurable geometry, or physical plausibility, resulting in models that inevitably inherit various dataset-specific biases and miss essential components or properties required to represent complete and realistic motions. There remains a pressing need to develop large-scale, standardized 4D benchmarks which encompass diverse object categories, articulated motions, and real-world dynamics.

To date, data-driven 4D models still frequently generate visually compelling but physically implausible dynamics. To this end, existing learning paradigms could evolve beyond reconstruction or supervision-driven training, moving toward self-supervised, causal, and physics-informed approaches that can infer motion, interaction, and intent directly from sparse and multi-modal input. In general, integrating semantic, material, and physical properties into 4D representations offers a promising path toward interpretable, generalizable, and application-ready models for vision, graphics, and robotics. On the other hand, disentangled representations where geometry, motion, appearance, and lighting are independently manipulable would benefit controllability and editability.

References

- [ACRDS23] ABOU-CHAKRA J., RANA K., DAYOUB F., SÜNDERHAUF N.: Physically embodied gaussian splatting: Embedding physical priors into a visual 3d world model for robotics. In *Conference on Robot Learning* (2023), no. 7th. 9
- [Ado15] ADOBE: Mixamo. <https://www.mixamo.com>, 2015. 14
- [AHR*23] ATTAL B., HUANG J.-B., RICHARDT C., ZOLLHOEFER M., KOPF J., O'TOOLE M., KIM C.: Hyperreel: High-fidelity 6-dof video with ray-conditioned sampling. In *Proceedings of the IEEE/CVF Conference on Computer Vision and Pattern Recognition* (2023). 5, 9, 20
- [AKS24] ALLDIECK T., KOLOTOUROU N., SMINCHISDESCU C.: Score distillation sampling with learned manifold corrective. In *European Conference on Computer Vision* (2024), Springer, pp. 1–18. 17
- [ALV*23] ARAÚJO J. P., LI J., VETRIVEL K., AGARWAL R., WU J., GOPINATH D., CLEGG A. W., LIU K.: Circle: Capture in rich contextual environments. In *Proceedings of the IEEE/CVF Conference on Computer Vision and Pattern Recognition* (2023), pp. 21211–21221. 14
- [ASS*23] ARMANDPOUR M., SADEGHIAN A., SADEGHIAN A., WANG H., HU C., WANG Z.: Re-imagine the negative prompt algorithm: Transform 2d diffusion into 3d, alleviate janus problem and beyond. *arXiv preprint arXiv:2304.04968* (2023). 13
- [ATFS24] ANDRILUKA M., TABANPOUR B., FREEMAN C. D., SMINCHISDESCU C.: Learned neural physics simulation for articulated 3d human pose reconstruction. In *European Conference on Computer Vision* (2024), Springer, pp. 320–336. 9
- [ATK19] ABBATEMATTEO B., TELLEX S., KONIDARIS G.: Learning to generalize kinematic models to novel objects. In *Proceedings of the 3rd Conference on Robot Learning* (2019). 8
- [BBBB23] BERLINCIONI L., BERRETTI S., BERTINI M., BIMBO A. D.: 4dsr-gcn: 4d video point cloud upsampling using graph convolutional networks. In *Proceedings of the 1st International Workshop on Multimedia Content Generation and Evaluation: New Methods and Practice* (2023), pp. 57–65. 5
- [BDK*23] BLATTMANN A., DOCKHORN T., KULAL S., MENDELVITCH D., KILIAN M., LORENZ D., LEVI Y., ENGLISH Z., VOLETI V., LETTS A., ET AL.: Stable video diffusion: Scaling latent video diffusion models to large datasets. *arXiv preprint arXiv:2311.15127* (2023). 15
- [BHKH19] BRAHMBHATT S., HAM C., KEMP C. C., HAYS J.: Contactdb: Analyzing and predicting grasp contact via thermal imaging. In *Proceedings of the IEEE/CVF conference on computer vision and pattern recognition* (2019), pp. 8709–8719. 12
- [BKY*24] BAE J., KIM S., YUN Y., LEE H., BANG G., UH Y.: Per-gaussian embedding-based deformation for deformable 3d gaussian splatting. *arXiv preprint arXiv:2404.03613* (2024). 17
- [BNVZ21] BAIN M., NAGRANI A., VAROL G., ZISSERMAN A.: Frozen in time: A joint video and image encoder for end-to-end retrieval. *Proceedings of the IEEE/CVF International Conference on Computer Vision* (2021), 1728–1738. 13
- [BPL*16] BATTAGLIA P., PASCANU R., LAI M., JIMENEZ REZENDE D., ET AL.: Interaction networks for learning about objects, relations and physics. *Advances in neural information processing systems* 29 (2016). 7
- [BRD*24] BARAD K. R., RICHARD A., DENTLER J., OLIVARES-MENDEZ M., MARTINEZ C.: Object-centric reconstruction and tracking of dynamic unknown objects using 3d gaussian splatting. In *2024 International Conference on Space Robotics (iSpaRo)* (June 2024), IEEE, p. 202–209. URL: <http://dx.doi.org/10.1109/iSpaRo60631.2024.10688304>, doi:10.1109/iSpaRo60631.2024.10688304. 10
- [BRL*23] BLATTMANN A., ROMBACH R., LING H., DOCKHORN T., KIM S. W., FIDLER S., KREIS K.: Align your latents: High-resolution video synthesis with latent diffusion models. In *Proceedings of the IEEE/CVF Conference on Computer Vision and Pattern Recognition* (2023). 11, 13
- [BSR*24] BAHMANI S., SKOROKHOV I., RONG V., WETZSTEIN G., GUIBAS L., WONKA P., TULYAKOV S., PARK J. J., TAGLIASACCHI A., LINDELL D. B.: 4d-fy: Text-to-4d generation using hybrid score distillation sampling. In *Proceedings of the IEEE/CVF Conference on Computer Vision and Pattern Recognition* (2024). 6, 13, 15, 16, 17, 18, 20, 21
- [BSR*25] BAHMANI S., SHEN T., REN J., HUANG J., JIANG Y., TURKI H., TAGLIASACCHI A., LINDELL D. B., GOJCIC Z., FIDLER S., ET AL.: Lyra: Generative 3d scene reconstruction via video diffusion model self-distillation. *arXiv preprint arXiv:2509.19296* (2025). 17
- [BT11] BRENDLE W., TODOROVIC S.: Learning spatiotemporal graphs of human activities. In *2011 International Conference on Computer Vision* (2011), IEEE, pp. 778–785. 7
- [BTT*20] BRAHMBHATT S., TANG C., TWIGG C. D., KEMP C. C., HAYS J.: Contactpose: A dataset of grasps with object contact and hand pose. In *European Conference on Computer Vision* (2020), Springer, pp. 361–378. 12
- [BXP*22] BHATNAGAR B. L., XIE X., PETROV I., SMINCHISDESCU C., THEOBALT C., PONS-MOLL G.: Behave: Dataset and method for tracking human object interactions. In *IEEE Conference on Computer Vision and Pattern Recognition (CVPR)* (jun 2022), IEEE. 11, 14
- [CBL*20] CAESAR H., BANKITI V., LANG A. H., VORA S., LIONG V. E., XU Q., KRISHNAN A., PAN Y., BALDAN G., BEJBOM O.: nusenes: A multimodal dataset for autonomous driving. *Proceedings of the IEEE/CVF conference on computer vision and pattern recognition* (2020), 11621–11631. 5, 14, 20
- [CCPL25] CAO Z., CHEN Z., PAN L., LIU Z.: Physx-3d: Physical-grounded 3d asset generation. *arXiv preprint arXiv:2507.12465* (2025). 14
- [CCX*25a] CHEN X., CHEN Y., XIU Y., GEIGER A., CHEN A.: Easi3r: Estimating disentangled motion from dust3r without training. *arXiv preprint arXiv:2503.24391* (2025). 11
- [CCX*25b] CHEN Y., CHEN X., XUE Y., CHEN A., XIU Y., GERARD P.-M.: Human3r: Everyone everywhere all at once. *arXiv preprint arXiv:2510.06219* (2025). 16
- [CCZ*26] CHEN H., CHEN X., ZHANG Y., XU Z., CHEN A.: Motion 3-to-4: 3d motion reconstruction for 4d synthesis. *arXiv preprint arXiv:2601.14253* (2026). 18
- [CFF*22] CAI H., FENG W., FENG X., WANG Y., ZHANG J.: Neural surface reconstruction of dynamic scenes with monocular rgb-d camera. *NeurIPS* 35 (2022). 9, 15
- [CFG*15] CHANG A. X., FUNKHOUSER T., GUIBAS L., HANRAHAN P., HUANG Q., LI Z., SAVARESE S., SAVVA M., SONG S., SU H., ET AL.: Shapenet: An information-rich 3d model repository. In *Proceedings of the IEEE conference on computer vision and pattern recognition* (2015), pp. 81–89. 13, 14
- [CGD*22] COLLINS J., GOEL S., DENG K., LUTHRA A., XU L., GUNDOGDU E., ZHANG X., YAGO VICENTE T. F., DIDERIKSEN T., ARORA H., GUILLAUMIN M., MALIK J.: Abo: Dataset and benchmarks for real-world 3d object understanding. *CVPR* (2022). 13
- [CGJ*23] CHEN Y., GU C., JIANG J., ZHU X., ZHANG L.: Periodic vibration gaussian: Dynamic urban scene reconstruction and real-time rendering. *ArXiv:2311.18561* (2023). 10
- [CHC*24] CHEN C., HUANG S., CHEN X., CHEN G., HAN X., ZHANG K., GONG M.: Ct4d: Consistent text-to-4d generation with animatable meshes. *arXiv preprint arXiv:2408.08342* (2024). 3
- [CHY*25] CHEN G., HE Y., YU M., YU F. R., XU G., MA F., LI M., ZHOU G.: Inter3d: A benchmark and strong baseline for human-interactive 3d object reconstruction. *arXiv preprint arXiv:2502.14004* (2025). 15

- [CJ23] CAO A., JOHNSON J.: Hexplane: A fast representation for dynamic scenes. In *Proceedings of the IEEE/CVF Conference on Computer Vision and Pattern Recognition* (2023). 6
- [CKA*22] CHRISTEN S., KOCABAS M., AKSAN E., HWANGBO J., SONG J., HILLIGES O.: D-grasp: Physically plausible dynamic grasp synthesis for hand-object interactions. In *Proceedings of the IEEE/CVF Conference on Computer Vision and Pattern Recognition* (2022), pp. 20577–20586. 12
- [CLH*25] CAO Y., LU J., HUANG Z., SHEN Z., ZHAO C., HONG F., CHEN Z., LI X., WANG W., LIU Y., LIU Z.: Reconstructing 4d spatial intelligence: A survey, 2025. URL: <https://arxiv.org/abs/2507.21045>, arXiv:2507.21045. 2
- [CLZ*24] CAO W., LUO C., ZHANG B., NIESSNER M., TANG J.: Motion2vecsets: 4d latent vector set diffusion for non-rigid shape reconstruction and tracking. In *Proceedings of the IEEE/CVF conference on computer vision and pattern recognition* (2024), pp. 20496–20506. 5
- [CLZ*25] CHEN Z., LIU T., ZHUO L., REN J., TAO Z., ZHU H., HONG F., PAN L., LIU Z.: 4dnex: Feed-forward 4d generative modeling made easy. *arXiv preprint arXiv:2508.13154* (2025). 18, 19, 21
- [CMCL21] CHOI H., MOON G., CHANG J. Y., LEE K. M.: Beyond static features for temporally consistent 3d human pose and shape from a video. In *Proceedings of the IEEE/CVF conference on computer vision and pattern recognition* (2021), pp. 1964–1973. 7
- [CPA*20] CORONA E., PUMAROLA A., ALENYA G., MORENO-NOGUER F., ROGEZ G.: Ganhand: Predicting human grasp affordances in multi-object scenes. In *Proceedings of the IEEE/CVF conference on computer vision and pattern recognition* (2020), pp. 5031–5041. 12
- [CPH*24] CAO Y., PAN L., HAN K., WONG K.-Y. K., LIU Z.: Avatargo: Zero-shot 4d human-object interaction generation and animation. In *The Thirteenth International Conference on Learning Representations* (2024). 11, 16, 20
- [CSWK24] CHIGNOLI M., SLOTINE J.-J., WENSING P. M., KIM S.: Urdf+: An enhanced urdf for robots with kinematic loops. In *2024 IEEE-RAS 23rd International Conference on Humanoid Robots (Humanoids)* (2024), IEEE, pp. 197–204. 8, 9
- [CWM*24] CHEN Z., WALSMAN A., MEMMEL M., MO K., FANG A., VEMURI K., WU A., FOX D., GUPTA A.: Urdformer: A pipeline for constructing articulated simulation environments from real-world images. *arXiv preprint arXiv:2405.11656* (2024). 9
- [CYH*24] CHEN Z., YANG J., HUANG J., DE LUTIO R., ESTURO J. M., IVANOVIC B., LITANY O., GOJCIC Z., FIDLER S., PAVONE M., SONG L., WANG Y.: OmniRe: Omni Urban Scene Reconstruction, 2024. doi:10.48550/arXiv.2408.16760. 11
- [CYX*21] CHAO Y.-W., YANG W., XIANG Y., MOLCHANOV P., HANDA A., TREMBLAY J., NARANG Y. S., VAN WYK K., IQBAL U., BIRCHFIELD S., ET AL.: Dexycb: A benchmark for capturing hand grasping of objects. In *Proceedings of the IEEE/CVF conference on computer vision and pattern recognition* (2021), pp. 9044–9053. 14
- [CZB*21] CHEN X., ZHENG Y., BLACK M. J., HILLIGES O., GEIGER A.: Snarf: Differentiable forward skinning for animating non-rigid neural implicit shapes. In *ICCV* (2021). 8
- [CZH*25] CHEN Z., ZHAO R., HAN X., GUO X., WANG S., QIAO Z.: Physics-driven local-whole elastic deformation modeling for point cloud representation learning. *arXiv preprint arXiv:2505.13812* (2025). 9
- [CZTW25] CHEN J., ZHANG B., TANG X., WONKA P.: V2m4: 4d mesh animation reconstruction from a single monocular video. *arXiv preprint arXiv:2503.09631* (2025). 1, 3, 13, 16
- [DD24] DILLER C., DAI A.: Cg-hoi: Contact-guided 3d human-object interaction generation. In *Proceedings of the IEEE/CVF Conference on Computer Vision and Pattern Recognition* (2024), pp. 19888–19901. 19
- [DDS*09] DENG J., DONG W., SOCHER R., LI L.-J., LI K., FEI-FEI L.: Imagenet: A large-scale hierarchical image database. In *2009 IEEE conference on computer vision and pattern recognition* (2009), Ieee, pp. 248–255. 15
- [DFK*22] DOWNS L., FRANCIS A., KOENIG N., KINMAN B., HICKMAN R., REYMANN K., MCHUGH T. B., VANHOUCHE V.: Google scanned objects: A high-quality dataset of 3d scanned household items. *2022 International Conference on Robotics and Automation (ICRA)* (2022), 2553–2560. 13
- [DLW*23] DEITKE M., LIU R., WALLINGFORD M., NGO H., MICHEL O., KUSUPATI A., FAN A., LAFORTE C., VOLETI V., GADRE S. Y., ET AL.: Objaverse-xl: A universe of 10m+ 3d objects. In *Advances in Neural Information Processing Systems* (2023), vol. 36, pp. 35799–35813. 13, 19
- [DMY*24] DUISTERHOF B. P., MANDI Z., YAO Y., LIU J.-W., SEIDENSCHWARZ J., SHOU M. Z., DEVA R., SONG S., BIRCHFIELD S., WEN B., ICHNOWSKI J.: DeformGS: Scene flow in highly deformable scenes for deformable object. *WAFR* (2024). 10, 17
- [DSW*25] DAI S., SU X., WAN B., HU R., XU K.: Textmesh4d: High-quality text-to-4d mesh generation. *arXiv preprint arXiv:2506.24121* (2025). 3, 5, 8, 16, 21
- [DTT*24] DELITZAS A., TAKMAZ A., TOMBARI F., SUMNER R., POLLEFEYS M., ENGELMANN F.: Scenefun3d: Fine-grained functionality and affordance understanding in 3d scenes. In *Proceedings of the IEEE/CVF Conference on Computer Vision and Pattern Recognition* (2024), pp. 14531–14542. 12
- [DWD*24] DUAN Y., WEI F., DAI Q., HE Y., CHEN W., CHEN B.: 4d-rotor gaussian splatting: towards efficient novel view synthesis for dynamic scenes. In *ACM SIGGRAPH 2024 Conference Papers* (2024), pp. 1–11. 6, 11, 16, 21
- [DXW*21] DENG S., XU X., WU C., CHEN K., JIA K.: 3d affordancenet: A benchmark for visual object affordance understanding. In *proceedings of the IEEE/CVF conference on computer vision and pattern recognition* (2021), pp. 1778–1787. 12
- [DZLY23] DONG Y., ZHANG Z., LIU Y., YI L.: Nsm4d: Neural scene model based online 4d point cloud sequence understanding. *arXiv preprint arXiv:2310.08326* (2023). 5
- [DZY*21] DU Y., ZHANG Y., YU H.-X., TENENBAUM J. B., WU J.: Neural radiance flow for 4d view synthesis and video processing. In *2021 IEEE/CVF International Conference on Computer Vision (ICCV)* (2021), IEEE Computer Society, pp. 14304–14314. 10
- [ECC*21] ETTINGER S., CHENG S., CAINE B., LIU C., ZHAO H., PRADHAN S., CHAI Y., SAPP B., QI C. R., ZHOU Y., ET AL.: Large scale interactive motion forecasting for autonomous driving: The waymo open motion dataset. In *Proceedings of the IEEE/CVF international conference on computer vision* (2021), pp. 9710–9719. 14
- [EZH22] EISNER B., ZHANG H., HELD D.: Flowbot3d: Learning 3d articulation flow to manipulate articulated objects. *arXiv preprint arXiv:2205.04382* (2022). 9
- [FHCD25] FAN S., HUANG W., CAI X., DU B.: 3d human interaction generation: A survey. *arXiv preprint arXiv:2503.13120* (2025). 11
- [FJG*21] FU H., JIA R., GAO L., GONG M., ZHAO B., MAYBANK S., TAO D.: 3d-future: 3d furniture shape with texture. *International Journal of Computer Vision* 129, 12 (2021), 3313–3337. 13
- [FKB*24] FISCHER T., KULHANEK J., BULÒ S. R., PORZI L., POLLEFEYS M., KONTSCIEDER P.: Dynamic 3d gaussian fields for urban areas. In *NeurIPS* (2024). 11
- [FKMW*23] FRIDOVICH-KEIL S., MEANTI G., WARBURG F. R., RECHT B., KANAZAWA A.: K-planes: Explicit radiance fields in space, time, and appearance. In *Proceedings of the IEEE/CVF Conference on Computer Vision and Pattern Recognition* (2023). 6, 18
- [FPB*24] FISCHER T., PORZI L., BULO S. R., POLLEFEYS M., KONTSCIEDER P.: Multi-level neural scene graphs for dynamic urban environments. In *CVPR* (2024). 21
- [FSL*24] FENG Y., SHANG Y., LI X., SHAO T., JIANG C., YANG Y.: Pie-nerf: Physics-based interactive elastodynamics with nerf. In *Proceedings of the IEEE/CVF Conference on Computer Vision and Pattern Recognition* (2024), pp. 4450–4461. 9

- [FTT*23] FAN Z., TAHERI O., TZIONAS D., KOCABAS M., KAUFMANN M., BLACK M. J., HILLIGES O.: ARCTIC: A dataset for dexterous bimanual hand-object manipulation. In *Proceedings IEEE Conference on Computer Vision and Pattern Recognition (CVPR)* (2023). 14
- [FYW*22] FANG J., YI T., WANG X., XIE L., ZHANG X., LIU W., NIESSNER M., TIAN Q.: Fast dynamic radiance fields with time-aware neural voxels. In *SIGGRAPH Asia 2022 Conference Papers* (2022), pp. 1–9. 6
- [FZO*20] FIERARU M., ZANFIR M., ONEATA E., POPA A.-I., OLARU V., SMINCHESCU C.: Three-dimensional reconstruction of human interactions. In *Proceedings of the IEEE/CVF Conference on Computer Vision and Pattern Recognition* (2020), pp. 7214–7223. 14
- [FZW*25] FENG H., ZHANG J., WANG Q., YE Y., YU P., BLACK M. J., DARRELL T., KANAZAWA A.: St4rtrack: Simultaneous 4d reconstruction and tracking in the world. *arXiv preprint arXiv:2504.13152* (2025). 5, 10, 16, 19, 20
- [FZZ*25] FAN J., ZENG X., ZHANG J., GONG M., YANG Y., TAO D.: Advances in radiance field for dynamic scene: From neural field to gaussian field, 2025. URL: <https://arxiv.org/abs/2505.10049>, [arXiv:2505.10049](https://arxiv.org/abs/2505.10049). 2
- [GCD*22] GUO X., CHEN G., DAI Y., YE X., SUN J., TAN X., DING E.: Neural deformable voxel grid for fast optimization of dynamic view synthesis. In *ACCV* (2022). 9
- [Gib77] GIBSON J. J.: The theory of affordances. *Perceiving, acting, and knowing: toward an ecological psychology* (1977), pp–67. 12
- [GJC*23] GUO C., JIANG T., CHEN X., SONG J., HILLIGES O.: Vid2avatar: 3d avatar reconstruction from videos in the wild via self-supervised scene decomposition. In *Proceedings of the IEEE/CVF Conference on Computer Vision and Pattern Recognition* (2023). 16
- [GLSU13] GEIGER A., LENZ P., STILLER C., URTASUN R.: Vision meets robotics: The kitti dataset. *The International Journal of Robotics Research* 32, 11 (2013), 1231–1237. 5
- [GPA*25] GOYAL P., PETROV D., ANDREWS S., BEN-SHABAT Y., LIU H.-T. D., KALOGERAKIS E.: Geopard: Geometric pretraining for articulation prediction in 3d shapes. *arXiv preprint arXiv:2504.02747* (2025). 16, 21
- [GPR*23] GOEL S., PAVLAKOS G., RAJASEGARAN J., KANAZAWA A., MALIK J.: Humans in 4d: Reconstructing and tracking humans with transformers. In *Proceedings of the IEEE/CVF International Conference on Computer Vision* (2023), pp. 14783–14794. 6, 8
- [GRT*25] GAT I., RAAB S., TEVET G., RESHEF Y., BERMANO A. H., COHEN-OR D.: Anytop: Character animation diffusion with any topology. *arXiv preprint arXiv:2502.17327* (2025). 16
- [GSKH21] GAO C., SARAF A., KOPF J., HUANG J.-B.: Dynamic view synthesis from dynamic monocular video. In *Proceedings of the IEEE/CVF International Conference on Computer Vision* (2021), pp. 5712–5721. 5
- [GSLD25] GAO D., SIDDIQUI Y., LI L., DAI A.: Meshart: Generating articulated meshes with structure-guided transformers. In *Proceedings of the Computer Vision and Pattern Recognition Conference* (2025), pp. 618–627. 16
- [GTT*21] GRADY P., TANG C., TWIGG C. D., VO M., BRAHMBHATT S., KEMP C. C.: Contactopt: Optimizing contact to improve grasps. In *Proceedings of the IEEE/CVF Conference on Computer Vision and Pattern Recognition* (2021), pp. 1471–1481. 12
- [GWB*22] GRAUMAN K., WESTBURY A., BYRNE E., CHAVIS Z., FURNARI A., GIRDHAR R., HAMBURGER J., JIANG H., LIU M., LIU X., ET AL.: Ego4d: Around the world in 3,000 hours of egocentric video. In *Proceedings of the IEEE/CVF conference on computer vision and pattern recognition* (2022), pp. 18995–19012. 14
- [GWT*24] GRAUMAN K., WESTBURY A., TORRESANI L., KITANI K., MALIK J., AFOURAS T., ASHUTOSH K., BAIYYA V., BANSAL S., BOOTE B., ET AL.: Ego-exo4d: Understanding skilled human activity from first-and third-person perspectives. In *Proceedings of the IEEE/CVF Conference on Computer Vision and Pattern Recognition* (2024), pp. 19383–19400. 13, 14, 19
- [GXC*24] GAO Q., XU Q., CAO Z., MILDENHALL B., MA W., CHEN L., TANG D., NEUMANN U.: Gaussianflow: Splatting gaussian dynamics for 4d content creation. *arXiv preprint arXiv:2403.12365* (2024). 6, 10
- [GXH*23] GAN W., XU H., HUANG Y., CHEN S., YOKOYA N.: V4d: Voxel for 4d novel view synthesis. *IEEE Transactions on Visualization and Computer Graphics* 30, 2 (2023), 1579–1591. 11, 16
- [GXL*25] GUO J., XIN Y., LIU G., XU K., LIU L., HU R.: Articulated: Self-supervised digital twin modeling of articulated objects using 3d gaussian splatting. In *Proceedings of the Computer Vision and Pattern Recognition Conference* (2025), pp. 27144–27153. 15, 16, 17
- [GXZ*23] GENG H., XU H., ZHAO C., XU C., YI L., HUANG S., WANG H.: Gapartnet: Cross-category domain-generalizable object perception and manipulation via generalizable and actionable parts. In *Proceedings of the IEEE/CVF Conference on Computer Vision and Pattern Recognition* (2023), pp. 7081–7091. 14
- [GYR*23] GUO Y., YANG C., RAO A., LIANG Z., WANG Y., QIAO Y., AGRAWALA M., LIN D., DAI B.: Animatediff: Animate your personalized text-to-image diffusion models without specific tuning. *arXiv preprint arXiv:2307.04725* (2023). 15
- [GYZW25] GAO Y., YU H.-X., ZHU B., WU J.: Fluidnexus: 3d fluid reconstruction and prediction from a single video. In *Proceedings of the Computer Vision and Pattern Recognition Conference* (2025), pp. 26091–26101. 9
- [GZD*25] GHOSH A., ZHOU B., DABRAL R., WANG J., GOLYANIK V., THEOBALT C., SLUSALLEK P., GUO C.: Duetgen: Music driven two-person dance generation via hierarchical masked modeling. In *Proceedings of the Special Interest Group on Computer Graphics and Interactive Techniques Conference Conference Papers* (2025), pp. 1–11. 19
- [HCV*21] HASSAN M., CEYLAN D., VILLEGAS R., SAITO J., YANG J., ZHOU Y., BLACK M. J.: Stochastic scene-aware motion prediction. In *Proceedings of the IEEE/CVF International Conference on Computer Vision* (2021), pp. 11374–11384. 14, 19
- [HGH*22] HUANG S., GOJIC Z., HUANG J., WIESER A., SCHINDLER K.: Dynamic 3d scene analysis by point cloud accumulation. In *European Conference on Computer Vision* (2022), Springer, pp. 674–690. 5
- [HGT*21] HASSAN M., GHOSH P., TESCH J., TZIONAS D., BLACK M. J.: Populating 3d scenes by learning human-scene interaction. In *Proceedings of the IEEE/CVF Conference on Computer Vision and Pattern Recognition* (2021), pp. 14708–14718. 12
- [HGW*23] HASSAN M., GUO Y., WANG T., BLACK M., FIDLER S., PENG X. B.: Synthesizing physical character-scene interactions. In *ACM SIGGRAPH 2023 Conference Proceedings* (2023), pp. 1–9. 12, 19
- [HH25] HU Q., HU W.: Dynamic point cloud denoising via gradient fields. *ACM Transactions on Multimedia Computing, Communications and Applications* 21, 4 (2025), 1–24. 5
- [HHC*25] HU Y., HE Y., CHEN J., YUAN W., QIU K., LIN Z., ZHU S., DONG Z., ZHANG J.: Forge4d: Feed-forward 4d human reconstruction and interpolation from uncalibrated sparse-view videos. *arXiv preprint arXiv:2509.24209* (2025). 18, 19
- [HHY*24] HUANG Z., HE Y., YU J., ZHANG F., SI C., JIANG Y., ZHANG Y., WU T., JIN Q., CHANPAISIT N., ET AL.: Vbench: Comprehensive benchmark suite for video generative models. In *Proceedings of the IEEE/CVF Conference on Computer Vision and Pattern Recognition* (2024). 15
- [HLX*21] HABERMANN M., LIU L., XU W., ZOLLHOEFER M., PONS-MOLL G., THEOBALT C.: Real-time deep dynamic characters. *ACM Transactions on Graphics (ToG)* 40, 4 (2021), 1–16. 14, 18
- [HLZ*25] HUANG H., LIU Y., ZHENG G., WANG J., DOU Z., YANG S.: Mvtokenflow: High-quality 4d content generation using multiview token flow. In *The Thirteenth International Conference on Learning Representations* (2025). 16

- [HSY*24] HUANG Y.-H., SUN Y.-T., YANG Z., LYU X., CAO Y.-P., QI X.: Sc-gs: Sparse-controlled gaussian splatting for editable dynamic scenes. In *Proceedings of the IEEE/CVF conference on computer vision and pattern recognition* (2024), pp. 4220–4230. 9, 17
- [HVT*19] HASSON Y., VAROL G., TZIONAS D., KALEVATYKH I., BLACK M. J., LAPTEV I., SCHMID C.: Learning joint reconstruction of hands and manipulated objects. In *Proceedings of the IEEE/CVF conference on computer vision and pattern recognition* (2019), pp. 11807–11816. 14
- [HWZ*24] HUANG N., WEI X., ZHENG W., AN P., LU M., ZHAN W., TOMIZUKA M., KEUTZER K., ZHANG S.: S^3 gaussian: Self-supervised street gaussians for autonomous driving. *CoRR* (2024). 18
- [HZG*23] HONG Y., ZHANG K., GU J., BI S., ZHOU Y., LIU D., LIU F., SUNKAVALLI K., BUI T., TAN H.: Lrm: Large reconstruction model for single image to 3d. *arXiv preprint arXiv:2311.04400* (2023). 18, 21
- [HZZ*24] HUANG T., ZENG Y., LI H., ZUO W., LAU R. W.: Dreamphysics: Learning physical properties of dynamic 3d gaussians with video diffusion priors. *arXiv e-prints* (2024), arXiv:2406. 9
- [IJZ*24] ILIASH D., JIANG H., ZHANG Y., SAVVA M., CHANG A. X.: S2O: Static to openable enhancement for articulated 3D objects. *arXiv preprint arXiv:2409.18896* (2024). 7, 14
- [IMH05] IGARASHI T., MOSCOVICH T., HUGHES J. F.: As-rigid-as-possible shape manipulation. *ACM transactions on Graphics (TOG)* 24, 3 (2005), 1134–1141. 15, 18
- [IPOS13] IONESCU C., PAPAVA D., OLARU V., SMINCHISDESCU C.: Human3.6m: Large scale datasets and predictive methods for 3d human sensing in natural environments. *IEEE transactions on pattern analysis and machine intelligence* 36, 7 (2013), 1325–1339. 14
- [IRG*23] IŞIK M., RÜNZ M., GEORGOPOULOS M., KHAKHULIN T., STARCK J., AGAPITO L., NIESSNER M.: Humanrf: High-fidelity neural radiance fields for humans in motion. *ACM Transactions on Graphics (TOG)* 42, 4 (2023), 1–12. 13, 14
- [JHBZ22] JIANG B., HONG Y., BAO H., ZHANG J.: Selfrecon: Self reconstruction your digital avatar from monocular video. In *CVPR* (2022). 10
- [JKFFN20] JI J., KRISHNA R., FEI-FEI L., NIEBLES J. C.: Action genome: Actions as compositions of spatio-temporal scene graphs. In *Proceedings of the IEEE/CVF conference on computer vision and pattern recognition* (2020), pp. 10236–10247. 7
- [JKZ*24] JIANG D., KE Z., ZHOU X., HOU Z., YANG X., HU W., QIU T., GUO C.: Timeformer: Capturing temporal relationships of deformable 3d gaussians for robust reconstruction. *arXiv preprint arXiv:2411.11941* (2024). 17
- [JLC*23] JIANG N., LIU T., CAO Z., CUI J., ZHANG Z., CHEN Y., WANG H., ZHU Y., HUANG S.: Full-body articulated human-object interaction. In *Proceedings of the IEEE/CVF International Conference on Computer Vision* (2023), pp. 9365–9376. 14
- [JLWW21] JIANG H., LIU S., WANG J., WANG X.: Hand-object contact consistency reasoning for human grasps generation. In *Proceedings of the IEEE/CVF international conference on computer vision* (2021), pp. 11107–11116. 12
- [JMSC22] JIANG H., MAO Y., SAVVA M., CHANG A. X.: Opd: Single-view 3d openable part detection. In *Computer Vision—ECCV 2022: 17th European Conference, Tel Aviv, Israel, October 23–27, 2022, Proceedings, Part XXXIX* (2022), Springer, pp. 410–426. 7
- [JN23] JUN H., NICHOL A.: Shap-e: Generating conditional 3d implicit functions. *arXiv preprint arXiv:2305.02463* (2023). 17
- [JSL*17] JOO H., SIMON T., LI X., LIU H., TAN L., GUI L., BANERJEE S., GODISART T. S., NABBE B., MATTHEWS I., KANADE T., NOBUHARA S., SHEIKH Y.: Panoptic studio: A massively multiview system for social interaction capture. *IEEE Transactions on Pattern Analysis and Machine Intelligence* (2017). 14
- [JTL*24] JIN L., TUCKER R., LI Z., FOUHEY D., SNAVELY N., HOLYNSKI A.: Stereo4d: Learning how things move in 3d from internet stereo videos. *arXiv preprint arXiv:2412.09621* (2024). 13, 14, 19
- [JWF*24] JI S., WU G., FANG J., CEN J., YI T., LIU W., TIAN Q., WANG X.: Segment any 4d gaussians. *arXiv preprint arXiv:2407.04504* (2024). 15
- [JYC*24] JIANG Y., YU C., CAO C., WANG F., HU W., GAO J.: Animate3d: Animating any 3d model with multi-view video diffusion. *Advances in Neural Information Processing Systems* 37 (2024), 125879–125906. 13
- [JZG*24] JIANG Y., ZHANG L., GAO J., HU W., YAO Y.: Consistent4d: Consistent 360° dynamic object generation from monocular video. In *The Twelfth International Conference on Learning Representations* (2024). 6, 15, 16, 17, 18
- [JZL*24] JIANG N., ZHANG Z., LI H., MA X., WANG Z., CHEN Y., LIU T., ZHU Y., HUANG S.: Scaling up dynamic human-scene interaction modeling. In *Proceedings of the IEEE/CVF Conference on Computer Vision and Pattern Recognition* (2024), pp. 1737–1747. 14
- [JZL*25] JIANG Z., ZHENG C., LAINA I., LARLUS D., VEDALDI A.: Geo4d: Leveraging video generators for geometric 4d scene reconstruction. *arXiv preprint arXiv:2504.07961* (2025). 18, 19
- [KAB20] KOCABAS M., ATHANASIOU N., BLACK M. J.: Vibe: Video inference for human body pose and shape estimation. In *Proceedings of the IEEE/CVF conference on computer vision and pattern recognition* (2020), pp. 5253–5263. 7
- [KBM*20] KUNDU J. N., BUCKCHASH H., MANDIKAL P., JAMKHANDI A., RADHAKRISHNAN V. B., ET AL.: Cross-conditioned recurrent networks for long-term synthesis of inter-person human motion interactions. In *Proceedings of the IEEE/CVF winter conference on applications of computer vision* (2020), pp. 2724–2733. 19
- [KGB*25] KÄSTINGSCHÄFER M., GIERUC T., BERNHARD S., CAMPBELL D., INSAFUTDINOV E., NAJAFI E., BROX T.: Seed4d: A synthetic ego-exo dynamic 4d data generator, driving dataset and benchmark. In *2025 IEEE/CVF Winter Conference on Applications of Computer Vision (WACV)* (2025), IEEE, pp. 7752–7764. 15
- [KGP02] KOVAR L., GLEICHER M., PIGHIN F.: Motion graphs. *ACM Transactions on Graphics* 21, 3 (2002), 473–482. 7
- [KHHR23] KHURANA T., HU P., HELD D., RAMANAN D.: Point cloud forecasting as a proxy for 4d occupancy forecasting. In *IEEE/CVF Conference on Computer Vision and Pattern Recognition (CVPR)* (2023). 5
- [KHK*25] KIM S., HA J., KIM Y. H., LEE Y., PARK F. C.: Screwsplat: An end-to-end method for articulated object recognition. *arXiv preprint arXiv:2508.02146* (2025). 9
- [KKLD23] KERBL B., KOPANAS G., LEIMKÜHLER T., DRETTAKIS G.: 3d gaussian splatting for real-time radiance field rendering. *ACM TOG* 42, 4 (2023). URL: <https://repo-sam.inria.fr/fungraph/3d-gaussian-splatting/>. 6, 18
- [KKNJ25] KIM J., KIM J., NA J., JOO H.: Parahome: Parameterizing everyday home activities towards 3d generative modeling of human-object interactions. In *Proceedings of the Computer Vision and Pattern Recognition Conference* (2025), pp. 1816–1828. 13, 14
- [KKY24] KIM P. J., KIM S., YOO J.: Stream: Spatio-temporal evaluation and analysis metric for video generative models. *arXiv preprint arXiv:2403.09669* (2024). 15
- [KMJ*24] KHANNA M., MAO Y., JIANG H., HARESH S., SHACKLETT B., BATRA D., CLEGG A., UNDERSANDER E., CHANG A. X., SAVVA M.: Habitat synthetic scenes dataset (hssd-200): An analysis of 3d scene scale and realism tradeoffs for objectgoal navigation. In *Proceedings of the IEEE/CVF Conference on Computer Vision and Pattern Recognition* (2024), pp. 16384–16393. 13
- [KMR*23] KIRILLOV A., MINTUN E., RAVI N., MAO H., ROLLAND C., GUSTAFSON L., XIAO T., WHITEHEAD S., BERG A. C., LO W.-Y., ET AL.: Segment anything. In *ICCV* (2023). 15

- [KO21] KUMRU M., OZKAN E.: Three-dimensional extended object tracking and shape learning using gaussian processes. *IEEE Transactions on Aerospace and Electronic Systems* 57, 5 (Oct. 2021), 2795–2814. URL: <http://dx.doi.org/10.1109/TAES.2021.3067668>, doi:10.1109/taes.2021.3067668. 10
- [KRG*24] KULKARNI N., REMPE D., GENOVA K., KUNDU A., JOHNSON J., FOUHEY D., GUIBAS L.: Nifty: Neural object interaction fields for guided human motion synthesis. In *Proceedings of the IEEE/CVF Conference on Computer Vision and Pattern Recognition* (2024), pp. 947–957. 12
- [KSS24] KANDUKURI R. K., STRECKE M., STUECKLER J.: Physics-based rigid body object tracking and friction filtering from rgb-d videos. In *2024 International Conference on 3D Vision (3DV)* (Mar. 2024), IEEE, p. 1259–1269. URL: <http://dx.doi.org/10.1109/3DV62453.2024.00111>, doi:10.1109/3dv62453.2024.00111. 10
- [KVH84] KAJIYA J. T., VON HERZEN B. P.: Ray tracing volume densities. *ACM SIGGRAPH computer graphics* 18, 3 (1984), 165–174. 5
- [KVN24] KATSUMATA K., VO D. M., NAKAYAMA H.: A compact dynamic 3d gaussian representation for real-time dynamic view synthesis. In *European Conference on Computer Vision* (2024), Springer, pp. 394–412. 11, 17
- [KYZ*20] KARUNRATANAKUL K., YANG J., ZHANG Y., BLACK M. J., MUANDET K., TANG S.: Grasping field: Learning implicit representations for human grasps. In *2020 International Conference on 3D Vision (3DV)* (2020), IEEE, pp. 333–344. 12
- [KZFM19] KANAZAWA A., ZHANG J. Y., FELSEN P., MALIK J.: Learning 3d human dynamics from video. In *Proceedings of the IEEE/CVF Conference on Computer Vision and Pattern Recognition* (2019). 7
- [LBB*17] LI T., BOLKART T., BLACK M. J., LI H., ROMERO J.: Learning a model of facial shape and expression from 4D scans. *ACM Transactions on Graphics, (Proc. SIGGRAPH Asia)* 36, 6 (2017), 194:1–194:17. URL: <https://doi.org/10.1145/3130800.3130813>. 6
- [LCL24] LI Z., CHEN Y., LIU P.: Dreammesh4d: Video-to-4d generation with sparse-controlled gaussian-mesh hybrid representation. *Advances in Neural Information Processing Systems* 37 (2024), 21377–21400. 3, 5, 16
- [LCLX24] LI Z., CHEN Z., LI Z., XU Y.: Spacetime gaussian feature splatting for real-time dynamic view synthesis. In *Proceedings of the IEEE/CVF Conference on Computer Vision and Pattern Recognition* (2024). 17
- [LCM*22] LIU J.-W., CAO Y.-P., MAO W., ZHANG W., ZHANG D. J., KEPPO J., SHAN Y., QIE X., SHOU M. Z.: Devrf: Fast deformable voxel radiance fields for dynamic scenes. *NeurIPS* 35 (2022). 6, 9, 15
- [LCQ*21] LU F., CHEN G., QU S., LI Z., LIU Y., KNOLL A.: Pointnet: Point cloud frame interpolation network. In *Proceedings of the AAAI Conference on Artificial Intelligence* (2021), vol. 35, pp. 2251–2259. 5
- [LDS*23] LEI J., DENG C., SHEN B., GUIBAS L., DANILIDIS K.: Nap: Neural 3d articulation prior. *arXiv preprint arXiv:2305.16315* (2023). 7, 9
- [LDZ*24] LU J., DENG J., ZHU R., LIANG Y., YANG W., ZHANG T., ZHOU X.: Dn-4dgs: Denoised deformable network with temporal-spatial aggregation for dynamic scene rendering. *arXiv preprint arXiv:2410.13607* (2024). 17
- [LDZY24] LIN Y., DAI Z., ZHU S., YAO Y.: Gaussian-flow: 4d reconstruction with dynamic 3d gaussian particle. In *Proceedings of the IEEE/CVF Conference on Computer Vision and Pattern Recognition* (2024). 6, 17
- [LGL*23] LONG X., GUO Y.-C., LIN C., LIU Y., DOU Z., LIU L., MA Y., ZHANG S.-H., HABERMANN M., THEOBALT C., ET AL.: Wonder3d: Single image to 3d using cross-domain diffusion. *arXiv preprint arXiv:2310.15008* (2023). 15
- [LGXC24] LI Y.-J., GLADKOVA M., XIA Y., CREMERS D.: Sadg: Segment any dynamic gaussian without object trackers. *arXiv preprint arXiv:2411.19290* (2024). 15
- [LHB*25] LU J., HUANG C.-H. P., BHATTACHARYA U., HUANG Q., ZHOU Y.: Humoto: A 4d dataset of mocap human object interactions. *arXiv preprint arXiv:2504.10414* (2025). 11, 15, 21
- [LHC*25] LIU T., HUANG Z., CHEN Z., WANG G., HU S., SHEN L., SUN H., CAO Z., LI W., LIU Z.: Free4d: Tuning-free 4d scene generation with spatial-temporal consistency. In *Proceedings of the IEEE/CVF International Conference on Computer Vision* (2025). 16
- [LHL*25] LIU J., HAN J., LIU L., AVILES-RIVERO A. I., JIANG C., LIU Z., WANG H.: Mamba4d: Efficient 4d point cloud video understanding with disentangled spatial-temporal state space models. In *Proceedings of the Computer Vision and Pattern Recognition Conference* (2025), pp. 17626–17636. 5
- [LIC*25] LIU J., ILIASH D., CHANG A. X., SAVVA M., MAHDAVI-AMIRI A.: SINGAPO: Single Image Controlled Generation of Articulated Parts in Objects. In *Proceedings of the International Conference on Learning Representations (ICLR)* (2025). 7, 16, 20, 21
- [LJL*25] LIU Y., JIA B., LU R., NI J., ZHU S.-C., HUANG S.: Artgs: Building interactive replicas of complex articulated objects via gaussian splatting. *ArXiv:2502.19459* (2025). 16, 17, 18
- [LJK20] LI M., KAUFMAN D. M., JIANG C.: Codimensional incremental potential contact. *arXiv preprint arXiv:2012.04457* (2020). 11
- [LKL24] LUITEN J., KOPANAS G., LEIBE B., RAMANAN D.: Dynamic 3d gaussians: Tracking by persistent dynamic view synthesis. In *International Conference on 3D Vision (3DV)* (2024). 8, 9, 10, 16, 17
- [LKT*24] LING H., KIM S. W., TORRALBA A., FIDLER S., KREIS K.: Align your gaussians: Text-to-4d with dynamic 3d gaussians and composed diffusion models. In *Proceedings of the IEEE/CVF Conference on Computer Vision and Pattern Recognition* (2024). 13, 21
- [LLF21] LI Z., LI T., FARIMANI A. B.: Tpu-gan: Learning temporal coherence from dynamic point cloud sequences. In *International Conference on Learning Representations* (2021). 5
- [LLH*22] LIN L., LIU Y., HU Y., YAN X., XIE K., HUANG H.: Capturing, reconstructing, and simulating: the urbanscene3d dataset. In *European Conference on Computer Vision* (2022), Springer, pp. 93–109. 20
- [LLP*25] LIN C., LIN Y., PAN P., YU Y., YAN H., FRAGKIADAKI K., MU Y.: Movies: Motion-aware 4d dynamic view synthesis in one second, 2025. URL: <https://arxiv.org/abs/2507.10065>, arXiv:2507.10065. 18, 19
- [LLT*25] LU R., LIU Y., TANG J., NI J., WANG Y., WAN D., ZENG G., CHEN Y., HUANG S.: Dreamart: Generating interactive articulated objects from a single image. *arXiv preprint arXiv:2507.05763* (2025). 7, 19
- [LLW*25] LIU Q., LIU Y., WANG J., LYU X., WANG P., WANG W., HOU J.: MoDGS: Dynamic gaussian splatting from casually-captured monocular videos with depth priors. In *The Thirteenth International Conference on Learning Representations* (2025). URL: <https://openreview.net/forum?id=2prShxdLkX>. 6, 9, 15
- [LLY*24] LI W., LIU J., YAN H., CHEN R., LIANG Y., CHEN X., TAN P., LONG X.: Craftsman3d: High-fidelity mesh generation with 3d native generation and interactive geometry refiner, 2024. 3
- [LLZ*23] LIU Y., LIN C., ZENG Z., LONG X., LIU L., KOMURA T., WANG W.: Syncdreamer: Generating multiview-consistent images from a single-view image. In *The Twelfth International Conference on Learning Representations* (2023). 13, 15
- [LME*23] LI Z., MÜLLER T., EVANS A., TAYLOR R. H., UNBERATH M., LIU M.-Y., LIN C.-H.: Neuralangelo: High-fidelity neural surface reconstruction. In *Proceedings of the IEEE/CVF Conference on Computer Vision and Pattern Recognition (CVPR)* (June 2023), pp. 8456–8465. 21

- [LMR*15] LOPER M., MAHMOOD N., ROMERO J., PONS-MOLL G., BLACK M. J.: SMPL: A skinned multi-person linear model. *ACM Trans. Graphics (Proc. SIGGRAPH Asia)* 34, 6 (Oct. 2015), 248:1–248:16. 6, 8, 9, 14
- [LMS23] LIU J., MAHDAVI-AMIRI A., SAVVA M.: Paris: Part-level reconstruction and motion analysis for articulated objects. In *ICCV* (2023). 7, 16
- [LNSW21] LI Z., NIKLAUS S., SNAVELY N., WANG O.: Neural scene flow fields for space-time view synthesis of dynamic scenes. In *Proceedings of the IEEE/CVF Conference on Computer Vision and Pattern Recognition* (2021). 5, 9, 10
- [LQC*23] LI X., QIAO Y.-L., CHEN P. Y., JATAVALLABHULA K. M., LIN M., JIANG C., GAN C.: Pac-nerf: Physics augmented continuum neural radiance fields for geometry-agnostic system identification. *arXiv preprint arXiv:2303.05512* (2023). 9
- [LQG19] LIU X., QI C. R., GUIBAS L. J.: Flownet3d: Learning scene flow in 3d point clouds. In *Proceedings of the IEEE/CVF conference on computer vision and pattern recognition* (2019), pp. 529–537. 5
- [LRM*24] LIANG H., REN J., MIRZAEI A., TORRALBA A., LIU Z., GILITSCHENSKI I., FIDLER S., OZTIRELI C., LING H., GOJCIC Z., ET AL.: Feed-forward bullet-time reconstruction of dynamic scenes from monocular videos. *arXiv preprint arXiv:2412.03526* (2024). 18, 19
- [LSCK23] LEE J., SUNG M., CHOI H., KIM T.-K.: Im2hands: Learning attentive implicit representation of interacting two-hand shapes. In *CVPR* (2023). 18
- [LSN*24] LEE J., SAITO S., NAM G., SUNG M., KIM T.-K.: Interhandgen: Two-hand interaction generation via cascaded reverse diffusion. In *Proceedings of the IEEE/CVF Conference on Computer Vision and Pattern Recognition* (2024), pp. 527–537. 18, 19
- [LSS*19] LOMBARDI S., SIMON T., SARAGIH J., SCHWARTZ G., LEHRMANN A., SHEIKH Y.: Neural volumes: Learning dynamic renderable volumes from images. *TOG* 38, 4 (2019). doi:10.1145/3306346.3323020. 18
- [LSY23] LI J., SONG Z., YANG B.: Nvfi: Neural velocity fields for 3d physics learning from dynamic videos. *Advances in Neural Information Processing Systems* 36 (2023), 34723–34751. 9
- [LSZ*22] LI T., SLAVCHEVA M., ZOLLHOEFER M., GREEN S., LASSNER C., KIM C., SCHMIDT T., LOVEGROVE S., GOESELE M., NEWCOMBE R., ET AL.: Neural 3d video synthesis from multi-view video. In *Proceedings of the IEEE/CVF conference on computer vision and pattern recognition* (2022), pp. 5521–5531. 5, 9, 14
- [LTMAS24] LIU J., TAM H. I. I., MAHDAVI-AMIRI A., SAVVA M.: CAGE: Controllable Articulation GEneration. In *Proceedings of the IEEE Conference on Computer Vision and Pattern Recognition (CVPR)* (2024). 3, 7
- [LTT*21] LI Y., TAKEHARA H., TAKETOMI T., ZHENG B., NIESSNER M.: 4dcomplete: Non-rigid motion estimation beyond the observable surface. In *Proceedings of the IEEE/CVF International Conference on Computer Vision* (2021), pp. 12706–12716. 10, 13, 14
- [LTV*22] LI R., TANKE J., VO M., ZOLLHOEFER M., GALL J., KANAZAWA A., LASSNER C.: Tava: Template-free animatable volumetric actors. In *ECCV* (2022). 8
- [LW25] LIN WU ZHIXIANG CHEN J. L.: Hoi-dyn: Learning interaction dynamics for human-object motion diffusion. *NeurIPS* (2025). 19
- [LWC*23] LI Z., WANG Q., COLE F., TUCKER R., SNAVELY N.: Dynibar: Neural dynamic image-based rendering. In *CVPR* (2023). 6
- [LWH*25] LEI J., WENG Y., HARLEY A. W., GUIBAS L., DANIILIDIS K.: Mosca: Dynamic gaussian fusion from casual videos via 4d motion scaffolds. In *Proceedings of the Computer Vision and Pattern Recognition Conference* (2025), pp. 6165–6177. 6, 10, 16, 20
- [LWL23] LI J., WU J., LIU C. K.: Object motion guided human motion synthesis. *ACM Transactions on Graphics (TOG)* 42, 6 (2023), 1–11. 1, 14, 19
- [LWVH*23] LIU R., WU R., VAN HOORICK B., TOKMAKOV P., ZAKHAROV S., VONDRICK C.: Zero-1-to-3: Zero-shot one image to 3d object. *Proceedings of the IEEE/CVF International Conference on Computer Vision* (2023), 9298–9309. 13, 17
- [LWW*25] LIU H., WANG X., WAN Z., MA Y., CHEN J., FAN Y., SHEN Y., SONG Y., CHEN Q.: Avatarartist: Open-domain 4d avatarization. In *Proceedings of the Computer Vision and Pattern Recognition Conference* (2025), pp. 10758–10769. 16
- [LXF*22] LIU L., XU W., FU H., QIAN S., YU Q., HAN Y., LU C.: Akb-48: A real-world articulated object knowledge base. In *Proceedings of the IEEE/CVF Conference on Computer Vision and Pattern Recognition* (2022), pp. 14809–14818. 8, 14
- [LXL*24] LE L., XIE J., LIANG W., WANG H.-J., YANG Y., MA Y. J., VEDDER K., KRISHNA A., JAYARAMAN D., EATON E.: Articulateanything: Automatic modeling of articulated objects via a vision-language foundation model. *arXiv preprint arXiv:2410.13882* (2024). 9
- [LXY*25] LIU I., XU Z., YIFAN W., TAN H., XU Z., WANG X., SU H., SHI Z.: Riganything: Template-free autoregressive rigging for diverse 3d assets. *ACM Transactions on Graphics (TOG)* 44, 4 (2025), 1–12. 7, 16
- [LXZ*24] LU H., XU T., ZHENG W., ZHAN Y. Z. W., DU D., TOMIZUKA M., KEUTZER K., CHEN Y.: Drivingrecon: Large 4d gaussian reconstruction model for autonomous driving. *arXiv preprint arXiv:2412.09043* (2024). 18, 19
- [LYLW24] LI H., YU H.-X., LI J., WU J.: Zerohsi: Zero-shot 4d human-scene interaction by video generation. *arXiv preprint arXiv:2412.18600* (2024). 1, 11
- [LYS*24] LIU Y., YANG H., SI X., LIU L., LI Z., ZHANG Y., LIU Y., YI L.: Taco: Benchmarking generalizable bimanual tool-action-object understanding. In *Proceedings of the IEEE/CVF Conference on Computer Vision and Pattern Recognition* (2024), pp. 21740–21751. 14
- [LYX*24a] LIANG H., YIN Y., XU D., LIANG H., WANG Z., PLATAN-IOTIS K. N., ZHAO Y., WEI Y.: Diffusion4d: fast spatial-temporal consistent 4d generation via video diffusion models. In *Proceedings of the 38th International Conference on Neural Information Processing Systems* (2024). 13, 14
- [LYX*24b] LIAO T., YI H., XIU Y., TANG J., HUANG Y., THIES J., BLACK M. J.: TADA! Text to Animatable Digital Avatars. In *International Conference on 3D Vision (3DV)* (2024). 7, 16, 20
- [LZL*24] LIANG H., ZHANG W., LI W., YU J., XU L.: Intergen: Diffusion-based multi-human motion generation under complex interactions. *International Journal of Computer Vision* 132, 9 (2024), 3463–3483. 11, 19
- [LZL*25] LI Y., ZOU Z.-X., LIU Z., WANG D., LIANG Y., YU Z., LIU X., GUO Y.-C., LIANG D., OUYANG W., ET AL.: Triposg: High-fidelity 3d shape synthesis using large-scale rectified flow models. *arXiv preprint arXiv:2502.06608* (2025). 3, 13
- [LZRV24a] LI R., ZHENG C., RUPPRECHT C., VEDALDI A.: Draga-part: Learning a part-level motion prior for articulated objects. In *European Conference on Computer Vision* (2024), Springer, pp. 165–183. 7
- [LZRV24b] LI R., ZHENG C., RUPPRECHT C., VEDALDI A.: Puppet-master: Scaling interactive video generation as a motion prior for part-level dynamics. *arXiv preprint arXiv:2408.04631* (2024). 7, 13, 14
- [LZT*19] LIU L., ZHENG Y., TANG D., YUAN Y., FAN C., ZHOU K.: Neuroskinning: Automatic skin binding for production characters with deep graph networks. *ACM Transactions on Graphics (TOG)* 38, 4 (2019), 1–12. 8
- [LZWL24] LI Z., ZHENG Z., WANG L., LIU Y.: Animatable gaussians: Learning pose-dependent gaussian maps for high-fidelity human avatar modeling. In *Proceedings of the IEEE/CVF conference on computer vision and pattern recognition* (2024), pp. 19711–19722. 8
- [LZX*24] LI Y., ZHAO N., XIAO J., FENG C., WANG X., CHUA T.-S.:

- Lasos: Language-guided affordance segmentation on 3d object. In *Proceedings of the IEEE/CVF Conference on Computer Vision and Pattern Recognition* (2024), pp. 14251–14260. [12](#)
- [LZYX*22] LIN W., ZHENG C., YONG J.-H., XU F.: Occlusionfusion: Occlusion-aware motion estimation for real-time dynamic 3d reconstruction. In *Proceedings of the IEEE/CVF Conference on Computer Vision and Pattern Recognition* (2022), pp. 1736–1745. [10](#)
- [LZZ*24] LI B., ZHENG C., ZHU W., MAI J., ZHANG B., WONKA P., GHANEM B.: Vivid-zoo: Multi-view video generation with diffusion model. *Advances in Neural Information Processing Systems 37* (2024), 62189–62222. [13, 14](#)
- [MCY*25] MA Z., CHEN X., YU S., BI S., ZHANG K., ZIWEN C., XU S., YANG J., XU Z., SUNKAVALLI K., ET AL.: 4d-irm: Large space-time reconstruction model from and to any view at any time. *arXiv preprint arXiv:2506.18890* (2025). [11, 16, 18, 19](#)
- [MGT*19] MAHMOOD N., GHORBANI N., TROJE N. F., PONS-MOLL G., BLACK M. J.: Amass: Archive of motion capture as surface shapes. *Proceedings of the IEEE/CVF international conference on computer vision* (2019), 5442–5451. [14](#)
- [MHS*22] MAO W., HARTLEY R. I., SALZMANN M., ET AL.: Contact-aware human motion forecasting. *Advances in Neural Information Processing Systems 35* (2022), 7356–7367. [12](#)
- [MLQ*25] MIAO Q., LI K., QUAN J., MIN Z., MA S., XU Y., YANG Y., LUO Y.: Advances in 4d generation: A survey. *ArXiv abs/2503.14501* (2025). [doi:10.48550/arXiv.2503.14501.2](#)
- [MRH22] MUSTAFA A., RUSSELL C., HILTON A.: 4d temporally coherent multi-person semantic reconstruction and segmentation. *International journal of computer vision 130*, 6 (2022), 1583–1606. [1](#)
- [MST*20] MILDENHALL B., SRINIVASAN P. P., TANCIK M., BARRON J. T., RAMAMOORTHI R., NG R.: Nerf: Representing scenes as neural radiance fields for view synthesis. In *ECCV* (2020). [5](#)
- [MYR*20] MA Q., YANG J., RANJAN A., PUJADES S., PONS-MOLL G., TANG S., BLACK M. J.: Learning to Dress 3D People in Generative Clothing. In *Computer Vision and Pattern Recognition (CVPR)* (June 2020). [7](#)
- [MZJ*22] MAO Y., ZHANG Y., JIANG H., CHANG A., SAVVA M.: Multiscan: Scalable rgbd scanning for 3d environments with articulated objects. *Advances in neural information processing systems 35* (2022), 9058–9071. [14](#)
- [MZS*25] MU Y., ZHANG Z., SHI Y., MATSUMOTO M., IMAMURA K., TEVET G., GUO C., TAYLOR M., SHU C., XI P., ET AL.: Smp: Reusable score-matching motion priors for physics-based character control. *arXiv preprint arXiv:2512.03028* (2025). [20](#)
- [NCOZMA25] NAG S., COHEN-OR D., ZHANG H., MAHDAVI-AMIRI A.: In-2-4d: Inbetweening from two single-view images to 4d generation. *arXiv preprint arXiv:2504.08366* (2025). [1, 3, 6, 9, 15, 16, 19](#)
- [NMOG19] NIEMEYER M., MESCHEDER L., OECHSLE M., GEIGER A.: Occupancy flow: 4d reconstruction by learning particle dynamics. In *Proceedings of the IEEE/CVF international conference on computer vision* (2019), pp. 5379–5389. [5, 10](#)
- [ODM*24] OQUAB M., DARCEY T., MOUTAKANNI T., VO H., SZAFRANIEC M., KHALIDOV V., FERNANDEZ P., HAZIZA D., MASSA F., EL-NOUBY A., ET AL.: Dinov2: Learning robust visual features without supervision. *Transactions on Machine Learning Research Journal* (2024). [15](#)
- [OGK*25] ON J., GWAK K., KANG G., CHA J., HWANG S., HWANG H., BAEK S.: Bigs: Bimanual category-agnostic interaction reconstruction from monocular videos via 3d gaussian splatting. In *Proceedings of the Computer Vision and Pattern Recognition Conference* (2025), pp. 17437–17447. [11](#)
- [OMT*21] OST J., MANNAN F., THUEREY N., KNODT J., HEIDE F.: Neural scene graphs for dynamic scenes. In *Proceedings of the IEEE/CVF Conference on Computer Vision and Pattern Recognition* (2021), pp. 2856–2865. [5](#)
- [PCG*19] PAVLAKOS G., CHOUTAS V., GHORBANI N., BOLKART T., OSMAN A. A., TZIONAS D., BLACK M. J.: Expressive body capture: 3d hands, face, and body from a single image. In *Proceedings of the IEEE/CVF Conference on Computer Vision and Pattern Recognition* (2019). [6, 18](#)
- [PCPMN21] PUMAROLA A., CORONA E., PONS-MOLL G., MORENO-NOGUER F.: D-nerf: Neural radiance fields for dynamic scenes. *Proceedings of the IEEE/CVF Conference on Computer Vision and Pattern Recognition* (2021), 10318–10327. [9, 14, 15, 20](#)
- [PDW*21] PENG S., DONG J., WANG Q., ZHANG S., SHUAI Q., ZHOU X., BAO H.: Animatable neural radiance fields for modeling dynamic human bodies. In *ICCV* (2021). [8](#)
- [PBJM22] POOLE B., JAIN A., BARRON J. T., MILDENHALL B.: Dreamfusion: Text-to-3d using 2d diffusion. *arXiv preprint arXiv:2209.14988* (2022). [17](#)
- [PLC*25] PANG H. E., LIU S., CAI Z., YANG L., ZHANG T., LIU Z.: Disco4d: Disentangled 4d human generation and animation from a single image. In *Proceedings of the Computer Vision and Pattern Recognition Conference* (2025). [16, 21](#)
- [PPN21] PIGA N. A., PATTACINI U., NATALE L.: A differentiable extended kalman filter for object tracking under sliding regime. *Frontiers in Robotics and AI 8* (2021), 686447. [10](#)
- [PSB*21] PARK K., SINHA U., BARRON J. T., BOUAZIZ S., GOLDMAN D. B., SEITZ S. M., MARTIN-BRUALLA R.: Nerfies: Deformable neural radiance fields. In *Proceedings of the IEEE/CVF International Conference on Computer Vision* (2021). [9, 14](#)
- [PSH*21] PARK K., SINHA U., HEDMAN P., BARRON J. T., BOUAZIZ S., GOLDMAN D. B., MARTIN-BRUALLA R., SEITZ S. M.: Hypernerf: A higher-dimensional representation for topologically varying neural radiance fields. *ACM Trans. Graph.* 40, 6 (dec 2021). [5, 9, 14, 20](#)
- [PSJ*23] PARK S., SON M., JANG S., AHN Y. C., KIM J.-Y., KANG N.: Temporal interpolation is all you need for dynamic neural radiance fields. In *Proceedings of the IEEE/CVF conference on computer vision and pattern recognition* (2023), pp. 4212–4221. [11, 16](#)
- [PSX*24] POKHARIYA C., SHAH I. N., XING A., LI Z., CHEN K., SHARMA A., SRIDHAR S.: Manus: Markerless grasp capture using articulated 3d gaussians. In *CVPR* (2024). [11](#)
- [PYL*22] PENG Y., YAN Y., LIU S., CHENG Y., GUAN S., PAN B., ZHAI G., YANG X.: Cagenerf: Cage-based neural radiance field for generalized 3d deformation and animation. *Advances in Neural Information Processing Systems 35* (2022), 31402–31415. [9](#)
- [PZL24] PENG S., ZHANG Y., LI K.: Papr in motion: Seamless point-level 3d scene interpolation. In *IEEE/CVF Conference on Computer Vision and Pattern Recognition (CVPR)* (2024). [5, 16](#)
- [PZX*21] PENG S., ZHANG Y., XU Y., WANG Q., SHUAI Q., BAO H., ZHOU X.: Neural body: Implicit neural representations with structured latent codes for novel view synthesis of dynamic humans. *Proceedings of the IEEE/CVF Conference on Computer Vision and Pattern Recognition* (2021), 9054–9063. [9, 14, 20](#)
- [QCB*24] QIAN S., CHEN W., BAI M., ZHOU X., TU Z., LI L. E.: Affordancellm: Grounding affordance from vision language models. In *Proceedings of the IEEE/CVF Conference on Computer Vision and Pattern Recognition* (2024), pp. 7587–7597. [12](#)
- [QCZ*23] QIU L., CHEN G., ZHOU J., XU M., WANG J., HAN X.: Rec-mv: Reconstructing 3d dynamic cloth from monocular videos. In *CVPR* (2023). [8, 9, 10](#)
- [QLC*25] QU W., LI J., CHENG J., SHI J., MENG C., MA C., WANG H., DENG X., ZHANG Y.: Hogs: Bimanual hand-object interaction understanding with 3d gaussian splatting based data augmentation. In *Proceedings of the AAAI Conference on Artificial Intelligence* (2025), vol. 39, pp. 6639–6647. [11](#)
- [QYW*25] QIU X., YANG J., WANG Y., CHEN Z., WANG Y., WANG T.-H., XIAN Z., GAN C.: Articulate animesh: Open-vocabulary 3d articulated objects modeling. *arXiv preprint arXiv:2502.02590* (2025). [7, 16](#)

- [QYZW24] QIU R.-Z., YANG G., ZENG W., WANG X.: Feature splatting: Language-driven physics-based scene synthesis and editing. *arXiv preprint arXiv:2404.01223* (2024). 9
- [RBL*22] ROMBACH R., BLATTMANN A., LORENZ D., ESSER P., OMMER B.: High-resolution image synthesis with latent diffusion models. In *Proceedings of the IEEE/CVF Conference on Computer Vision and Pattern Recognition* (2022). 15, 21
- [RBZ*20] REMPE D., BIRDAL T., ZHAO Y., GOJCIC Z., SRIDHAR S., GUIBAS L. J.: Caspr: Learning canonical spatiotemporal point cloud representations. *Advances in neural information processing systems* 33 (2020), 13688–13701. 5
- [RCJ*21] RAI N., CHEN H., JI J., DESAI R., KOZUKA K., ISHIZAKA S., ADELI E., NIEBLES J. C.: Home action genome: Cooperative compositional action understanding. In *Proceedings of the IEEE/CVF Conference on Computer Vision and Pattern Recognition* (2021), pp. 11184–11193. 7
- [RGA*20] ROSINOL A., GUPTA A., ABATE M., SHI J., CARLONE L.: 3d dynamic scene graphs: Actionable spatial perception with places, objects, and humans. *arXiv preprint arXiv:2002.06289* (2020). 7, 16
- [RKH*21] RADFORD A., KIM J. W., HALLACY C., RAMESH A., GOH G., AGARWAL S., SASTRY G., ASKELL A., MISHKIN P., CLARK J., ET AL.: Learning transferable visual models from natural language supervision. In *International conference on machine learning* (2021), PmlR, pp. 8748–8763. 15
- [RKLMO4] REDON S., KIM Y. J., LIN M. C., MANOCHA D.: Fast continuous collision detection for articulated models. In *Proceedings of the Ninth ACM Symposium on Solid Modeling and Applications* (Goslar, DEU, 2004), SM '04, Eurographics Association, p. 145–156. 9
- [RLH*20] RANFTL R., LASINGER K., HAFNER D., SCHINDLER K., KOLTUN V.: Towards robust monocular depth estimation: Mixing datasets for zero-shot cross-dataset transfer. *TPAMI* 44, 3 (2020). 15
- [RPT*23] REN J., PAN L., TANG J., ZHANG C., CAO A., ZENG G., LIU Z.: Dreamgaussian4d: Generative 4d gaussian splatting. *arXiv preprint arXiv:2312.17142* (2023). 9, 16
- [RRKB11] RUBLEE E., RABAUD V., KONOLIGE K., BRADSKI G.: Orb: An efficient alternative to sift or surf. In *ICCV* (2011), Ieee. 10
- [RTB17] ROMERO J., TZIONAS D., BLACK M. J.: Embodied hands: Modeling and capturing hands and bodies together. *ACM Transactions on Graphics, (Proc. SIGGRAPH Asia)* 36, 6 (Nov. 2017). 6, 14, 18
- [RTG98] RUBNER Y., TOMASI C., GUIBAS L. J.: A metric for distributions with applications to image databases. In *Sixth international conference on computer vision (IEEE Cat. No. 98CH36271)* (1998), IEEE, pp. 59–66. 15
- [RTSB25] RON R., TEVET G., SAWDAYEE H., BERMANO A. H.: Hoidini: Human-object interaction through diffusion noise optimization. *arXiv preprint arXiv:2506.15625* (2025). 18, 19
- [RXM*24] REN J., XIE C., MIRZAEI A., KREIS K., LIU Z., TORRALBA A., FIDLER S., KIM S. W., LING H., ET AL.: L4gm: Large 4d gaussian reconstruction model. In *Advances in Neural Information Processing Systems* (2024), vol. 37, pp. 56828–56858. 6, 11, 16, 18, 19, 21
- [SBV*22] SCHUHMANN C., BEAUMONT R., VENCU R., GORDON C., WIGHTMAN R., CHERTI M., COOMBS T., KATTA A., MULLIS C., WORTSMAN M., ET AL.: Laion-5b: An open large-scale dataset for training next generation image-text models. In *Advances in Neural Information Processing Systems* (2022), vol. 35, pp. 25278–25294. 13
- [SCH*16] SAVVA M., CHANG A. X., HANRAHAN P., FISHER M., NIESSNER M.: Pigraps: learning interaction snapshots from observations. *ACM Transactions On Graphics (TOG)* 35, 4 (2016), 1–12. 12
- [SCL*23] SONG L., CHEN A., LI Z., CHEN Z., CHEN L., YUAN J., XU Y., GEIGER A.: Nerfplayer: A streamable dynamic scene representation with decomposed neural radiance fields. *IEEE Transactions on Visualization and Computer Graphics* 29, 5 (2023), 2732–2742. 5
- [SCZ*23] SHI R., CHEN H., ZHANG Z., LIU M., XU C., WEI X., CHEN L., ZENG C., SU H.: Zero123++: a single image to consistent multi-view diffusion base model. *arXiv preprint arXiv:2310.15110* (2023). 13, 15
- [SDT*22] SIMEONOV A., DU Y., TAGLIASACCHI A., TENENBAUM J. B., RODRIGUEZ A., AGRAWAL P., SITZMANN V.: Neural descriptor fields: Se (3)-equivariant object representations for manipulation. In *2022 International Conference on Robotics and Automation (ICRA)* (2022), IEEE, pp. 6394–6400. 12
- [SFT*25] SIYAO L., FENG Y., TAHERI O., LOY C. C., BLACK M. J.: Half-physics: Enabling kinematic 3d human model with physical interactions. *arXiv preprint arXiv:2507.23778* (2025). 9
- [SGH*26] SUI K., GHOSH A., HWANG I., ZHOU B., WANG J., GUO C.: A survey on human interaction motion generation. *International Journal of Computer Vision* 134, 3 (2026), 113. 11, 19
- [SGOC20] SANTESTEBAN I., GARCES E., OTADUY M. A., CASAS D.: Softsmpl: Data-driven modeling of nonlinear soft-tissue dynamics for parametric humans. In *Computer Graphics Forum* (2020), vol. 39, Wiley Online Library, pp. 65–75. 7
- [SGW*24] SUN Q., GUO Z., WAN Z., YAN J. N., YIN S., ZHOU W., LIAO J., LI H.: Eg4d: Explicit generation of 4d object without score distillation. In *The Thirteenth International Conference on Learning Representations* (2024). 6, 16, 19
- [SGXT20] SHIMADA S., GOLYANIK V., XU W., THEOBALT C.: Physcap: Physically plausible monocular 3d motion capture in real time. *ACM Transactions on Graphics* 39, 6 (dec 2020). 7
- [SGY*24] SIYAO L., GU T., YANG Z., LIN Z., LIU Z., DING H., YANG L., LOY C. C.: Duolando: Follower gpt with off-policy reinforcement learning for dance accompaniment. In *ICLR* (2024). 19
- [SHU*24] STEARNS C., HARLEY A., UY M., DUBOST F., TOMBARI F., WETZSTEIN G., GUIBAS L.: Dynamic gaussian marbles for novel view synthesis of casual monocular videos. In *SIGGRAPH Asia* (2024). 6, 10, 16
- [SJSC24] SUN X., JIANG H., SAVVA M., CHANG A.: Opdmulti: Openable part detection for multiple objects. In *2024 International Conference on 3D Vision (3DV)* (2024), IEEE, pp. 169–178. 7
- [SKD*20] SUN P., KRETZSCHMAR H., DOTIWALLA X., CHOUARD A., PATNAIK V., TSUI P., GUO J., ZHOU Y., CHAI Y., CAINE B., ET AL.: Scalability in perception for autonomous driving: Waymo open dataset. *Proceedings of the IEEE/CVF conference on computer vision and pattern recognition* (2020), 2446–2454. 14
- [SLW*25] SHI Y., LIU Y., WU Y., LIU X., ZHAO C., LUO J., ZHOU B.: Drive any mesh: 4d latent diffusion for mesh deformation from video. *arXiv preprint arXiv:2506.07489* (2025). 3
- [SLY*25] SONG C., LI X., YANG F., XU Z., WEI J., LIU F., FENG J., LIN G., ZHANG J.: Puppeteer: Rig and animate your 3d models. *arXiv preprint arXiv:2508.10898* (2025). 5, 13, 16
- [SPH*23] SINGER U., POLYAK A., HAYES T., YIN X., AN J., ZHANG S., HU Q., YANG H., ASHUAL O., GAFNI O., PARIKH D., GUPTA S., TAIGMAN Y.: Make-a-video: Text-to-video generation without text-video data. In *The Eleventh International Conference on Learning Representations* (2023). URL: <https://openreview.net/forum?id=nJfy1Dvgz1q>. 13, 15
- [SSB11] STURM J., STACHNISS C., BURGARD W.: A probabilistic framework for learning kinematic models of articulated objects. *Journal of Artificial Intelligence Research* 41 (Aug. 2011), 477–526. URL: <http://dx.doi.org/10.1613/jair.3229>, doi:10.1613/jair.3229. 9
- [SSC*13] STOMAKHIN A., SCHROEDER C., CHAI L., TERAN J., SELLE A.: A material point method for snow simulation. *ACM Transactions on Graphics (TOG)* 32, 4 (2013), 1–10. 9
- [SSP*23] SINGER U., SHEYNNIN S., POLYAK A., ASHUAL O., MAKAROV I., KOKKINOS F., GOYAL N., VEDALDI A., PARIKH D., JOHNSON J., TAIGMAN Y.: Text-to-4d dynamic scene generation. In

- Proceedings of the 40th International Conference on Machine Learning* (2023). 6, 13, 15, 16, 17, 18
- [SSP*24] SHAO R., SUN J., PENG C., ZHENG Z., ZHOU B., ZHANG H., LIU Y.: Control4d: Efficient 4d portrait editing with text. In *Proceedings of the IEEE/CVF Conference on Computer Vision and Pattern Recognition* (2024). 6
- [STR21] STOJANOV S., THAI A., REHG J. M.: Using shape to categorize: Low-shot learning with an explicit shape bias. In *Proceedings of the IEEE/CVF conference on computer vision and pattern recognition* (2021), pp. 1798–1808. 13
- [SWS*25] SONG C., WU Z., SU S.-Y., WANDT B., SIGAL L., RHODIN H.: Locality sensitive avatars from video. In *The Thirteenth International Conference on Learning Representations* (2025). URL: <https://openreview.net/forum?id=SVta2eQnt3>. 8
- [SWY*24] SHI Y., WANG P., YE J., MAI L., LI K., YANG X.: MV-Dream: Multi-view diffusion for 3d generation. In *The Twelfth International Conference on Learning Representations* (2024). 13, 15, 17
- [SYLK18] SUN D., YANG X., LIU M.-Y., KAUTZ J.: Pwc-net: Cnns for optical flow using pyramid, warping, and cost volume. In *CVPR* (2018). 10
- [SZKS19] STARKE S., ZHANG H., KOMURA T., SAITO J.: Neural state machine for character-scene interactions. *ACM Transactions on Graphics* 38, 6 (2019), 178. 12
- [SZL*24] SONG W., ZHANG X., LI S., GAO Y., HAO A., HOU X., CHEN C., LI N., QIN H.: Hoianimator: Generating text-prompt human-object animations using novel perceptive diffusion models. In *Proceedings of the IEEE/CVF Conference on Computer Vision and Pattern Recognition* (2024), pp. 811–820. 18
- [SZL*25] SONG C., ZHANG J., LI X., YANG F., CHEN Y., XU Z., LIEW J. H., GUO X., LIU F., FENG J., LIN G.: Magicarticulate: Make your 3d models articulation-ready. In *Proceedings of the Computer Vision and Pattern Recognition Conference (CVPR)* (June 2025), pp. 15998–16007. 5, 7, 16
- [SZT*23] SHAO R., ZHENG Z., TU H., LIU B., ZHANG H., LIU Y.: Tensor4d: Efficient neural 4d decomposition for high-fidelity dynamic reconstruction and rendering. In *Proceedings of the IEEE/CVF Conference on Computer Vision and Pattern Recognition* (2023). 6
- [TADTBS*22] TUAN-ANH V., DUC-THANH N., BINH-SON H., QUANG-HIEU P., SAI-KIT Y.: Rfnet-4d: Joint object reconstruction and flow estimation from 4d point clouds. In *Proceedings of European Conference on Computer Vision (ECCV)* (2022). 5
- [TAL*22] TIWARI G., ANTIĆ D., LENSSEN J. E., SARAFIANOS N., TUNG T., PONS-MOLL G.: Pose-ndf: Modeling human pose manifolds with neural distance fields. In *European Conference on Computer Vision* (2022), Springer, pp. 572–589. 12
- [TCBT22] TAHERI O., CHOUTAS V., BLACK M. J., TZIONAS D.: Goal: Generating 4d whole-body motion for hand-object grasping. In *Proceedings of the IEEE/CVF Conference on Computer Vision and Pattern Recognition* (2022), pp. 13263–13273. 12, 19
- [TCC*24] TANG J., CHEN Z., CHEN X., WANG T., ZENG G., LIU Z.: Lgm: Large multi-view gaussian model for high-resolution 3d content creation. In *European Conference on Computer Vision* (2024), Springer, pp. 1–18. 11, 17, 18, 21
- [TD20] TEED Z., DENG J.: Raft: Recurrent all-pairs field transforms for optical flow. In *ECCV* (2020), Springer. 5, 10
- [TGBT20] TAHERI O., GHORBANI N., BLACK M. J., TZIONAS D.: GRAB: A dataset of whole-body human grasping of objects. In *European Conference on Computer Vision (ECCV)* (2020). URL: <https://grab.is.tue.mpg.de>. 12, 14
- [TLH*24] TONDERSKI A., LINDSTRÖM C., HESS G., LJUNGBERGH W., SVENSSON L., PETERSSON C.: Neurad: Neural rendering for autonomous driving. In *CVPR* (2024). 15
- [Tru] URL: <https://truebones.gumroad.com/l/skzMC>. 14
- [TTG*21] TRETSCHEK E., TEWARI A., GOLYANIK V., ZOLLHÖFER M., LASSNER C., THEOBALT C.: Non-rigid neural radiance fields: Reconstruction and novel view synthesis of a dynamic scene from monocular video. In *Proceedings of the IEEE/CVF international conference on computer vision* (2021), pp. 12959–12970. 9
- [TWH*22] TURPIN D., WANG L., HEIDEN E., CHEN Y.-C., MACKLIN M., TSOVKAS S., DICKINSON S., GARG A.: Grasp’d: Differentiable contact-rich grasp synthesis for multi-fingered hands. In *European Conference on Computer Vision* (2022), Springer, pp. 201–221. 12
- [TZT*25] TAUBNER F., ZHANG R., TULI M., BAHMANI S., LINDELL D. B.: Mvp4d: Multi-view portrait video diffusion for animatable 4d avatars. *arXiv preprint arXiv:2510.12785* (2025). 16
- [TZTL25] TAUBNER F., ZHANG R., TULI M., LINDELL D. B.: CAP4D: Creating animatable 4D portrait avatars with morphable multi-view diffusion models. In *Proceedings of the IEEE/CVF Conference on Computer Vision and Pattern Recognition (CVPR)* (June 2025), pp. 5318–5330. 16
- [TZW*25] TEAM A., ZHU H., WANG Y., ZHOU J., CHANG W., ZHOU Y., LI Z., CHEN J., SHEN C., PANG J., ET AL.: Aether: Geometric-aware unified world modeling. *arXiv preprint arXiv:2503.18945* (2025). 5
- [UFPC22] URAIN J., FUNK N., PETERS J., CHALVATZAKI G.: Se (3)-diffusionfields: Learning smooth cost functions for joint grasp and motion optimization through diffusion. *arXiv preprint arXiv:2209.03855* (2022). 12
- [VNZ25] VORA A., NAG S., ZHANG H.: Articulate that object part (atop): 3d part articulation via text and motion personalization. *arXiv preprint arXiv:2502.07278* (2025). 6, 7, 8, 13
- [VYB*24] VOLETI V., YAO C.-H., BOSS M., LETTS A., PANKRATZ D., TOCHILKIN D., LAFORTE C., ROMBACH R., JAMPANI V.: Sv3d: Novel multi-view synthesis and 3d generation from a single image using latent video diffusion. In *European Conference on Computer Vision* (2024). 3, 17
- [WCC*23] WANG Q., CHANG Y.-Y., CAI R., LI Z., HARIHARAN B., HOLYNSKI A., SNAVELY N.: Tracking everything everywhere all at once. In *ICCV* (2023). 9, 10
- [WCJ*24] WANG Z., CHEN Y., JIA B., LI P., ZHANG J., ZHANG J., LIU T., ZHU Y., LIANG W., HUANG S.: Move as you say interact as you can: Language-guided human motion generation with scene affordance. In *Proceedings of the IEEE/CVF Conference on Computer Vision and Pattern Recognition* (2024), pp. 433–444. 12
- [WCK*25] WANG J., CHEN M., KARAEEV N., VEDALDI A., RUPPRECHT C., NOVOTNY D.: Vggt: Visual geometry grounded transformer. In *Proceedings of the IEEE/CVF Conference on Computer Vision and Pattern Recognition* (2025). 5, 21
- [WCL*22] WANG Z., CHEN Y., LIU T., ZHU Y., LIANG W., HUANG S.: Humanise: Language-conditioned human motion generation in 3d scenes. *Advances in Neural Information Processing Systems* 35 (2022), 14959–14971. 14
- [WCS*22] WENG C.-Y., CURLESS B., SRINIVASAN P. P., BARRON J. T., KEMELMACHER-SHLIZERMAN I.: Humannerf: Free-viewpoint rendering of moving people from monocular video. In *CVPR* (2022). 8
- [WELG21] WANG C., ECKART B., LUCEY S., GALLO O.: Neural trajectory fields for dynamic novel view synthesis. *ArXiv:2105.05994* (2021). 10
- [WFY*25] WU S., FEI H., YANG J., LI X., LI J., ZHANG H., CHUA T.-S.: Learning 4d panoptic scene graph generation from rich 2d visual scene. In *Proceedings of the Computer Vision and Pattern Recognition Conference* (2025), pp. 24539–24549. 16
- [WGP*25] WU R., GAO R., POOLE B., TREVITHICK A., ZHENG C., BARRON J. T., HOLYNSKI A.: Cat4d: Create anything in 4d with multi-view video diffusion models. In *Proceedings of the IEEE/CVF Conference on Computer Vision and Pattern Recognition* (2025), pp. 26057–26068. 6, 16, 19, 21

- [WGPYZ24] WANG R., GADI PATIL A., YU F., ZHANG H.: Active coarse-to-fine segmentation of moveable parts from real images. In *European Conference on Computer Vision* (2024), Springer, pp. 111–127. 7
- [WHMM22] WENG T., HELD D., MEIER F., MUKADAM M.: Neural grasp distance fields for robot manipulation. *arXiv preprint arXiv:2211.02647* (2022). 12
- [WHZ*25] WEN B., HUANG D., ZHANG Z., ZHOU J., DENG J., GONG J., CHEN Y., MA L., LI Y.-L.: Reconstructing in-the-wild open-vocabulary human-object interactions. In *Proceedings of the Computer Vision and Pattern Recognition Conference* (2025), pp. 17426–17436. 11, 18
- [WIR*24] WU Q., ILIASH D., RITCHIE D., SAVVA M., CHANG A. X.: Diorama: Unleashing zero-shot single-view 3d scene modeling. *arXiv preprint arXiv:2411.19492* (2024). 5
- [WKS*22] WANG S., KWON Y., SHEN Y., ZHANG Q., STATE A., HUANG J.-B., FUCHS H.: Learning dynamic view synthesis with few rgbd cameras. *ArXiv:220410477* (2022). 15
- [WLC*24] WANG S., LEROY V., CABON Y., CHIDLOVSKII B., REVAUD J.: Dust3r: Geometric 3d vision made easy. In *Proceedings of the IEEE/CVF Conference on Computer Vision and Pattern Recognition* (2024), pp. 20697–20709. 5, 11
- [WLJ*23] WU S., LI R., JAKAB T., RUPPRECHT C., VEDALDI A.: Magicpony: Learning articulated 3d animals in the wild. In *CVPR* (2023). 15
- [WLL*23] WU Z., LIU T., LUO L., ZHONG Z., CHEN J., XIAO H., HOU C., LOU H., CHEN Y., YANG R., ET AL.: Mars: An instance-aware, modular and realistic simulator for autonomous driving. In *CAAI* (2023). 15
- [WLL*25] WU D., LIU L., LINLI Z., HUANG A., SONG L., YU Q., WU Q., LU C.: REArtGS: Reconstructing and generating articulated objects via 3d gaussian splatting with geometric and motion constraints. In *The Thirty-ninth Annual Conference on Neural Information Processing Systems* (2025). URL: <https://openreview.net/forum?id=6LGyChG6Ep>. 9
- [WML23] WANG C., MACDONALD L. E., JENI L. A., LUCEY S.: Flow supervision for deformable nerf. In *Proceedings of the IEEE/CVF Conference on Computer Vision and Pattern Recognition* (2023), pp. 21128–21137. 6, 10
- [WML23] WANG R., MAO W., LI H.: Deepsimho: stable pose estimation for hand-object interaction via physics simulation. *Advances in Neural Information Processing Systems* 36 (2023), 79685–79697. 12
- [WNGO24] WEI W., NEJADASL F. K., GEVERS T., OSWALD M. R.: T-mae: Temporal masked autoencoders for point cloud representation learning. In *European Conference on Computer Vision* (2024), Springer, pp. 178–195. 5
- [WPD*25] WANG W., PAN L., DOU Z., MEI J., LIAO Z., LOU Y., WU Y., YANG L., WANG J., KOMURA T.: Sims: Simulating stylized human-scene interactions with retrieval-augmented script generation. In *Proceedings of the IEEE/CVF International Conference on Computer Vision* (2025), pp. 14117–14127. 20
- [WSK*15] WU Z., SONG S., KHOSLA A., YU F., ZHANG L., TANG X., XIAO J.: 3d shapenets: A deep representation for volumetric shapes. In *Proceedings of the IEEE conference on computer vision and pattern recognition* (2015), pp. 1912–1920. 13
- [WWL*20] WU W., WANG Z. Y., LI Z., LIU W., FUXIN L.: Pointpwnet: Cost volume on point clouds for (self-) supervised scene flow estimation. In *European Conference on Computer Vision* (2020), Springer, pp. 88–107. 5
- [WWXL23] WANG Z., WU T., XU Z., LIN D.: Neuralangelo: High-fidelity neural surface reconstruction. In *Proceedings of the IEEE/CVF Conference on Computer Vision and Pattern Recognition* (2023), pp. 8456–8465. 9
- [WWY*25] WANG Y., WANG X., YI R., FAN Y., HU J., ZHU J., MA L.: 3d gaussian head avatars with expressive dynamic appearances by compact tensorial representations. In *Proceedings of the Computer Vision and Pattern Recognition Conference* (2025), pp. 21117–21126. 9
- [WWZ*22] WU Y., WANG J., ZHANG Y., ZHANG S., HILLIGES O., YU F., TANG S.: Saga: Stochastic whole-body grasping with contact. In *Proceedings of the European Conference on Computer Vision (ECCV)* (2022). 19
- [WYF*24] WU G., YI T., FANG J., XIE L., ZHANG X., WEI W., LIU W., TIAN Q., WANG X.: 4d gaussian splatting for real-time dynamic scene rendering. In *Proceedings of the IEEE/CVF Conference on Computer Vision and Pattern Recognition (CVPR)* (June 2024), pp. 20310–20320. 6, 16, 17
- [WYG*24] WANG Q., YE V., GAO H., AUSTIN J., LI Z., KANAZAWA A.: Shape of Motion: 4D Reconstruction from a Single Video. *ArXiv:240713764* (2024). 10, 15, 17, 20
- [WYJ*24] WU Z., YU C., JIANG Y., CAO C., WANG F., BAI X.: Sc4d: Sparse-controlled video-to-4d generation and motion transfer. In *European Conference on Computer Vision* (2024). 16
- [WYW*24] WANG Z., YE Z., WU H., CHEN J., YI L.: Semantic complete scene forecasting from a 4d dynamic point cloud sequence. In *Proceedings of the AAAI Conference on Artificial Intelligence* (2024), vol. 38, pp. 5867–5875. 5
- [WYWB25] WU Z., YU C., WANG F., BAI X.: Animateanymesh: A feed-forward 4d foundation model for text-driven universal mesh animation. *arXiv preprint arXiv:2506.09982* (2025). 3, 5, 13, 16, 18, 20, 21
- [WZF*23] WU T., ZHANG J., FU X., WANG Y., REN J., PAN L., WU W., YANG L., WANG J., QIAN C., ET AL.: Omniobject3d: Large-vocabulary 3d object dataset for realistic perception, reconstruction and generation. In *Proceedings of the IEEE/CVF Conference on Computer Vision and Pattern Recognition* (2023), pp. 803–814. 13
- [WZH*25] WANG* Q., ZHANG* Y., HOLYSKI A., EFROS A. A., KANAZAWA A.: Continuous 3d perception model with persistent state. In *CVPR* (2025). 5, 11, 16, 20, 21
- [WZM*24] WANG H., ZHU W., MIAO L., XU Y., GAO F., TIAN Q., WANG Y.: Aligning human motion generation with human perceptions. *arXiv preprint arXiv:2407.02272* (2024). 15
- [WZM*25] WANG Z., ZHENG Q., MA S., YE M., ZHAN Y., LI D.: End-to-end hoi reconstruction transformer with graph-based encoding. In *Proceedings of the Computer Vision and Pattern Recognition Conference* (2025), pp. 27706–27715. 19
- [WZT*22] WU T., ZHONG F., TAGLIASACCHI A., COLE F., OZTIRELI C.: D²nerf: Self-supervised decoupling of dynamic and static objects from a monocular video. *NeurIPS* 35 (2022). 5
- [WZY*25] WANG H., ZHANG W., YU R., HUANG T., REN J., JIA F., WANG Z., NIU X., CHEN X., CHEN J., ET AL.: Physhsi: Towards a real-world generalizable and natural humanoid-scene interaction system. *arXiv preprint arXiv:2510.11072* (2025). 20
- [WZZ*25] WANG Y., ZHOU J., ZHU H., CHANG W., ZHOU Y., LI Z., CHEN J., PANG J., SHEN C., HE T.: π^3 : Scalable permutation-equivariant visual geometry learning. *arXiv preprint arXiv:2507.13347* (2025). 1, 3, 5
- [XCW*22] XU C., CHEN Y., WANG H., ZHU S.-C., ZHU Y., HUANG S.: Partafford: Part-level affordance discovery from 3d objects. *arXiv preprint arXiv:2202.13519* (2022). 12
- [XFYX24] XU J., FAN Z., YANG J., XIE J.: Grid4d: 4d decomposed hash encoding for high-fidelity dynamic gaussian splatting. *Advances in Neural Information Processing Systems* 37 (2024), 123787–123811. 6
- [XH22] XU T., HARADA T.: Deforming radiance fields with cages. In *European Conference on Computer Vision* (2022), Springer, pp. 159–175. 9
- [XHZ*22] XUE H., HANG T., ZENG Y., SUN Y., LIU B., YANG H., FU J., GUO B.: Advancing high-resolution video-language representation with large-scale video transcriptions. *Proceedings of the IEEE/CVF*

- Conference on Computer Vision and Pattern Recognition (2022), 5036–5045. 13
- [XLB*24] XU D., LIANG H., BHATT N. P., HU H., LIANG H., PLATANIOS K. N., WANG Z.: Comp4d: Llm-guided compositional 4d scene generation. *arXiv preprint arXiv:2403.16993* (2024). 15
- [XLD*25] XU Z., LI Z., DONG Z., ZHOU X., NEWCOMBE R., LV Z.: 4dgt: Learning a 4d gaussian transformer using real-world monocular videos. *arXiv preprint arXiv:2506.08015* (2025). 11, 18, 19
- [XLWG23] XU S., LI Z., WANG Y.-X., GUI L.-Y.: Interdiff: Generating 3d human-object interactions with physics-informed diffusion. In *Proceedings of the IEEE/CVF International Conference on Computer Vision* (2023), pp. 14928–14940. 12, 19
- [XLWG25] XU S., LING H. Y., WANG Y.-X., GUI L.-Y.: Intermimic: Towards universal whole-body control for physics-based human-object interactions. In *Proceedings of the Computer Vision and Pattern Recognition Conference* (2025), pp. 12266–12277. 20
- [XLY*25] XIANG J., LV Z., XU S., DENG Y., WANG R., ZHANG B., CHEN D., TONG X., YANG J.: Structured 3d latents for scalable and versatile 3d generation. In *Proceedings of the Computer Vision and Pattern Recognition Conference* (2025), pp. 21469–21480. 3, 13, 14, 17, 21
- [XLY*24] XU L., LV X., YAN Y., JIN X., WU S., XU C., LIU Y., ZHOU Y., RAO F., SHENG X., ET AL.: Inter-x: Towards versatile human-human interaction analysis. In *Proceedings of the IEEE/CVF conference on computer vision and pattern recognition* (2024), pp. 22260–22271. 11
- [XLZ*25] XU S., LI D., ZHANG Y., XU X., LONG Q., WANG Z., LU Y., DONG S., JIANG H., GUPTA A., ET AL.: Interact: Advancing large-scale versatile 3d human-object interaction generation. In *Proceedings of the Computer Vision and Pattern Recognition Conference* (2025), pp. 7048–7060. 15
- [XQM*20] XIANG F., QIN Y., MO K., XIA Y., ZHU H., LIU F., LIU M., JIANG H., YUAN Y., WANG H., YI L., CHANG A. X., GUIBAS L. J., SU H.: SAPIEN: A simulated part-based interactive environment. In *The IEEE Conference on Computer Vision and Pattern Recognition (CVPR)* (June 2020). 7, 13, 14
- [XSM*25] XIA H., SU E., MEMMEL M., JAIN A., YU R., MBIZIWO-TIAPU N., FARHADI A., GUPTA A., WANG S., MA W.-C.: Drawer: Digital reconstruction and articulation with environment realism, 2025. URL: <https://arxiv.org/abs/2504.15278>, [arXiv:2504.15278](https://arxiv.org/abs/2504.15278). 7
- [XSW*23] XU L., SONG Z., WANG D., SU J., FANG Z., DING C., GAN W., YAN Y., JIN X., YANG X., ET AL.: Actformer: A gan-based transformer towards general action-conditioned 3d human motion generation. In *Proceedings of the IEEE/CVF International Conference on Computer Vision* (2023), pp. 2228–2238. 18, 19
- [XWW*23] XIAO Z., WANG T., WANG J., CAO J., ZHANG W., DAI B., LIN D., PANG J.: Unified human-scene interaction via prompted chain-of-contacts. *arXiv preprint arXiv:2309.07918* (2023). 20
- [XWX*25] XIAO Y., WANG J., XUE N., KARAEEV N., MAKAROV Y., KANG B., ZHU X., BAO H., SHEN Y., ZHOU X.: Spatialtrackerv2: 3d point tracking made easy. *arXiv preprint arXiv:2507.12462* (2025). 5
- [XYDM*24] XUETING L., YUAN Y., DE MELLO S., DAVIET G., LEAF J., MACKLIN M., KAUTZ J., IQBAL U.: Simavatar: Simulation-ready avatars with layered hair and clothing. *Arxiv* (2024). 7
- [XYV*24] XIE Y., YAO C.-H., VOLETI V., JIANG H., JAMPANI V.: Sv4d: Dynamic 3d content generation with multi-frame and multi-view consistency. In *The Thirteenth International Conference on Learning Representations* (2024). 6, 13, 14, 16, 19
- [XZC*23] XU H., ZHANG J., CAI J., REZATOFIHI H., YU F., TAO D., GEIGER A.: Unifying flow, stereo and depth estimation. *TPAMI* 45, 11 (2023). 15
- [XZQ*24] XIE T., ZONG Z., QIU Y., LI X., FENG Y., YANG Y., JIANG C.: Physgaussian: Physics-integrated 3d gaussians for generative dynamics. In *Proceedings of the IEEE/CVF Conference on Computer Vision and Pattern Recognition* (2024). 9, 10, 21
- [XZY*24] XU L., ZHOU Y., YAN Y., JIN X., ZHU W., RAO F., YANG X., ZENG W.: Regennet: Towards human action-reaction synthesis. In *Proceedings of the IEEE/CVF conference on computer vision and pattern recognition* (2024), pp. 1759–1769. 12
- [YAK*20] YIFAN W., AIGERMAN N., KIM V. G., CHAUDHURI S., SORKINE-HORNUNG O.: Neural cages for detail-preserving 3d deformations. In *Proceedings of the IEEE/CVF conference on computer vision and pattern recognition* (2020), pp. 75–83. 9
- [YCP*23] YANG J., CEN J., PENG W., LIU S., HONG F., LI X., ZHOU K., CHEN Q., LIU Z.: 4d panoptic scene graph generation. *Advances in Neural Information Processing Systems* 36 (2023), 69692–69705. 3, 7, 16
- [YCPH25] YIN M., CAO Y., PENG S., HAN K.: Splat4d: Diffusion-enhanced 4d gaussian splatting for temporally and spatially consistent content creation. In *Proceedings of the Special Interest Group on Computer Graphics and Interactive Techniques Conference Conference Papers* (2025), pp. 1–10. 19
- [YCW*23] YANG Z., CHEN Y., WANG J., MANIVASAGAM S., MA W.-C., YANG A. J., URTASUN R.: Unisim: A neural closed-loop sensor simulator. In *CVPR* (2023). 15
- [YGH*25] YANG Y., GUO Y.-C., HUANG Y., ZOU Z.-X., YU Z., LI Y., CAO Y.-P., LIU X.: Holopart: Generative 3d part amodal segmentation. *arXiv preprint arXiv:2504.07943* (2025). 7
- [YGG*24] YANG Z., GAO X., ZHOU W., JIAO S., ZHANG Y., JIN X.: Deformable 3d gaussians for high-fidelity monocular dynamic scene reconstruction. In *Proceedings of the IEEE/CVF conference on computer vision and pattern recognition* (2024), pp. 20331–20341. 9
- [YHR*24] YAO M., HUO Y., RAN Y., TIAN Q., WANG R., WANG H.: Neural radiance field-based visual rendering: A comprehensive review. *arXiv preprint arXiv:2404.00714* (2024). 6
- [YHY*20] YAN Z., HU R., YAN X., CHEN L., VAN KAICK O., ZHANG H., HUANG H.: Rpm-net: recurrent prediction of motion and parts from point cloud. *arXiv preprint arXiv:2006.14865* (2020). 7, 16
- [YHZ*25] YE J., HE Y., ZHOU Y., ZHU Y., XIAO K., LIU Y.-J., YANG W., HAN X.: Primitiveanything: Human-crafted 3d primitive assembly generation with auto-regressive transformer. *arXiv preprint arXiv:2505.04622* (2025). 7
- [YJB*23] YANG J., JOHNSON B., BERGER I., TSCHERNEZKI V., VEDALDI A., HARLEY A. W.: Emernerf: Emergent spatial-temporal scene decomposition via self-supervision. *arXiv preprint arXiv:2311.02077* (2023). 15
- [YKH*24] YANG L., KANG B., HUANG Z., XU X., FENG J., ZHAO H.: Depth anything: Unleashing the power of large-scale unlabeled data. In *CVPR* (2024). 15, 18
- [YLL23] YAN Z., LI C., LEE G. H.: Nerf-ds: Neural radiance fields for dynamic specular objects. In *CVPR* (2023). 15
- [YLSL21] YUAN W., LV Z., SCHMIDT T., LOVEGROVE S.: Star: Self-supervised tracking and reconstruction of rigid objects in motion with neural rendering. In *CVPR* (2021). 9
- [YPZ*24] YANG Z., PAN Z., ZHU X., ZHANG L., FENG J., JIANG Y.-G., TORR P. H.: 4d gaussian splatting: Modeling dynamic scenes with native 4d primitives. *arXiv preprint arXiv:2412.20720* (2024). 6, 11
- [YQG*24] YE C., QIU L., GU X., ZUO Q., WU Y., DONG Z., BO L., XIU Y., HAN X.: Stablenormal: Reducing diffusion variance for stable and sharp normal. *ACM Transactions on Graphics* (2024). 18
- [YQZ*24] YU F., QIAN Y., ZHANG X., GIL-URETA F., JACKSON B., BENNETT E., ZHANG H.: Dpa-net: Structured 3d abstraction from sparse views via differentiable primitive assembly. In *European Conference on Computer Vision* (2024), Springer, pp. 454–471. 7

- [YRH*24] YAO Y., REN S., HOU J., DENG Z., ZHANG J., WANG W.: Dynosurf: Neural deformation-based temporally consistent dynamic surface reconstruction. In *European Conference on Computer Vision* (2024). 21
- [YSI*23] YUAN Y., SONG J., IQBAL U., VAHDAT A., KAUTZ J.: Physdiff: Physics-guided human motion diffusion model. In *Proceedings of the IEEE/CVF international conference on computer vision* (2023), pp. 16010–16021. 8, 9, 12
- [YVN*22] YANG G., VO M., NEVEROVA N., RAMANAN D., VEDALDI A., JOO H.: Banmo: Building animatable 3d neural models from many casual videos. In *CVPR* (2022). 15
- [YWZ*24] YU H., WANG C., ZHUANG P., MENAPACE W., SIAROHIN A., CAO J., JENI L., TULYAKOV S., LEE H.-Y.: 4real: Towards photorealistic 4d scene generation via video diffusion models. In *Advances in Neural Information Processing Systems* (2024), vol. 37, pp. 45256–45280. 16
- [YXL18] YAN S., XIONG Y., LIN D.: Spatial temporal graph convolutional networks for skeleton-based action recognition. In *Proceedings of the AAAI conference on artificial intelligence* (2018), vol. 32. 7
- [YXL*25] YAO W., XIE S., LI L., ZHANG W., LAI Z., DAI S., ZHANG K., WANG Z.: Sd-gs: Structured deformable 3d gaussians for efficient dynamic scene reconstruction. *arXiv preprint arXiv:2507.07465* (2025). 6
- [YXV*25] YAO C.-H., XIE Y., VOLETI V., JIANG H., JAMPANI V.: Sv4d 2.0: Enhancing spatio-temporal consistency in multi-view video diffusion for high-quality 4d generation. *arXiv preprint arXiv:2503.16396* (2025). 6, 13, 17, 19
- [YXW*23] YIN Y., XU D., WANG Z., ZHAO Y., WEI Y.: 4dgen: Grounded 4d content generation with spatial-temporal consistency. *arXiv preprint arXiv:2312.17225* (2023). 6, 16
- [YXY*24] YU W., XING J., YUAN L., HU W., LI X., HUANG Z., GAO X., WONG T.-T., SHAN Y., TIAN Y.: Viewcrafter: Taming video diffusion models for high-fidelity novel view synthesis. *arXiv preprint arXiv:2409.02048* (2024). 17
- [YYPZ24] YANG Z., YANG H., PAN Z., ZHANG L.: Real-time photorealistic dynamic scene representation and rendering with 4d gaussian splatting. In *International Conference on Learning Representations (ICLR)* (2024). 6
- [YZL*21] YANG L., ZHAN X., LI K., XU W., LI J., LU C.: Cpf: Learning a contact potential field to model the hand-object interaction. In *Proceedings of the IEEE/CVF international conference on computer vision* (2021), pp. 11097–11106. 12
- [YZT*25] YANG L., ZHU K., TIAN J., ZENG B., LIN M., PEI H., ZHANG W., YAN S.: Widerange4d: Enabling high-quality 4d reconstruction with wide-range movements and scenes. *arXiv preprint arXiv:2503.13435* (2025). 15
- [YZY*25] YAO K., ZHANG L., YAN X., ZENG Y., ZHANG Q., XU L., YANG W., GU J., YU J.: Cast: Component-aligned 3d scene reconstruction from an rgb image. *ACM Transactions on Graphics (TOG)* 44, 4 (2025), 1–19. 5
- [ZBL*19] ZHOU Y., BARNES C., LU J., YANG J., LI H.: On the continuity of rotation representations in neural networks. In *Proceedings of the IEEE/CVF conference on computer vision and pattern recognition* (2019), pp. 5745–5753. 11
- [ZBS*22] ZHANG X., BHATNAGAR B. L., STARKE S., GUZOV V., PONS-MOLL G.: Couch: Towards controllable human-chair interactions. In *European Conference on Computer Vision* (2022), Springer, pp. 518–535. 14
- [ZBS*24] ZHANG X., BHATNAGAR B. L., STARKE S., PETROV I., GUZOV V., DHAMO H., PÉREZ-PELLITERO E., PONS-MOLL G.: Force: Dataset and method for intuitive physics guided human-object interaction. *CoRR* (2024). 12, 19
- [ZCW*24] ZHANG H., CHEN X., WANG Y., LIU X., WANG Y., QIAO Y.: 4diffusion: Multi-view video diffusion model for 4d generation. In *Advances in Neural Information Processing Systems* (2024), vol. 37, pp. 15272–15295. 6, 16
- [ZGV*25] ZHOU J. J., GAO H., VOLETI V., VASISHTA A., YAO C.-H., BOSS M., TORR P., RUPPRECHT C., JAMPANI V.: Stable virtual camera: Generative view synthesis with diffusion models. *arXiv preprint arXiv:2503.14489* (2025). 17
- [ZHH*24] ZHANG J., HERRMANN C., HUR J., JAMPANI V., DARRELL T., COLE F., SUN D., YANG M.-H.: Monst3r: A simple approach for estimating geometry in the presence of motion. *arXiv preprint arXiv:2410.03825* (2024). 5, 11, 16, 18, 19
- [ZHN*20] ZHANG Y., HASSAN M., NEUMANN H., BLACK M. J., TANG S.: Generating 3d people in scenes without people. In *Proceedings of the IEEE/CVF conference on computer vision and pattern recognition* (2020), pp. 6194–6204. 19
- [ZHY*25] ZHU H., HE T., YU X., GUO J., CHEN Z., BIAN J.: Ar4d: Autoregressive 4d generation from monocular videos. *arXiv preprint arXiv:2501.01722* (2025). 19
- [ZIE*18] ZHANG R., ISOLA P., EFROS A. A., SHECHTMAN E., WANG O.: The unreasonable effectiveness of deep features as a perceptual metric. In *CVPR* (2018). 15
- [ZJZ*24] ZENG Y., JIANG Y., ZHU S., LU Y., LIN Y., ZHU H., HU W., CAO X., YAO Y.: Stag4d: Spatial-temporal anchored generative 4d gaussians. In *European Conference on Computer Vision* (2024). 6, 15, 16, 17, 18
- [ZKJB17] ZUFFI S., KANAZAWA A., JACOBS D., BLACK M. J.: 3D menagerie: Modeling the 3D shape and pose of animals. In *IEEE Conf. on Computer Vision and Pattern Recognition (CVPR)* (July 2017). 6
- [ZL25] ZHOU H., LEE G. H.: Uni4d-llm: A unified spatiotemporal-aware vlm for 4d understanding and generation. *arXiv preprint arXiv:2509.23828* (2025). 15
- [ZLL*24] ZHAO Y., LIN C.-C., LIN K., YAN Z., LI L., YANG Z., WANG J., LEE G. H., WANG L.: Genxd: Generating any 3d and 4d scenes. In *The Thirteenth International Conference on Learning Representations* (2024). 16
- [ZLL*25] ZHAO Z., LAI Z., LIN Q., ZHAO Y., LIU H., YANG S., FENG Y., YANG M., ZHANG S., YANG X., ET AL.: Hunyuan3d 2.0: Scaling diffusion models for high resolution textured 3d assets generation. *arXiv preprint arXiv:2501.12202* (2025). 3, 13, 20
- [ZLN*24] ZHENG Y., LI X., NAGANO K., LIU S., HILLIGES O., DE MELLO S.: A unified approach for text-and image-guided 4d scene generation. In *Proceedings of the IEEE/CVF Conference on Computer Vision and Pattern Recognition* (2024). 15, 16
- [ZLS*24] ZHOU X., LIN Z., SHAN X., WANG Y., SUN D., YANG M.-H.: Drivinggaussian: Composite gaussian splatting for surrounding dynamic autonomous driving scenes. In *Proceedings of the IEEE/CVF Conference on Computer Vision and Pattern Recognition* (2024). 20
- [ZLZ*25] ZHU W., LI B., ZHENG C., MAI J., CHEN J., JIANG L., HAMDANI A., MARTINEZ S. R., LIN C.-W., ELHOSEINY M., ET AL.: 4d-bench: Benchmarking multi-modal large language models for 4d object understanding. *arXiv preprint arXiv:2503.17827* (2025). 15
- [ZMR*23] ZHU W., MA X., RO D., CI H., ZHANG J., SHI J., GAO F., TIAN Q., WANG Y.: Human motion generation: A survey. *IEEE Transactions on Pattern Analysis and Machine Intelligence* 46, 4 (2023), 2430–2449. 11, 14
- [ZQXY24] ZHANG T., QIAN G., XIE J., YANG J.: Fastpci: Motion-structure guided fast point cloud frame interpolation. In *European Conference on Computer Vision* (2024), Springer, pp. 251–267. 5
- [ZQZ*22] ZENG Y., QIAN Y., ZHANG Q., HOU J., YUAN Y., HE Y.: Idea-net: Dynamic 3d point cloud interpolation via deep embedding alignment. In *Proceedings of the IEEE/CVF Conference on Computer Vision and Pattern Recognition* (2022). 5
- [ZSY*25] ZHANG Z., SHI Y., YANG L., NI S., YE Q., WANG J.: OpenHOI: Open-world hand-object interaction synthesis with multi-modal large language model. In *The Thirty-ninth Annual Conference*

- on *Neural Information Processing Systems* (2025). URL: <https://openreview.net/forum?id=0biUwyjKkm>. 19
- [ZTF*18] ZHOU T., TUCKER R., FLYNN J., FYFFE G., SNAVELY N.: Stereo magnification: Learning view synthesis using multiplane images. *arXiv preprint arXiv:1805.09817* (2018). 19
- [ZWL*23] ZHENG Z., WU D., LU R., LU F., CHEN G., JIANG C.: Neuralpci: Spatio-temporal neural field for 3d point cloud multi-frame non-linear interpolation. In *Proceedings of the IEEE/CVF Conference on Computer Vision and Pattern Recognition* (2023), pp. 909–918. 5, 16
- [ZWY*24] ZHAO M., WANG Y., YU F., ZOU C., MAHDAVI-AMIRI A.: Sweepnet: Unsupervised learning shape abstraction via neural sweepers. In *European Conference on Computer Vision* (2024), Springer. 7
- [ZWZ*22] ZHAO K., WANG S., ZHANG Y., BEELER T., TANG S.: Compositional human-scene interaction synthesis with semantic control. In *European Conference on Computer Vision* (2022), Springer, pp. 311–327. 12
- [ZWZ*24] ZHANG L., WANG Z., ZHANG Q., QIU Q., PANG A., JIANG H., YANG W., XU L., YU J.: Clay: A controllable large-scale generative model for creating high-quality 3d assets. *ACM Transactions on Graphics (TOG)* 43, 4 (2024), 1–20. 13, 21
- [ZYD*25] ZHANG H., YAO C.-H., DONNÉ S., AHUJA N., JAMPANI V.: Stable part diffusion 4d: Multi-view rgb and kinematic parts video generation. *arXiv preprint arXiv:2509.10687* (2025). 7, 16, 20, 21
- [ZYW*24] ZHANG T., YU H.-X., WU R., FENG B. Y., ZHENG C., SNAVELY N., WU J., FREEMAN W. T.: Physdreamer: Physics-based interaction with 3d objects via video generation. In *European Conference on Computer Vision* (2024), Springer, pp. 388–406. 15, 21
- [ZYWL24] ZHONG L., YU H.-X., WU J., LI Y.: Reconstruction and simulation of elastic objects with spring-mass 3d gaussians. In *European Conference on Computer Vision* (2024), Springer, pp. 407–423. 9
- [ZYX*23] ZHAO Y., YAN Z., XIE E., HONG L., LI Z., LEE G. H.: Animate124: Animating one image to 4d dynamic scene. *arXiv preprint arXiv:2311.14603* (2023). 6, 9, 16
- [ZYZ*24] ZHAN X., YANG L., ZHAO Y., MAO K., XU H., LIN Z., LI K., LU C.: Oakink2: A dataset of bimanual hands-object manipulation in complex task completion. In *Proceedings of the IEEE/CVF Conference on Computer Vision and Pattern Recognition* (2024), pp. 445–456. 14
- [ZZL24] ZHANG M., ZHANG K., LI Y.: Dynamic 3d gaussian tracking for graph-based neural dynamics modeling. *arXiv preprint arXiv:2410.18912* (2024). 10
- [ZZY*24] ZHENG Y., ZHAO Q., YANG G., YIFAN W., XIANG D., DUBOST F., LAGUN D., BEELER T., TOMBARI F., GUIBAS L., WETZSTEIN G.: Physavatar: Learning the physics of dressed 3d avatars from visual observations. *arxiv* (2024). 3, 7, 16